Nonlinear Spectral Imaging of Fungi

Helene Knaus

2014

The research described in this report was performed within the Microbiology and the Molecular Biophysics groups of the Science Faculty of Utrecht University and was financed by the Dutch Technology Foundation STW, Applied Science division of NWO and the Technology Program of the Ministry of Economic Affairs with support from Productschap Tuinbouw.

ISBN: 978-90-393-6253-2

Cover: Collage of different nonlinear spectral images of fungal hyphae

Printed and published by CPI-Koninklijke Wöhrmann B.V, Zutphen

Printed on wood-free offset white FSC recycled paper

Printing of this thesis was financially supported by the Dutch Technology Foundation STW

Nonlinear Spectral Imaging of Fungi

Niet-lineaire spectrale microscopie van schimmels

(met een samenvatting in het Nederlands)

Proefschrift

ter verkrijging van de graad van doctor aan de Universiteit Utrecht op gezag van de rector magnificus, prof. dr. G.J. van der Zwaan, ingevolge het besluit van het college voor promoties in het openbaar te verdedigen op donderdag 11 december 2014 des ochtends te 10.30 uur

door

Helene Knaus

geboren op 31 januari 1982 te Dshambul, Kazachstan

Promotoren: Prof.dr. H. A. B. Wösten
Prof.dr. H. C. Gerritsen

Copromotor: Dr. G. A. Blab

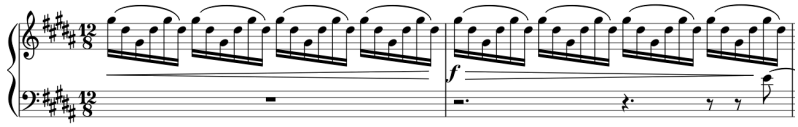

S. Rachmaninov Op. 32 No. 12

Contents

CHAPTER 1

General introduction

Part of this chapter has bee n published as: Helene Knaus, Gerhard A. Blab, G. Jerre van Veluw, Hans C. Gerritsen, Han A. B. Wösten (2013). Fungal Biology Review 27: 60-66

1

THE FUNGAL KINGDOM

The fungal kingdom consists of a diverse group of eukaryotic microorganisms. It has been estimated that it encompasses 1.5 million species, of which about 70.000 have been identified (Hawksworth 1991). Fungi can grow as unicellular organisms known as yeasts, while filamentous fungi grow by means of hyphae. The latter fungi form a network of hyphae known as mycelium or colony. Fungi play important roles in nature. They establish mutual beneficial and parasitic interactions and are essential for conversion of dead organic material. Besides their ecological role, fungi are important for mankind. Fungi can be harmful by infecting plants (among many, if not all, agricultural crops) animals, and humans. Moreover, they produce toxins and are an important cause of spoilage of food and buildings. On the other hand, fungi are used as a food source (e.g. Quorn®, mushrooms) or to prepare food (e.g. tofu, miso, cheese, bread) and alcoholic drinks (e.g. wine, beer, sake). Moreover, they are used in biotechnological applications, like the biodegradation of waste products (Borchert and Libra 2001, Maeda et al. 2005, Kanaly et al. 2005), as biocontrol agents (Butt et al. 2001), or as a cell factory. Fungal enzymes and metabolites such as citric acid (Andersen et al. 2011, Papagianni 2007) find a wide range of applications in the industry. Moreover, antibiotics (Elander 2003), mycotoxins, and enzymes produced by fungi are used as pharmaceuticals. The capability to perform post-translational protein modifications makes fungi important cell factories for humanized pharmaceutical compounds (Berends et al. 2009, Kozarski et al. 2011, Jeong et al. 2010). Fungi are also used in research as a model system for eukaryotic organisms, the most important being *Saccharomyces cerevisae.*

The life cycle of filamentous fungi

Asexual and sexual spores of filamentous fungi are dispersed by air, water, or vectors such as insects. At some stage, these spores contact a food source and start germinating. As a result, hyphae are formed that grow at their tip and that branch subapically. This and hyphal fusion results in a mycelium. Fungal mycelia colonize distinct patches of substrate such as a wheat kernel up to immense areas such as a forest. For instance, a genetic individual of the honey mushroom had colonized

1000 hectares of forest (Smith et al. 1992, Ferguson et al. 2003). At some point, formation of asexual or sexual spore forming structures, of which the mushrooms are the most conspicuous, is initiated. Their spores are dispersed and can start a new cycle.

Aspergillus niger and *Agaricus bisporus* were used as model systems in this Thesis. These fungi will be introduced in the next two sections.

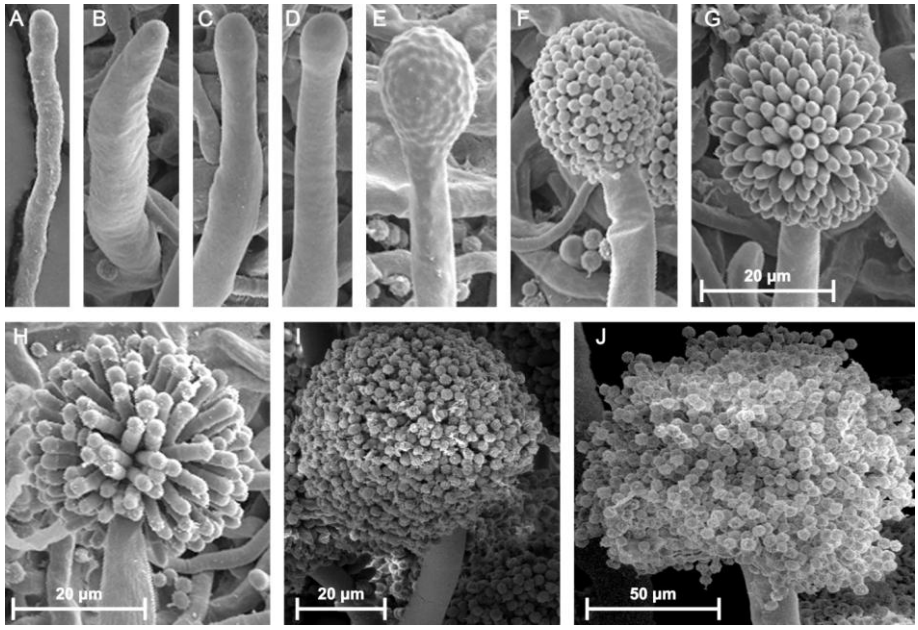

Figure 1. Scanning electron microscopy illustrating development of *A. niger*. The vegetative mycelium forms two types of aerial hyphae. One type is similar to vegetative hyphae (2-3 μm) (A), while the other type, called stalk, is 6-7 μm thick (B). The tips of the latter aerial hyphae swell to form a vesicle (C,D). Buds are formed on the vesicle (E) that develop into metulae (F, G). Phialides are formed on top of the metulae (H) that give rise to chains of conidia (I, J). The bar in G also holds for A-F (Taken from Krijgsheld et al., 2013; with permission).

The life cycle of *A. niger* and its role in nature and the industry

A. niger is part of the genus *Aspergillus*, which comprises upto 837 species (Geiser et al. 2007, Samson and Varga 2009).These fungi are among the most abundant fungi in the world. Aspergilli can be found in soil and decaying organic matter and are common food spoilage

fungi (Pitt et al. 2009). *A. niger* normally feeds on dead organic substrates but it can also be a pathogen of plants (Pawar et al. 2008), animals, and humans with a compromised immune system (Pitt 1994, Brakhage 2005).

A. niger secretes a wide variety and large amounts of enzymes that degrade polymers within the living or dead substrate into small molecules that can be taken up to serve as nutrients. For instance, glucoamylase is secreted to degrade starch, and xylanases to degrade hemicellulose within plant material (van den Brink and de Vries 2011). *A. niger* also excretes high amounts of organic acids such as citric acid. The capacity to produce and release large amounts of proteins and organic acids combined with the established fermentation technology and molecular biology makes *A. niger* an important cell factory. For instance, strains of *A. niger* have been isolated that produce more than 30 grams per liter of glucoamylase (Finkelstein et al. 1989).

A. niger is known to reproduce asexually but a sexual cycle has not yet been reported in the literature. Yet, its genome seems to have all genes to enable sexual reproduction (Pel et al. 2007). Asexual reproduction in *A. niger* is mediated by the formation of conidiophores that form spores called conidia. Conidiophore development begins with the formation of a specialized aerial hypha. This so called stalk has a width of 6-7 μm, while vegetative hypha have a diameter of 2-3 μm (Figure 1A,B) (Krijgsheld et al. 2013). Swelling of the tip of the stalk gives rise to the conidiophore vesicle (Figure 1C-E). Budding results in a layer of metulae on the vesicle surface (Figure 1F,G). These metulae in turn bud twice to produce a layer of phialides (Figure 1H) that give rise to chains of conidia (Figure 1I,J). In contrast to the vegetative mycelium that appears hyaline, conidia are black pigmented due to the presence of melanin.

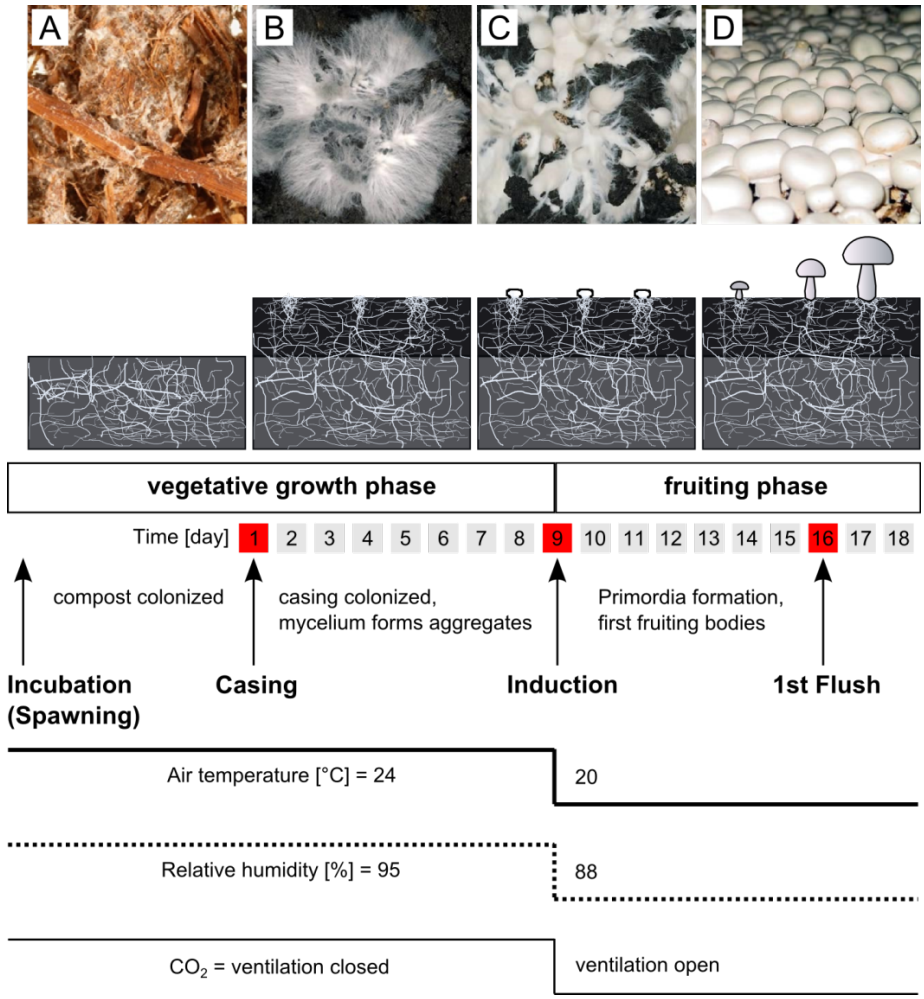

Figure 2. Cultivation conditions and development of *A. bisporus*. Top row shows fully colonized compost (A), vegetative mycelium on casing (B), primordia (C) and first fruiting body flush (D). Middle row gives a schematic view (cross section through the compost and casing layer) of development. Bottom row provides physicochemical factors during the cultivation. In this figure, cultivation is started with fully colonized compost that was topped with casing layer at day 1. The compost had already been inoculated with *A. bisporus* (spawning) 12 days before casing layer was added. After 9 days the mycelium has fully colonized the casing layer and fruiting body formation is induced by changing the environmental conditions. The first flush of fruiting bodies is observed 16 – 18 days after the compost was topped with casing. Pictures B and C by Hans van Pelt.

The life-cycle of *A. bisporus* and its role in nature and the industry

A. bisporus, the white button mushroom, is one of over 200 species of the genus *Agaricus*, which can be found all over the world (Calvo-Bado et al. 2000). *A. bisporus* belongs to the Basidiomycota (Hibbett et al. 2007) and forms mushrooms as part of its sexual cycle. These fruiting bodies produce basidiospores that are formed by specialized cells, basidia, in the gills of the mushroom cap (Wösten and Wessels 2006). *A. bisporus* plays an important role in the degradation of leaf litter and it has been hypothesized also to decay lignocellulosic material, as present in wood (Morin et al. 2012). *A. bisporus* is a model organism for the persistence of organisms growing in soils containing humic-rich compounds (from modified lignin and other recalcitrant aromatic compounds) and for the bioconversion of plant litter (Morin et al. 2012).

Besides its ecological importance, *A. bisporus* is one of the most cultivated edible mushrooms worldwide representing a multibillion industry. The mushrooms of *A. bisporus* are relatively rich in protein and fibres and are low in fat (Wani et al. 2010, Kurtzman Jr 1997). In addition, white button mushrooms contain minerals and bio-active compounds like antioxidative and immunomodulating polysaccharides (Kozarski et al. 2011, Wani et al. 2010, Kurtzman Jr 1997, Mattila et al. 2001).

A. bisporus is grown commercially on compost consisting of lignocellulose rich material, usually derived from wheat straw (Iiyami et al. 1996, Atkey and Wood 1984, Iiyama et al. 1994, Chen et al. 2000), horse or chicken manure, and gypsum. After colonization of the substrate, the compost is topped with casing layer. This layer offers a high water activity (Bels-Koning 1950, Flegg 1956, Kalberer 1987) and a microbial flora needed to induce mushroom formation (Eger 1961). Mushroom induction also requires lowering of temperature and CO_2 levels (Eastwood et al. 2013). The developmental stages of *A. bisporus* during the cultivation conditions applied in this thesis are presented in Figure 2. The first stage of mushroom development is the formation of fluffy hyphal knots (Eastwood et al. 2013, Umar and van Griensven 1997). These knots grow out into 1–2 mm sized fluffy initials. These undiffer-

entiated primordia develop into smooth undifferentiated primordia (Eastwood et al. 2013), of which 5–10 % develop into mature fruiting bodies (Noble et al. 2003). Stipe and cap tissue can be distinguished in 4 mm sized differentiated primordia. These tissues further develop when the mushroom is formed (Umar and van Griensven 1997). Gill tissue is developed in the cap as the fruiting body enlarges. Basidia are formed within this tissue and give rise to sexual basidiospores.

LABEL-FREE FLUORESCENCE MICROSCOPY IN FUNGI

Over the last few decades, fluorescence microscopy has developed into an indispensable tool to study biological processes (Gitai 2009, Kentner and Sourjik 2010, Toomre and Bewersdorf 2010, Zipfel et al. 2003, Hickey et al. 2004). It allows spatial and temporal localization of cells, organelles, gene expression and molecules within whole organisms down to the level of tissues and individual cells. In most cases, exogenous fluorophores are used in fluorescence microscopy. These fluorophores can be added to the medium or can be expressed within cells. Many fluorophores can be taken up by living cells and thus allow live-cell imaging. Other fluorophores can only penetrate the cell after they have been fixed (Hickey et al. 2004). For instance, fluorescent antibodies (Xiao et al. 1999) and probes used to localize specific RNA molecules (Teertstra et al. 2004) need fixation of cells. Fluorescent reporter proteins (e.g. GFP) enable localization of gene expression when cloned behind the promoter of interest, while fusing the reporter gene to the coding sequence of the target protein allows protein localization in living cells. Exogenous fluorophores may affect viability or can even be toxic. Moreover, they may have an impact on the functioning or the localization of organelles or macromolecules of interest. In case cell fixation is required, one should acknowledge that this procedure may influence cellular integrity (Wiedenmann et al. 2009, Dillingham and Wallace 2008). Label-free microscopy does not require cell fixation and has no impact on the distribution and functioning of molecules and organelles, nor on viability of cells and tissues.

Table 1. Endogenous fluorophores in fungi.

Endogenous Fluorophore	2p Excitation Maximum (nm)	Emission Maximum (nm)	Function
NAD(P)H (Huang et al. 2002)	710	460	NAD(P)H / NAD(P)$^+$ ratio describes energy metabolism and redox state (Palero et al. 2011, Canelas et al. 2008, Herbrich et al. 2012).
FAD (Huang et al. 2002)	710 and 900	530	Energy metabolism (Skala et al. 2007).
Riboflavin (Bi et al. 2006)	740	530	Component of FAD, FMN and flavoproteins (Esteve et al. 2001, Abbas and Sibirny 2011).
Lipofuscin (Chorvat Jr and Chorvatova 2009, Roshchina 2003, Bindewald-Wittich et al. 2006)	800	500 – 550	Peroxidized lipids and protein aggregates associated with oxidative stress (Yin 1996, Georgiou and Zees 2002, Jung et al. 2010).
Ergosterol (Nakashima et al. 1985)	620 (based on 1p absorption)	340	Membrane sterol used to quantify fungal biomass in substrates (Bonzom et al. 1999, Hendrix 1970, Newell 2001, Shapiro and Gealt 1982).
Melanin (synthetic) (Teuchner et al. 2000)	no maximum, but decreasing absorption spectrum between the near-UV and the near-IR	620	Cell wall associated pigment involved in virulence and defense against environmental stress such as oxidizing agents and UV light (Eisenman and Casadevall 2012, Hegnauer et al. 1985, Nosanchuk and Casadevall 2003, Soler-Rivas et al. 2000, Butler et al. 2005, Dadachova et al. 2007, Rosas et al. 2000).
Carotenoids (Vivas et al. 2011, Jorgensen et al. 1992)	640	570	Anti-oxidative pigments (Will et al. 1984, Schrantz and Lemoine 1995, Strobel et al. 2009).

Label-free fluorescence microscopy is based on auto-fluorescence originating from endogenous fluorophores. A limited number of biomolecules are autofluorescent including collagen, elastin, keratin, flavins, NAD(P)H, melanin, chlorophyll, lignin and xanthophyll (Palero et al. 2008, Chorvat Jr and Chorvatova 2009, Roshchina 2003). Endogenous fluorophores that have been identified in fungi include flavins, NAD(P)H, and melanin (Table 1). They are for instance involved in

energy metabolism or in pathogenesis and defense mechanisms. Thus, monitoring these molecules non-invasively in their natural environment can provide insight in processes in cells and tissues (Palero et al. 2011, Palero et al. 2007, Lin et al. 2009, Stringari et al. 2012, Arcangeli et al. 2000, Vishwasrao et al. 2005, Rodrigues et al. 2011, Bader et al. 2011). Most endogenous fluorophores require UV excitation. One-photon (1p) UV-excitation is challenging technically as it requires specialized excitation sources and optics. Moreover, UV radiation is phototoxic for biological specimens. These issues can be circumvented by nonlinear excitation. In nonlinear excitation, mostly applied as two-photon (2p) excitation, fluorophores are excited by simultaneous absorption of two near infrared photons. 2p excitation has important advantages over 1p excitation (Denk et al. 1990). Firstly, 2p excitation is limited to the focal volume, thereby reducing the overall photodamage of the specimen. Secondly, most tissues are nearly transparent in the near-IR. This provides increased penetration depth (Gu et al. 2000, Theer and Denk 2006, Gerritsen and de Grauw 1999), allowing optical sectioning of thick biological samples (e.g. up to 100 μm in mammalian skin tissue).

Nonlinear microscopy (NLM) has the capacity of linking structural information and biochemical properties of the specimen. The spatial image is acquired point by point, while moving the focal volume laterally across the specimen and recording the 2p excited (auto)fluorescent emission. Spectrum, lifetime and polarization of the emitted fluorescence contain biochemical information (Lakowicz 2006). Each fluorophore has a characteristic emission spectrum, defined by the maximum emission wavelength and the shape of the spectrum. The lifetime of a fluorophore can also be used as a finger print of the fluorophore. This is the average time that a fluorophore stays in its excited state before relaxing to the ground state. Fluorescent molecules have a preferential direction for both the absorption and the emission of light. Absorption is maximal when the polarization direction of the excitation light is oriented in the preferred direction. Similarly, the emission of the fluorescence light is maximal along the preferred emission direction. Under polarized excitation (e.g. laser light) the emission of a static fluorophore will be polarized, whereas a rotating fluorophore will emit depolarized light. The degree to which molecular orientation de-

polarizes the emission is described by anisotropy. Thus, anisotropy is a measure of the rotational diffusion of a fluorophore. Low anisotropy values can be explained by small, fast rotating or unbound molecules, whereas high anisotropy values refer to big, slow rotating or bound molecules. Changes of the molecular surrounding can alter emission spectra (Palero et al. 2011, Arcangeli et al. 2000, Teuchner et al. 2000), fluorescence lifetime (Tyagi and Penzkofer 2010, Lakowicz et al. 1992) and / or anisotropy (Vishwasrao et al. 2005, Kierdaszuk et al. 1996). This allows quantitative analysis of the environment of the fluorophore. Thus, by spatially mapping the spectrum, lifetime and anisotropy, endogenous fluorophores can be localized and characterized within their environment.

In most cases a specimen contains various autofluorescent molecules. Depending on the excitation wavelength some of these autofluorescent molecules will not be excited (Table 1). Nonetheless, the detected spectrum, lifetime and anisotropy are often the result of the contribution of different endogenous fluorophores. As all fluorophores are characterized by their emission spectrum and lifetime, it is possible to decompose the total emission and follow individual endogenous fluorophores. In well characterized biological systems such as human tissue the type and number of endogenous fluorophores is limited (Chorvat Jr and Chorvatova 2009). Hence, biochemical and spatial information can be correlated and followed over time. For instance, it is possible to monitor metabolism (Stringari et al. 2012, Vishwasrao et al. 2005), and to discriminate between free and bound NAD(P)H (Palero et al. 2011). Inspired by these recent developments in human tissue imaging, (possible) applications of label-free fluorescence microscopy in fungal biology shall be discussed in the following section.

Label-free microscopy in fungal biology

Autofluorescent molecules have great potential to study fundamental aspects of fungal growth and development or applied aspects such as bioprocess monitoring. For instance, recording emission spectra for a distinct set of excitation wavelengths was shown to be a valuable tool to monitor fungal physiology in bioreactors (Marose et al. 2008, Ganzlin et al. 2007). Proteins, coenzymes, and vitamins were simulta-

neously detected in- and outside fungal cells and hyphae. However, analyzing auto-fluorescence using microscopic techniques has not been widely used to study fungal biology. Monitoring colonization of plant roots by arbuscular mycorrhizae revealed that all fungal structures (hyphae, vesicles and spores) were autofluorescent under blue light excitation, irrespectively of being dead or alive (Dreyer et al. 2006). Lin et al. (2009) used NLM combined with spectroscopy, known as nonlinear spectral microscopy (NLSM), as a tool for taxonomy. The emission spectra of *Aspergillus flavus*, *Micosporum gypseum*, *Micosoprum canis*, *Trichophyton rubrum*, and *Trichophyton tonsurans* were split by optical filters into the blue, green and red wavelength range. It was found that fluorescence intensity ratios were species specific. An initial study on the use of NLSM in fungal cell biology showed that the endogenous fluorophores of *Arthrobotrys ferox* spores are located in the cell wall and membranes (Arcangeli et al. 2000). NLSM was further applied to detect local biochemical changes due to environmental conditions. It was observed that spores undergoing UV-B irradiation showed a red-shifted emission spectrum. Herbrich et al. (2012) localized free and enzyme-bound NAD(P)H as well as melanin in spores of *Aspergillus ochraceus*. These molecules have overlapping spectral characteristics, making a spectral decomposition challenging. However, their fluorescence lifetimes do differ. By decomposing the overall fluorescence lifetime, melanin was mainly found in the cell-wall, while NAD(P)H was identified in the cytoplasm. Notably, fluorescence lifetime imaging microscopy (FLIM) localized regions within the spore that are enriched in enzyme-bound and regions that are enriched in free NAD(P)H. The ratio of protein-bound and free NAD(P)H is an indicator for the metabolic activity. Therefore, it was proposed that metabolic activity is carried out in distinct regions of the spore. However, lifetime components comparable to free NAD(P)H can also be found within the lifetime decay signal of bound NAD(P)H (Gafni and Brand 1976). Thus, free and bound NAD(P)H cannot always be ambiguously assigned. Anisotropy can be used as a sensitive alternative to distinguish between free and enzyme-bound NAD(P)H (Vishwasrao et al. 2005). In contrast to lifetime or spectral measurements, anisotropy depends on the rotational diffusion of the fluorophores. The rotational diffusion depends on the volume of the fluorophores

and can be used to distinguish between free and bound states, and to monitor local viscosity.

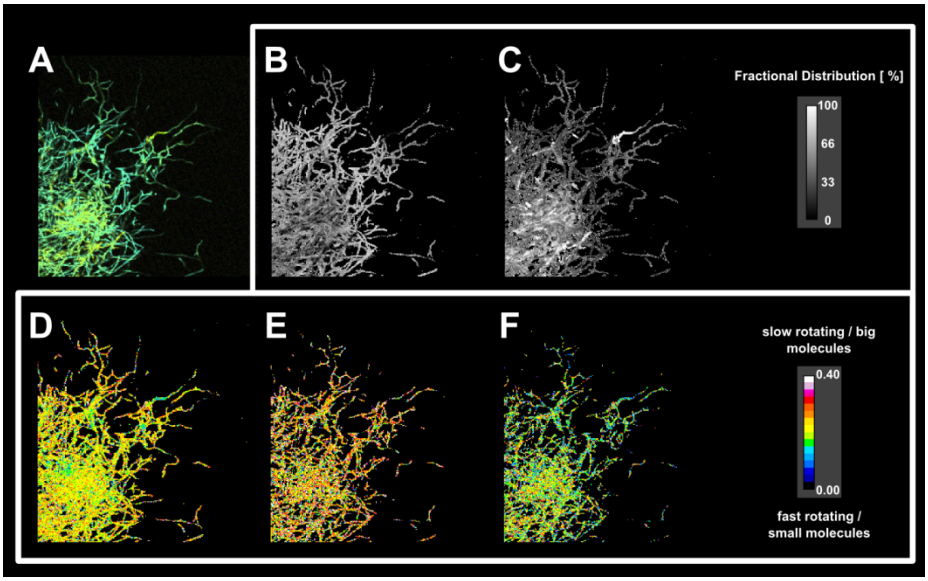

Figure 3. NLSM combined with simultaneous anisotropy measurements on an *A. niger* colony grown in liquid medium with maltose as a carbon source. Light of 740 nm was used for excitation. (A) RGB real-color representation of the spectral data. Blue (B) and yellow-green (C) emitting component (decomposed of the total spectrum by spectral phasor). The average anisotropy image calculated over the entire emission (D) and the anisotropy image for the emission of the blue (E) and yellow-green (F) component.

I did pilot studies to use polarization dependent spectral information to study metabolism and heterogeneity within and between mycelia and hyphae of filamentous fungi. To visualize this multidimensional dataset, consisting of spectral and spatial information, the spectra are represented in Red-Green-Blue (RGB)-values of the visible spectral wavelength range as perceived by eye (Figure 3A). Within a maltose-grown colony of *A. niger* regions are observed that are spectrally predominantly blue and others that are mostly yellow-green. Spectral decomposition, using the spectral phasor (Fereidouni et al. 2012), reveals two main components contributing to the total measured emission spectrum. One component is in the blue (Figure 3B) the other in the yellow-green (Figure 3C) wavelength range. The blue component can

be identified as NAD(P)H and the yellow-green one might be lipofuscin. Lipofuscin accumulates in the presence of reactive oxygen species (ROS) and is known to be produced by some fungi (Georgiou and Zees 2002, Georgiou et al. 2006). However, it is unknown whether *A. niger* produces lipofuscin. There is a higher percentage of the yellow-green emitting compound (Figure 3C) within the center of the colony when compared to its periphery. NAD(P)H (Figure 3B) is quite homogeneously distributed between zones of the colony, but heterogeneity is observed between hyphae within a particular zone. Interestingly, low content of NAD(P)H correlates with high content of the yellow-green emitting compound. Being an indirect antioxidant, NAD(P)H reduces oxidative stress. As such, it could decrease lipofuscin accumulation (Jung et al. 2010). Spatial mapping of the average anisotropy (calculated over the entire emission) of the *A. niger* mycelium shows some heterogeneity within the mycelium (Figure 3D). However, heterogeneity is higher when calculating anisotropy for the emission range of NAD(P)H (Figure 3E) and the yellow-green emitting compound (Figure 3F). These data are in line with previous findings showing that zones within fungal colonies (Wösten et al. 1991, Masai et al. 2006, Kasuga and Glass 2008, Moukha et al. 1993, Levin et al. 2007, Krijgsheld et al. 2012) as well as hyphae within zones (de Bekker et al. 2011, Vinck et al. 2005, Vinck et al. 2011, van Veluw et al. 2012, Bleichrodt et al. 2012) are heterogeneous with respect to gene expression, growth, and secretion. It would be of high interest to relate gene expression (monitored by using GFP as a reporter) with the metabolic state of hyphae as measured by NLSM.

Label-free microscopy - perspectives in fungal biology

First applications show that label-free fluorescence microscopy can provide new insights in fungal biology. Up to now most fungal studies focus on relative changes of the total fluorescence emission. However, a more detailed characterization (i.e. anisotropy and decomposition of spectra as well as fluorescence lifetime) of the emitted fluorescence provides biochemical data and thus enables us to monitor metabolism, stress reactions and developmental processes. Currently, miniaturized portable biomedical imaging devices are being developed, such as NLSM integrated into endoscopy needles for clinical applications

(Brown et al. 2012). This progress is facilitated with the characterization of the endogenous fluorophores present in human tissue and the development of robust, user-friendly data analysis methods. Techniques such as linear unmixing (Garini et al. 2006), blind source separation or nonnegative matrix factorization (Neher et al. 2009) and the phasor analysis (Fereidouni et al. 2012, Verveer and Hanley 2009) can also be used to decompose spectra and lifetime of fluorophores in fungi. A full chemical characterization of fluorescent components in fungi will increase applicability and will improve biochemical understanding of fungal hyphae and cells.

Up to now data is mostly post-processed. However, by integrating emission decomposition techniques into the imaging acquisition software one can gain immediate results on biologically intact samples. This means that distribution of components within mycelia or even within hyphae or cells can be quantified and followed in real time. This can be particularly interesting for biotechnological applications, for instance to monitor metabolism and secondary metabolites in small- and large-scale bioreactors. Combining morphological and biochemical properties can also lead to new developments in fungal taxonomy, biomedical diagnostics (e.g. identifying fungal pathogens on skin) as well as quality control of fungal products such as mushrooms.

SCOPE OF THIS THESIS

The aim of this Thesis was to set up a NLSM system and to apply this technique to study fungal growth and development.

Chapter 2 describes design, calibration, and testing of a spectral imaging system optimized for label-free characterization of living fungi using autofluorescence of endogenous fluorophores. As a specimen usually contains several endogenous fluorophores, the spectral phasor analysis has been tested to decompose spectral data. Moreover, spectral imaging was combined with anisotropy measurements.

Autofluorescence of NAD(P)H, FAD and melanin of mushroom caps was monitored during a 17 day storage period at 4 °C (**Chapter 3**). Mushrooms did not show changes in morphology or color as detecta-

ble by eye during this period. However, changes were observed in spectra. This showed that NLSM can be used to monitor the metabolic state of mushrooms during postharvest storage. A degree of freshness was defined based on FAD / NAD(P)H and melanin / NAD(P)H ratios.

The FAD / NAD(P)H ratio was used in **Chapter 4** to monitor the metabolic state during development of *A. bisporus*. Data implies that aerial structures are more metabolically active than vegetative growing mycelium in the compost and casing layer. Moreover, the FAD / NAD(P)H ratio together with preliminary experiments suggest that smaller mushrooms (1 - 4 cm cap diameter) have a better shelf-life when compared to bigger mushrooms (8 cm cap diameter). The presence of melanin was also monitored in **Chapter 4**. Although invisible by eye, melanin was more abundant in the vegetative mycelium within compost than in the mycelium in the casing layer or in the aerial structures. This indicates that melanin is important for the colonization of substrates.

Another way to investigate the presence of fungal melanin-like pigments is described in **Chapter 5**. It is shown that regardless of the melanin type and synthesis pathway, melanin fluorescence is enhanced upon illumination with a high level of near-infrared light. This effect is irreversible and is observed in cell walls of *A. bisporus* and *A. niger*, suggesting that melanin-like pigments form a structural component of the fungal cell wall. This is an unexpected finding since these mycelia appear white or hyaline by eye. Fluorescence enhancement was also observed in white spores of an *A. niger* strain that are blocked in the initial step of the DHN melanin synthesis pathway. This indicates that another melanin synthesis pathway functions in *A. niger* apart from the DHN pathway.

Results are summarized and discussed in **Chapter 6**.

REFERENCES

Abbas CA, Sibirny AA (2011) Genetic control of biosynthesis and transport of riboflavin and flavin nucleotides and construction of robust biotechnological producers. MMBR 75: 321-360

Andersen MR, Salazar MP, Schaap PJ, van de Vondervoort PJ, Culley D, Thykaer J, Frisvad JC, Nielsen KF, Albang R, Albermann K, Berka RM, Braus GH, Braus-Stromeyer SA, Corrochano LM, Dai Z, van Dijck PW, Hofmann G, Lasure LL, Magnuson JK, Menke H, Meijer M, Meijer SL, Nielsen JB, Nielsen ML, van Ooyen AJ, Pel HJ, Poulsen L, Samson RA, Stam H, Tsang A, van den Brink JM, Atkins A, Aerts A, Shapiro H, Pangilinan J, Salamov A, Lou Y, Lindquist E, Lucas S, Grimwood J, Grigoriev IV, Kubicek CP, Martinez D, van Peij NN, Roubos JA, Nielsen J, Baker SE (2011) Comparative genomics of citric-acid-producing *Aspergillus niger* ATCC 1015 versus enzyme-producing CBS 513.88. Genome Res 21: 885-897

Arcangeli C, Yu W, Cannistraro S, Gratton E (2000) Two-photon autofluorescence microscopy and spectroscopy of Antarctic fungus: New approach for studying effects of UV-B irradiation. Biopolymers 57: 218-225

Atkey PT, Wood DA (1984) Electron microscopic study of wheat straw degradation during composting. Appl Biochem Biotechnol 9: 335-336

Bader AN, Pena AM, Johan van Voskuilen C, Palero JA, Leroy F, Colonna A, Gerritsen HC (2011) Fast nonlinear spectral microscopy of in vivo human skin. Biomed Opt Express 2: 365-373

Bels-Koning H (1950) Experiments with casing soils, water supply and climate. Mushroom Science 1: 78-84

Berends E, Scholtmeijer K, Wösten HAB, Bosch D, Lugones LG (2009) The use of mushroom-forming fungi for the production of N-glycosylated therapeutic proteins. Trends Microbiol 17: 439-443

Bi YH, Huang ZL, Liu B, Zou QJ, Yu JH, Zhao YD, Luo QM (2006) Two-photon-excited fluorescence and two-photon spectrofluoroelectrochemistry of riboflavin. Electrochem commun 8: 595-599

Bindewald-Wittich A, Han M, Schmitz-Valckenberg S, Snyder SR, Giese G, Bille JF, Holz FG (2006) Two-Photon–Excited Fluorescence Imaging of Human RPE Cells with a Femtosecond Ti: Sapphire Laser. Invest Ophthalmol Vis Sci 47: 4553-4557

Bleichrodt RJ, Veluw GJ, Recter B, Maruyama J, Kitamoto K, Wösten HAB (2012) Hyphal heterogeneity in *Aspergillus oryzae* is the result of dynamic closure of septa by Woronin bodies. Mol Microbiol 86: 1334-1344

Bonzom PM, Nicolaou A, Zloh M, Baldeo W, Gibbons WA (1999) NMR lipid profile of *Agaricus bisporus*. Phytochemistry 50: 1311-1321

Borchert M, Libra JA (2001) Decolorization of reactive dyes by the white rot fungus *Trametes versicolor* in sequencing batch reactors. Biotechnol Bioeng 75: 313-321

Brakhage AA (2005) Systemic fungal infections caused by *Aspergillu*s species: epidemiology, infection process and virulence determinants. Curr Drug Targets 6: 875-886

Brown CM, Rivera DR, Pavlova I, Ouzounov DG, Williams WO, Mohanan S, Webb WW, Xu C (2012) In vivo imaging of unstained tissues using a compact and flexible multiphoton microendoscope. J Biomed Opt 17: 040505-1-040505-3

Butler M, Gardiner R, Day A (2005) Fungal melanin detection by the use of copper sulfide-silver. Mycologia 97: 312-319

Butt TM, Jackson C, Magan N (2001) Fungi as biocontrol agents: progress problems and potential. CABI

Calvo-Bado L, Noble R, Challen M, Dobrovin-Pennington A, Elliott T (2000) Sexuality and genetic identity in the *Agaricus* section *Arvenses*. Appl Environ Microbiol 66: 728-734

Canelas AB, van Gulik WM, Heijnen JJ (2008) Determination of the cytosolic free NAD/NADH ratio in Saccharomyces cerevisiae under steady-state and highly dynamic conditions. Biotechnol Bioeng 100: 734-743

Chen Y, Chefetz B, Rosario R, van Heemst J, Romaine C, Hatcher P (2000) Chemical nature and composition of compost during mushroom growth. Compost Sci Util 8: 347-359

Chorvat Jr D, Chorvatova A (2009) Multi-wavelength fluorescence lifetime spectroscopy: a new approach to the study of endogenous fluorescence in living cells and tissues. Laser Phys Lett 6: 175-193

Dadachova E, Bryan RA, Huang X, Moadel T, Schweitzer AD, Aisen P, Nosanchuk JD, Casadevall A (2007) Ionizing radiation changes the electronic properties of melanin and enhances the growth of melanized fungi. PLoS One 2: e457

de Bekker C, van Veluw GJ, Vinck A, Wiebenga LA, Wösten HAB (2011) Heterogeneity of *Aspergillus niger* microcolonies in liquid shaken cultures. Appl Environ Microbiol 77: 1263-1267

Denk W, Strickler JH, Webb WW (1990) Two-photon laser scanning fluorescence microscopy. Science 248: 73-76

Dillingham MS, Wallace MI (2008) Protein modification for single molecule fluorescence microscopy. Org Biomol Chem 6: 3031-3037

Dreyer B, Morte A, Perez-Gilabert M, Honrubia M (2006) Autofluorescence detection of arbuscular mycorrhizal fungal structures in palm roots: an underestimated experimental method. Mycol Res 110: 887-897

Eastwood DC, Herman B, Noble R, Dobrovin-Pennington A, Sreenivasaprasad S, Burton KS (2013) Environmental regulation of reproductive phase change in *Agaricus bisporus* by 1-octen-3-ol, temperature and CO_2. Fungal Genet Biol 55: 54-66

Eger G (1961) Untersuchungen ueber die Funktion der Deckschicht bei der Fruechtkoerperbildung des Kulturchampignons, *Psalliota bispora* Lge. Archiv fuer Mikrobiologie 39: 313-334

Eisenman HC, Casadevall A (2012) Synthesis and assembly of fungal melanin. Appl Microbiol Biotechnol 93: 931-940

Elander R (2003) Industrial production of β-lactam antibiotics. Appl Microbiol Biotechnol 61: 385-392

Esteve MJ, Farré R, Frígola A, García-Cantabella JM (2001) Simultaneous determination of thiamin and riboflavin in mushrooms by liquid chromatography. J Agric Food Chem 49: 1450-1454

Fereidouni F, Bader AN, Gerritsen HC (2012) Spectral phasor analysis allows rapid and reliable unmixing of fluorescence microscopy spectral images. Opt Express 20: 12729-12741

Ferguson B, Dreisbach T, Parks C, Filip G, Schmitt C (2003) Coarse-scale population structure of pathogenic *Armillaria* species in a mixed-conifer forest in the Blue Mountains of northeast Oregon. Can J For Res 33: 612-623

Finkelstein DB, Rambosek J, Crawford MS, Soliday CL, McAda PC, Leach J (1989) Protein secretion in *Aspergillus niger*. In: Hershberger CL, Queener SW and Hegeman G (eds) Genetics and molecular biology of industrial microorganisms. American Society of Microbiology, Washington DC, pp 295-300

Flegg P (1956) The casing layer in the cultivation of the mushroom (*Psalliota hortensis*). Eur J Soil Sci 7: 168-176

Gafni A, Brand L (1976) Fluorescence decay studies of reduced nicotinamide adenine dinucleotide in solution and bound to liver alcohol dehydrogenase. Biochemistry (NY) 15: 3165-3171

Ganzlin M, Marose S, Lu X, Hitzmann B, Scheper T, Rinas U (2007) In situ multi-wavelength fluorescence spectroscopy as effective tool to simultaneously monitor spore germination, metabolic activity and quantitative protein production in recombinant *Aspergillus niger* fed-batch cultures. J Biotechnol 132: 461-468

Garini Y, Young IT, McNamara G (2006) Spectral imaging: principles and applications. Cytometry A 69: 735-747

Geiser D, Klich M, Frisvad JC, Peterson S, Varga J, Samson RA (2007) The current status of species recognition and identification in *Aspergillus*. Stud Mycol 59: 1-10

Georgiou CD, Patsoukis N, Papapostolou I, Zervoudakis G (2006) Sclerotial metamorphosis in filamentous fungi is induced by oxidative stress. Integr Comp Biol 46: 691-712

Georgiou CD, Zees A (2002) Lipofuscins and sclerotial differentiation in phytopathogenic fungi. Mycopathologia 153: 203-208

Gerritsen HC, De Grauw CJ (1999) Imaging of optically thick specimen using two-photon excitation microscopy. Microsc Res Tech 47: 206-209

Gitai Z (2009) New fluorescence microscopy methods for microbiology: sharper, faster, and quantitative. Curr Opin Microbiol 12: 341-346

Gu M, Gan X, Kisteman A, Xu MG (2000) Comparison of penetration depth between two-photon excitation and single-photon excitation in imaging through turbid tissue media. Appl Phys Lett 77: 1551-1553

Hawksworth DL (1991) The fungal dimension of biodiversity: magnitude, significance, and conservation. Mycol Res 95: 641-655

Hegnauer H, Nyhlén LE, Rast DM (1985) Ultrastructure of native and synthetic *Agaricus bisporus* melanins - Implications as to the compartmentation of melanogenesis in fungi. Exp Mycol 9: 1-29

Hendrix J (1970) Sterols in growth and reproduction of fungi. Annu Rev Phytopathol 8: 111-130

Herbrich S, Gehder M, Krull R, Gericke KH (2012) Label-Free Spatial Analysis of Free and Enzyme-Bound NAD(P)H in the Presence of High Concentrations of Melanin. J Fluoresc 22: 349-355

Hibbett DS, Binder M, Bischoff JF, Blackwell M, Cannon PF, Eriksson OE, Huhndorf S, James T, Kirk PM, Lücking R (2007) A higher-level phylogenetic classification of the fungi. Mycol Res 111: 509-547

Hickey PC, Swift SR, Roca MG, Read ND (2004) Live-cell imaging of filamentous fungi using vital fluorescent dyes and confocal microscopy, Microbial Imaging. In: Savidge T and Pothoulakis C (eds) Methods in Microbiology. Elsevier, pp 63-87

Huang S, Heikal AA, Webb WW (2002) Two-photon fluorescence spectroscopy and microscopy of NAD(P)H and flavoprotein. Biophys J 82: 2811-2825

Iiyama K, Stone BA, Macauley BJ (1994) Compositional changes in compost during composting and growth of *Agaricus bisporus*. Appl Environ Microbiol 60: 1538-1546

Iiyami K, Lam TBT, Stone BA, Macauley BJ (1996) Characterisation of material generated on the surface of wheat straw during composting for mushroom production. J Sci Food Agric 70: 461-467

Jeong SC, Jeong YT, Yang BK, Islam R, Koyyalamudi SR, Pang G, Cho KY, Song CH (2010) White button mushroom (*Agaricus bisporus*) lowers blood glucose and cholesterol levels in diabetic and hypercholesterolemic rats. Nutr Res 30: 49-56

Jorgensen K, Stapelfeldt H, Skibsted LH (1992) Fluorescence of carotenoids. Effect of oxygenation and cis/trans isomerization. Chem Phys Lett 190: 514-519

Jung T, Hohn A, Grune T (2010) Lipofuscin: detection and quantification by microscopic techniques. Methods Mol Biol 594: 173-193

Kalberer PP (1987) Water potentials of casing and substrate and osmotic potentials of fruit bodies of *Agaricus bisporus*. Scientia Horticulturae 32: 175-182

Kanaly RA, Kim IS, Hur H (2005) Biotransformation of 3-methyl-4-nitrophenol, a main product of the insecticide fenitrothion, by *Aspergillus niger*. J Agric Food Chem 53: 6426-6431

Kasuga T, Glass NL (2008) Dissecting colony development of *Neurospora crassa* using mRNA profiling and comparative genomics approaches. Eukaryotic cell 7: 1549-1564

Kentner D, Sourjik V (2010) Use of fluorescence microscopy to study intracellular signaling in bacteria. Annu Rev Microbiol 64: 373-390

Kierdaszuk B, Malak H, Gryczynski I, Callis P, Lakowicz JR (1996) Fluorescence of reduced nicotinamides using one-and two-photon excitation. Biophys Chem 62: 1-13

Kozarski M, Klaus A, Niksic M, Jakovljevic D, Helsper JP, Van Griensven LJ (2011) Antioxidative and immunomodulating activities of polysaccharide extracts of the medicinal mushrooms *Agaricus bisporus*, *Agaricus brasiliensis*, *Ganoderma lucidum* and *Phellinus linteus*. Food Chem 129: 1667-1675

Krijgsheld P, Alterlaar AFM, Post H, Ringrose JH, Müller WH, Heck AJR, Wösten HAB (2012) Spatially resolving the secretome within the mycelium of the cell factory *Aspergillus niger*. J Proteome Res 11: 2807-2818

Krijgsheld P, Bleichrodt R, van Veluw GJ, Wang F, Müller WH, Dijksterhuis J, Wösten HAB (2013) Development in *Aspergillus*. Stud Mycol 74: 1-29

Kurtzman Jr RH (1997) Nutrition from mushrooms, understanding and reconciling available data. Mycoscience 38: 247-253

Lakowicz JR (2006) Principles of fluorescence spectroscopy. Springer Science & Business Media LLC, New York, USA

Lakowicz JR, Szmacinski H, Nowaczyk K, Johnson ML (1992) Fluorescence lifetime imaging of free and protein-bound NADH. Proc Natl Acad Sc USA 89: 1271-1275

Levin AM, De Vries RP, Conesa A, De Bekker C, Talon M, Menke HH, van Peij NNME, Wösten HAB (2007) Spatial differentiation in the vegetative mycelium of *Aspergillus niger*. Eukaryotic cell 6: 2311-2322

Lin SJ, Tan HY, Kuo CJ, Wu RJ, Wang SH, Chen WL, Jee SH, Dong CY (2009) Multiphoton autofluorescence spectral analysis for fungus imaging and identification. Appl Phys Lett 95: 043703

Maeda H, Yamagata Y, Abe K, Hasegawa F, Machida M, Ishioka R, Gomi K, Nakajima T (2005) Purification and characterization of a biodegradable plastic-degrading enzyme from *Aspergillus oryzae*. Appl Microbiol Biotechnol 67: 778-788

Marose S, Lindemann C, Scheper T (2008) Two-Dimensional Fluorescence Spectroscopy: A New Tool for On-Line Bioprocess Monitoring. Biotechnol Prog 14: 63-74

Masai K, Maruyama J, Sakamoto K, Nakajima H, Akita O, Kitamoto K (2006) Square-plate culture method allows detection of differential gene expression and screening of

novel, region-specific genes in *Aspergillus oryzae*. Appl Microbiol Biotechnol 71: 881-891

Mattila P, Könkö K, Eurola M, Pihlava J, Astola J, Vahteristo L, Hietaniemi V, Kumpulainen J, Valtonen M, Piironen V (2001) Contents of vitamins, mineral elements, and some phenolic compounds in cultivated mushrooms. J Agric Food Chem 49: 2343-2348

Morin E, Kohler A, Baker AR, Foulongne-Oriol M, Lombard V, Nagye LG, Ohm RA, Patyshakuliyeva A, Brun A, Aerts AL, Bailey AM, Billette C, Coutinho PM, Deakin G, Doddapaneni H, Floudas D, Grimwood J, Hildén K, Kües U, Labutti KM, Lapidus A, Lindquist EA, Lucas SM, Murat C, Riley RW, Salamov AA, Schmutz J, Subramanian V, Wösten HAB, Xu J, Eastwood DC, Foster GD, Sonnenberg AS, Cullen D, de Vries RP, Lundell T, Hibbett DS, Henrissat B, Burton KS, Kerrigan RW, Challen MP, Grigoriev IV M, F. (2012) Genome sequence of the button mushroom *Agaricus bisporu*s reveals mechanisms governing adaptation to a humic-rich ecological niche. Proc Natl Acad Sc USA 109: 17501-17506

Moukha SM, Wösten HAB, Mylius EJ, Asther M, Wessels JGH (1993) Spatial and temporal accumulation of mRNAs encoding two common lignin peroxidases in *Phanerochaete chrysosporium*. J Bacteriol 175: 3672-3678

Nakashima N, Meech SR, Auty AR, Jones AC, Phillips D (1985) Fluorescence properties of ergosterol. Journal of photochemistry 30: 207-214

Neher RA, Mitkovski M, Kirchhoff F, Neher E, Theis FJ, Zeug A (2009) Blind source separation techniques for the decomposition of multiply labeled fluorescence images. Biophys J 96: 3791-3800

Newell S (2001) Fungal biomass and productivity. Methods in microbiology 30: 357-372

Noble R, Fermor TR, Lincoln S, Dobrovin-Pennington A, Evered C, Mead A, Li R (2003) Primordia initiation of mushroom (*Agaricus bisporus*) strains on axenic casing materials. Mycologia 95: 620-629

Nosanchuk JD, Casadevall A (2003) The contribution of melanin to microbial pathogenesis. Cell Microbiol 5: 203-223

Palero JA, Bader AN, de Bruijn HS, van den Heuvel A, Sterenborg HJCM, Gerritsen HC (2011) In vivo monitoring of protein-bound and free NADH during ischemia by nonlinear spectral imaging microscopy. Biomed Opt Express 2: 1030-1039

Palero JA, de Bruijn HS, Sterenborg HJCM, van Weelden H, Gerritsen HC (2008) In vivo nonlinear spectral imaging microscopy of visible and ultraviolet irradiated hairless mouse skin tissues. Photochem Photobiol Sci 7: 1422-1425

Palero JA, de Bruijn HS, van der Ploeg van den Heuvel A, Sterenborg HJCM, Gerritsen HC (2007) Spectrally resolved multiphoton imaging of in vivo and excised mouse skin tissues. Biophys J 93: 992-1007

Papagianni M (2007) Advances in citric acid fermentation by *Aspergillus niger*: Biochemical aspects, membrane transport and modeling. Biotechnol Adv 25: 244-263

Pawar N, Patil V, Kamble S, Dixit G (2008) First report of *Aspergillus niger* as a plant pathogen on *Zingiber officinal*e from India. Plant Dis 92: 1368-1368

Pel HJ, De Winde JH, Archer DB, Dyer PS, Hofmann G, Schaap PJ, Turner G, de Vries RP, Albang R, Albermann K (2007) Genome sequencing and analysis of the versatile cell factory *Aspergillus niger* CBS 513.88. Nat Biotechnol 25: 221-231

Pitt J (1994) The current role of *Aspergillus* and *Penicillium* in human and animal health. J Med Vet Mycol 32: 17-32

Pitt JI, Hocking AD, Diane A (2009) Fungi and food spoilage. Springer

Rodrigues RM, Macko P, Palosaari T, Whelan MP (2011) Autofluorescence microscopy: a non-destructive tool to monitor mitochondrial toxicity. Toxicol Lett 206: 281-288

Rosas ÁL, Nosanchuk JD, Gómez BL, Edens WA, Henson JM, Casadevall A (2000) Isolation and serological analyses of fungal melanins. J Immunol Methods 244: 69-80

Roshchina VV (2003) Autofluorescence of plant secreting cells as a biosensor and bioindicator reaction. J Fluoresc 13: 403-420

Samson R, Varga J (2009) What is a species in *Aspergillus*? Medical Mycology 47: S13-S20

Schrantz J, Lemoine Y (1995) Carotenoid composition of mycelium and apothecia in the discomycete Scutellinia umbrarum. Phytochemistry 40: 33-35

Shapiro BE, Gealt MA (1982) Ergosterol and lanosterol from Aspergillus nidulans. J Gen Microbiol 128: 1053-1056

Skala MC, Riching KM, Gendron-Fitzpatrick A, Eickhoff J, Eliceiri KW, White JG, Ramanujam N (2007) In vivo multiphoton microscopy of NADH and FAD redox states, fluorescence lifetimes, and cellular morphology in precancerous epithelia. Proc Natl Acad Sc USA 104: 19494-19499

Smith ML, Bruhn JN, Anderson JB (1992) The fungus *Armillaria bulbosa* is among the largest and oldest living organisms. Nature 356: 428-431

Soler-Rivas C, Arpin N, Olivier JM, Wichers HJ (2000) Discoloration and tyrosinase activity in *Agaricus bisporus* fruit bodies infected with various pathogens. Mycol Res 104: 351-356

Stringari C, Sierra R, Donovan PJ, Gratton E (2012) Label-free separation of human embryonic stem cells and their differentiating progenies by phasor fluorescence lifetime microscopy. J Biomed Opt 17: 046012-1-046012-11

Strobel I, Breitenbach J, Scheckhuber CQ, Osiewacz HD, Sandmann G (2009) Carotenoids and carotenogenic genes in Podospora anserina: engineering of the carotenoid composition extends the life span of the mycelium. Curr Genet 55: 175-184

Teertstra WR, Lugones LG, Wösten HAB (2004) In situ hybridisation in filamentous fungi using peptide nucleic acid probes. Fungal Genet Biol 41: 1099-1103

Teuchner K, Ehlert J, Freyer W, Leupold D, Altmeyer P, Stücker M, Hoffmann K (2000) Fluorescence studies of melanin by stepwise two-photon femtosecond laser excitation. J Fluoresc 10: 275-275

Theer P, Denk W (2006) On the fundamental imaging-depth limit in two-photon microscopy. J Opt Soc Am A Opt Image Sci Vis 23: 3139-3149

Toomre D, Bewersdorf J (2010) A new wave of cellular imaging. Annu Rev Cell Dev Biol 26: 285-314

Tyagi A, Penzkofer A (2010) pH dependence of the absorption and emission behaviour of lumiflavin in aqueous solution. J Photochem Photobiol A Chem 215: 108-117

Umar MH, van Griensven LJLD (1997) Morphological studies on the life span, developmental stages, senescence and death of fruit bodies of *Agaricus bisporus*. Mycol Res 101: 1409-1422

van den Brink J, de Vries RP (2011) Fungal enzyme sets for plant polysaccharide degradation. Appl Microbiol Biotechnol 91: 1477-1492

van Veluw GJ, Teertstra WR, de Bekker C, Vinck A, van Beek N, Muller WH, Arentshorst M, van der Mei HC, Ram AFJ, Dijksterhuis J, Wösten HAB (2012) Heteroge-

neity in liquid shaken cultures of *Aspergillus niger* inoculated with melanised conidia or conidia of pigmentation mutants. Stud Mycol 74: 47-57

Verveer PJ, Hanley QS (2009) Frequency domain FLIM theory, Instrumentation and data analysis. In: Gadella TWJ (ed) FRET and FLIM Techniques. Elsevier, Amsterdam, pp 59-94

Vinck A, de Bekker C, Ossin A, Ohm RA, de Vries RP, Wösten HAB (2011) Heterogenic expression of genes encoding secreted proteins at the periphery of *Aspergillus niger* colonies. Environ Microbiol 13: 216-225

Vinck A, Terlou M, Pestman WR, Martens EP, Ram AF, Van Den Hondel CA, Wösten HAB (2005) Hyphal differentiation in the exploring mycelium of *Aspergillus niger*. Mol Microbiol 58: 693-699

Vishwasrao HD, Heikal AA, Kasischke KA, Webb WW (2005) Conformational dependence of intracellular NADH on metabolic state revealed by associated fluorescence anisotropy. J Biol Chem 280: 25119-25126

Vivas MG, Silva DL, Boni L, Zalesny R, Bartkowiak W, Mendonca CR (2011) Two-photon absorption spectra of carotenoids compounds. J Appl Phys 109: 103529-103529-8

Wani BA, Bodha R, Wani A (2010) Nutritional and medicinal importance of mushrooms. J Med Plant Res 4: 2598-2604

Wiedenmann J, Oswald F, Nienhaus GU (2009) Fluorescent proteins for live cell imaging: opportunities, limitations, and challenges. IUBMB Life 61: 1029-1042

Will OH, Newland NA, Reppe CR (1984) Photosensitivity of pigmented and nonpigmented strains ofUstilago violacea. Curr Microbiol 10: 295-301

Wösten HAB, Moukha SM, Sietsma JH, Wessels JGH (1991) Localization of growth and secretion of proteins in *Aspergillus niger*. J Gen Microbiol 137: 2017-2023

Wösten H, Wessels J (2006) The emergence of fruiting bodies in basidiomycetes, Growth, differentiation and sexuality. In: Kües U and Fischer R (eds) The Mycota. Springer, Heidelberg, pp 393-414

Xiao Y, Kreber B, Breuil C (1999) Localisation of fungal hyphae in wood using immunofluorescence labelling and confocal laser scanning microscopy. Int Biodeterior Biodegradation 44: 185-190

Yin D (1996) Biochemical basis of lipofuscin, ceroid, and age pigment-like fluorophores. Free Radic Biol Med 21: 871-888

Zipfel WR, Williams RM, Webb WW (2003) Nonlinear magic: multiphoton microscopy in the biosciences. Nat Biotechnol 21: 1369-1377

CHAPTER 2

Nonlinear microscopy for spectrally resolved anisotropy imaging of fungi

Helene Knaus, Gerhard A. Blab, Alexandra V. Agronskaia, Dave J. van den Heuvel, Han A. B. Wösten, Hans C. Gerritsen

ABSTRACT

Optical microscopy capturing spectrum, polarization, and lifetime of emitted fluorescence enables biochemical mapping of biological samples. Here it is shown that the combination of a commercial multiphoton laser-scanning microscope and a home-build spectrograph ensures user-friendly operation. The system was calibrated and optimized for label-free – i.e. utilizing inherently fluorescent metabolic components of the cell – characterization of fungi in vivo, providing a detection range of 440 nm to 620 nm. Simultaneous anisotropy imaging was implemented to obtain complementary information about the biochemical properties of the specimen. The design offers a new tool to study fundamental and applied aspects of growth and development of organisms such as fungi.

INTRODUCTION

Fungi are consumed (e.g. Quorn®, mushrooms), are used for food production (e.g. cheese, bread, tofu), and are important cell factories for the industrial-scale production of enzymes and primary and secondary metabolites such as antibiotics. On the other hand, fungi are a main cause of spoilage of food and buildings, and pathogens of agricultural crops, animals and humans. Consequently, it is important to monitor presence of fungi and their metabolic state and to understand fungal growth and development. Studying intact fungi in their natural environment is challenging as most tools rely on the introduction of markers, sectioning of samples or the use of cell extracts (Harris et al. 2006, Moss et al. 2008, Kuhn et al. 2003, Hua et al. 2011, Butler et al. 2005, Eisenman et al. 2005). Nonlinear imaging provides a non-invasive and non-destructive technique to study fungi in their natural environment.

Visualizing the distribution and local biochemical properties of biomolecules in space and time is crucial to understand biological processes at a cellular level. Fluorescence microscopy is an important tool to study these processes (Hickey et al. 2004, Kentner and Sourjik 2010, Zipfel et al. 2003). It allows spatial and temporal localization of biomolecules and is minimally invasive when endogenous fluorophores are used as markers for cellular processes. For instance, NAD(P)H and FAD can be used for metabolic monitoring (Stringari et al. 2012, Vishwasrao et al. 2005, Palero et al. 2011). Most of these biomarkers are excited in the UV-range, which usually causes phototoxicy in biological specimens inside the focal volume and along the axis of illumination. Non-linear excitation greatly reduces the incidence of phototoxicity. In the case of nonlinear excitation, mostly applied as two-photon (2p) excitation, fluorescence is excited by simultaneous absorption of two near infrared (NIR) photons. The probability of a 2p absorption process is proportional to the square of the excitation intensity. This nonlinear property causes absorption to be strongly confined to the focal volume. By using NIR excitation wavelengths, also the scattering inside the specimen is reduced, and thus optical sectioning of thick specimens is possible (Gu et al. 2000, Theer and Denk 2006, Gerritsen and De Grauw 1999, Denk et al. 1990).

For many applications it is crucial to link spatial and biochemical information within the specimen. Biochemical characterization can be achieved by simultaneously exploiting several properties (spectrum, polarization, lifetime) of the endogenous fluorescence. In this regard spectral imaging is a well-established technique allowing simultaneous quantitative analysis of different fluorophores based on their emission spectra. For instance, it is possible to biochemically characterize mammalian tissues (Palero et al. 2008, Bader et al. 2011) or to use abnormalities in the spectra for medical diagnostics (Levitt et al. 2011). Polarization of fluorescence (anisotropy) can be used to characterize the cellular environment of the fluorophore. Anisotropy measurements yield information about the rotational diffusion of the fluorescent molecule, which is indicative of cellular viscosity or the interaction of the fluorophore with, for instance, an enzyme (Vishwasrao et al. 2005, Kierdaszuk et al. 1996).

Here, a user-friendly nonlinear spectral imaging set up is described, that also can be used for spectrally resolved anisotropy in fungal hyphae and tissues. The system has been optimized for the emission wavelength range between 440 nm and 620 nm, where most endogenous fungal fluorophores emit (see Chapter 1, Table 1). In addition, data analysis of the spectrally resolved anisotropy microscope is discussed.

INSTRUMENT DESCRIPTION

A schematic diagram of the nonlinear microscope for spectrally resolved anisotropy imaging is shown in Figure 1. This setup is based on a commercial Nikon C1 confocal scan-head and a Nikon Eclipse Ti-U inverted microscope (Nikon Instruments Europe, Amsterdam, The Netherlands). It is equipped with a home-built detection unit (see below). All optical paths were shielded to ensure working safety.

The excitation source is a tunable Chameleon Ultra II mode-locked titanium-sapphire laser (Coherent Europe, Utrecht, The Netherlands). This laser generates 140 fs pulses at a repetition rate of 80 MHz, a typical output power of 3.7 W at 800 nm and can be tuned from 680 nm to 1080 nm. To avoid pulse-broadening and other artifacts, the fiber cou-

pling unit of the scanner was removed and the laser beam was coupled directly into the Nikon C1 scanner. Before entering the scanner, the laser beam is 2 times attenuated and expanded 4 fold using a 25 mm and a 100 mm focal length lens to yield a beam diameter of 5 mm. The beam passes a Glan-Laser polarizer (GL10-B, Thorlabs, Lubeck, Germany) and 2 steering mirrors are used to guide the laser beam to the scan head. A dual neutral density filter wheel (range of optical densities from 0.08 to 3.0 in 0.1 increments, Newport Corporation, Utrecht, The Netherlands) was placed directly before the scan head to control the power at the specimen. A half-wave plate (AHWP10M-980, Thorlabs) in the excitation path was used to rotate the laser polarization to align it with the parallel and perpendicular detection channels of the emission. A T680dcspxr multiphoton dichroic mirror (Chroma Technology, Olching, Germany) is used to separate the fluorescence emission light form the excitation light. All data described in this Thesis were acquired with an open pinhole, as a pinhole is not strictly necessary in the case of 2p excitation.

Emission is either guided by a flipping mirror to a fiber-coupled photo multiplier detector (PMT, C1 detector Unit, Nikon Europe) or to the home-built anisotropy resolved spectrograph. To suppress scattered laser light, two short-pass emission filters were used, one (FF01-720/SP-25 BrightLine®, Semrock) before the fiber coupling of the PMT and one (FF01-680/SP-25 BrightLine®, Semrock) before a periscope that directs the emission to the spectrograph by means of two high reflectance MaxMirrors (Semrock, Rochester, NY, USA).

The first optical element of the anisotropy resolved spectrograph is a Quartz Wollaston prism with a 0.5 degree divergence angle (MWQ25-05-HEAR 450-750 nm; Karl Lambrecht, Chicago, USA). This prism splits the emission in parallel and perpendicular polarized beams. Next, these two beams are dispersed by a 056-0120 BK7 Equilateral Prism (OptoSigma, Santa Ana, CA, USA). The usable spectral range runs from 440 nm to 620 nm and covers the emission bands of the endogenous fluorophores in mushrooms and mycelium. The dispersed spectra are focused by an achromatic doublet lens (026-0770, diameter 25 mm, focal length 119.8 mm, broadband anti-reflection coated 425-675 nm; OptoSigma) onto an IxonEM 860 electron multiplication CCD

camera (Andor, Belfast, UK). The thermoelectrically cooled, back-illuminated camera is equipped with a 128 x 128 pixel EMCCD chip, having a pixel size of 24 x 24 μm and a full frame rate of 513 fps. Small sections of the EMCCD chip can be read out with rates as high as 14025 fps.

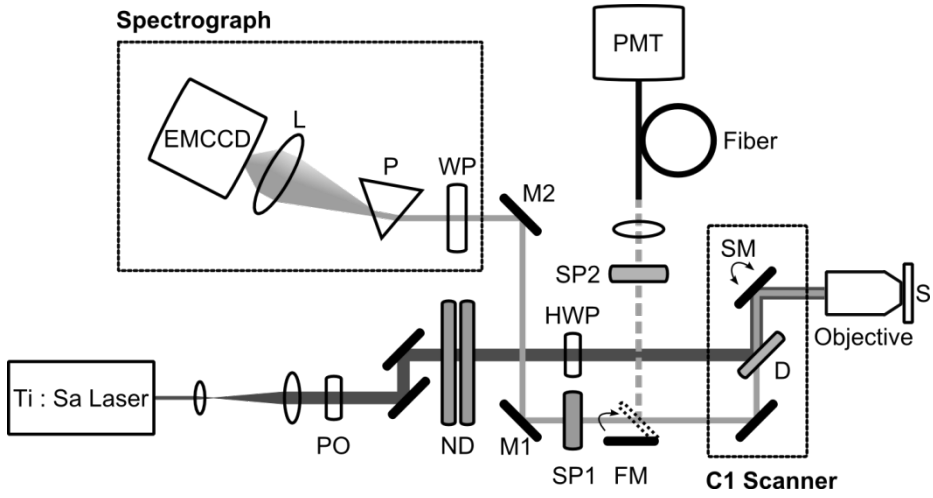

Figure 1. Schematic representation of the nonlinear microscope for spectrally resolved anisotropy imaging. The excitation beam passes the polarizer (PO), the neutral density filter wheels (ND) and the half-wave plate (HWP) towards the C1 scanner that scans the laser beam across the sample (S) using scanning mirrors (SM). The excitation light is separated from the emission by a dichroic mirror (D) and short pass filters (SP1, SP2). The emission can be guided by a flipping mirror (FM) towards a fiber-coupled PMT or via two mirrors (M1, M2) towards the spectrograph. Here, the emission is first split by a Wollaston prism (WP) in a parallel and perpendicular beam (with respect to the excitation). The two beams are dispersed by a prism (P) and focused by a lens (L) onto the EMCCD-camera.

INSTRUMENT CALIBRATION

Wavelength calibration and system responsivity

The raw data of the anisotropy resolved spectrograph consists of an array of intensities read from the pixels of the camera. In order to obtain true spectral information, a wavelength calibration is required. In addition, any wavelength-dependent response of the system needs to

be determined and to be corrected for. This is necessary to allow comparison with spectra recorded on other systems. Wavelength calibration and measurement of the wavelength-dependent system responsivity were carried out using a combination of different band-pass filters and three well characterized fluorophores (7-methoxycoumarin-4-acetic acid (MC), coumarin120 (C120) and lucifer yellow (LY)) covering the whole spectral range of interest. MC (Sigma-Aldrich Chemie, Zwijndrecht, The Netherlands) was solubilized in PBS buffer (pH 7.4), while C120 (Sigma-Aldrich Chemie) and LY (Life Technologies Europe, Bleiswijk, The Netherlands) were solubilized in methanol (Merck) and prior to spectral measurements diluted to a final concentration of 10 μM in phosphate buffered saline (PBS; pH 7.4). MC and C120 were excited at 720 nm, while a wavelength of 840 nm was used for LY.

For wavelength calibration, 2p emission spectra of all three dyes were recorded with and without the following optical filters: a 390/482/563/640 nm BrightLine filter (Semrock), 633 nm, 514 nm, and 442 nm RazorEdge filters (Semrock), a HQ 585/40m and a HQ 510/50m filter (Chroma Technology), and Ex 450-490 and BA 420 Nikon Fluorescence Filter Cube filters. The spectra were analyzed by taking the first derivative of the ratio of spectra measured with and without filter. These derivatives were then fitted with Gaussian functions and the maxima of these functions were used to determine the cutoff-points of the filters (in pixels) in the raw data. The transmission of the same filters was also measured with a commercial spectrometer (HP 8452a, Hewlett Packard Beun de Ronde, Abcoude, The Netherlands) and the cutoff points (in nanometers) determined in the same manner. The results are depicted as a scatter plot in Figure 2A (black squares). The final wavelength calibration was obtained by fitting these data points with a fourth order polynomial (Figure 2A, black curve), which is an appropriate approximation for prism based spectrograph systems (Bader et al. 2011). This approach allowed fast verification of the wavelength calibration at the beginning of each measurement by recording a 2p emission spectrum using at least one of the filters previously used for the calibration and confirming its cutoff pixel positions. Moreover, as 2p excited emission is used for the wavelength calibration, this approach is independent of shifts in the focal position, which

can occur when an external light source is used. The dispersion $\Delta\lambda$ per pixel (Figure 2A, grey curve), of the spectrograph was determined from the polynomial fit, using the coefficients, C_i, obtained in the wavelength calibration with k being the pixel index:

$$\Delta\lambda=\lambda_{k+1/2}-\lambda_{k-1/2} = C_4+C_2(1/4+3k^2)+k(C_1+2C_3+4C_1k^2).$$

To obtain the spectral responsivity (Figure 2B) a method similar to (Gardecki and Maroncelli 1998) was used: 2p emission spectra of freshly prepared C120 and LY solutions were recorded with the anisotropy resolved spectral imaging microscope and compared to their one-photon (1p) emission standard (Edinburgh Instruments FLS 920 Spectrometer, Livingston, UK). The 1p emission spectrum had been used as a reference, as the 1p and 2p emission spectra do not change for these dyes (Bestvater et al. 2002, Lakowicz et al. 1997, Xu and Webb 1996). Before calculating the instrument responsivity, 2p spectra were first dispersion corrected and then normalized. First, spectral responsivity was calculated for both fluorophores independently by dividing the 2p emission spectra by their corresponding 1p reference-spectra. Next, to cover the whole spectral range, these two individual system responsivities were linked at the intersection of the spectra (494 nm and 30 % of the total fluorescence intensity) by scaling the LY spectrum. The derived curve was used as the system responsivity in the given spectral range.

As the optics affects the spectral responsivity, the responsivity was measured for both objectives (Nikon Instruments Europe) used during this study. The wavelength-dependent instrument response for the CFI S Fluor 20x/0.75 NA air objective (black curve) and the CFI Apo LWD 25x/1.1 NA water immersion objective (grey curve) between 440 nm and 620 nm is presented in Figure 2B. Small differences between the objectives are visible, but overall the shapes of the responsivities are similar.

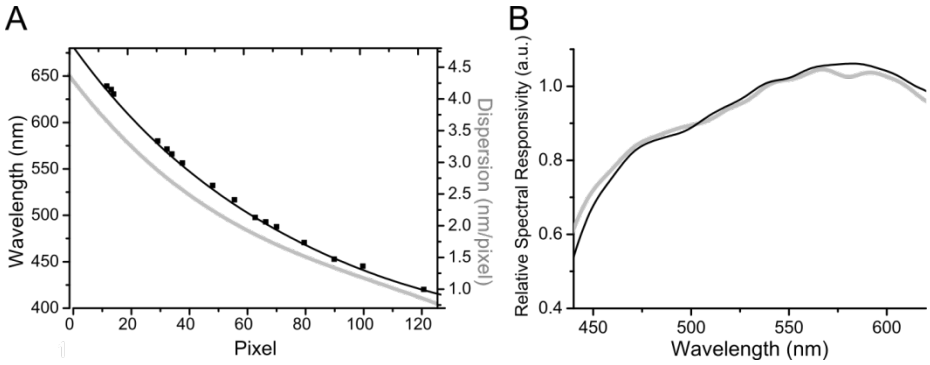

Figure 2. Calibration of the spectrally resolved anisotropy microscope. (A) The wavelength scale was calibrated using the edges of band-pass filters (black squares) and fitting with a forth order polynomial (black curve). The grey curve represents the dispersion of the spectrograph. (B) The wavelength dependent responsivity of the instrument, excluding dispersion, using the CFI S Fluor 20x/0.75 NA air objective (black curve) and the CFI Apo LWD 25x/1.1 NA water immersion objective (grey curve).

Anisotropy calibration

Similar to the calibration of the wavelength-dependent instrument responsivity, a calibration of the polarization response is necessary. Yet, there is no generally accepted method to test the accuracy of fluorescence polarization measurements (Ameloot et al. 2013). However, the calibration is usually described in terms of the G-factor, the ratio of the sensitivity of the parallel and perpendicular detection channels. A simple way to determine the G-factor consists of measuring an aqueous dye solution with a known anisotropy value. In this case, fast rotation of fluorophores (rotational diffusion time << fluorescence lifetime) results in completely depolarized emission, or an anisotropy value of zero. To calculate the G-factor (G) and anisotropy (r) the following equation was used (Lakowicz 2006): $r = (I_{\parallel} - GI_{\perp})\times(I_{\parallel} + 2GI_{\perp})^{-1}$, where $I_{\parallel}$ and $I_{\perp}$ are the parallel and perpendicular intensities. Thus, the G-factor can be calculated as $G = I_{\parallel}\times (I_{\perp})^{-1}$, in the aforementioned case when anisotropy equals zero. The G-factor was calculated using 5 μM fluorescein in water, which is supposed to provide an anisotropy value of zero (Bader et al. 2007). The G-factor proved to be wavelength independent and was averaged at 0.94. Spectrally resolved anisotropies of fluorescein in water (grey curve) and GFP in glycerol (black

curve), both using 0.94 as the G-factor, are presented in Figure 3. The latter was used to test the G-factor for the high anisotropy case. Glycerol reduces rotational diffusion (> fluorescence lifetime), resulting in an expected anisotropy value of 0.51 in case of 2p excitation (Volkmer et al. 2000, Bader et al. 2009). As shown in Figure 3, anisotropy of GFP in glycerol was wavelength independent, but amounted only 0.46. This lower anisotropy is not caused by a misalignment of excitation polarization and the orientation of the detection channels. This was confirmed by repeating the calibration after introducing a half-wave plate into the excitation path (Figure 1) in order to maximize GFP anisotropy. As this did not improve the results, it is most likely that the lower value of GFP anisotropy is the result of the fact that use of a high numerical aperture objective can lower the apparent anisotropy (Axelrod 1979).

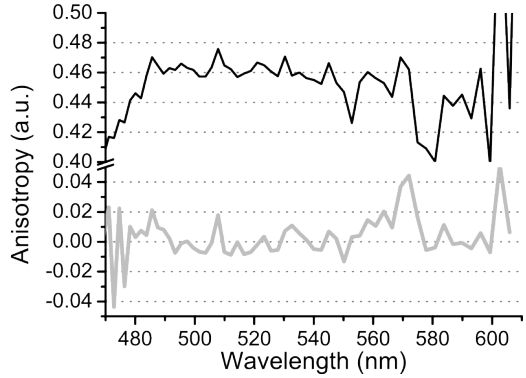

Figure 3. Wavelength dependence of anisotropy measurements. An aqueous 5 μM fluorescein solution, known to provide an anisotropy value of zero (grey curve), yielded a G-factor of 0.94. Using this value, anisotropy of 3.7 μM GFP in 50 : 50 v / v glycerol / PBS, pH 7.4 was calculated to be 0.46 (black curve). For measurements a 20x air objective with a numerical aperture of 0.75 was used.

DATA ACQUISITION

Nonlinear spectral imaging microscopy is a scanning technique. The image is built up by raster scanning the laser focus over the sample and recording the fluorescence emission spectrum at each position. For proper operation, the scanner and the spectrograph need to be

synchronized by using the same master clock for acquisition and scanning. This is realized by employing the external trigger mode of the camera and supplying it with the pixel clock from the scanner. However, the pixel clock of the Nikon C1 scanner is continuously running, also during the retrace of the scanners, once a scan has been started. Therefore, a custom built electronics board (workshop Utrecht University, The Netherlands) capable of combining the pixel and the line clock (signal that indicates the usable part of a scan line) was used.

The microscope scanner (equipped with a Nikon slow scan board) was operated using EZ-C1 software (Confocal Gold Version 3.90T1; C1 Firmware Version 4.10, Nikon), while the camera was running on Andor Solis X-4493 software (Version 4.21.30007.0, Andor). Camera acquisition was run in Kinetic mode, External triggering, Multi-Track read out and Frame Transfer mode. The Electron Multiplier Gain was set at 200.

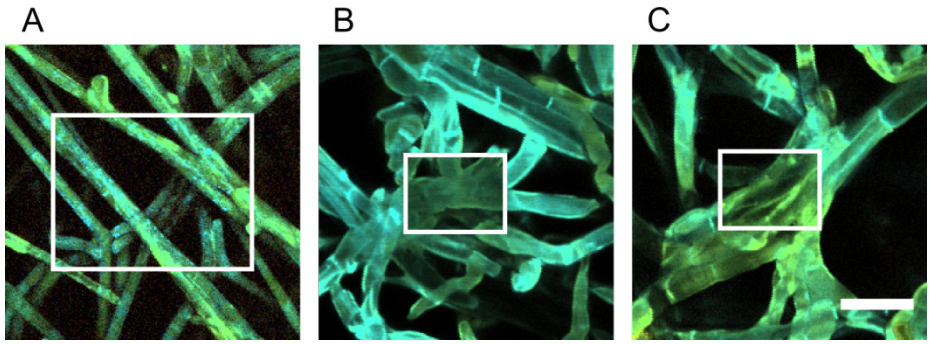

Figure 4. RGB real color representation of nonlinear spectral images of the cap of a freshly harvested *A. bisporus* mushroom. Prior to acquisition of the images shown above, a zoomed-in region was imaged, depicted by the rectangles. Because of bleaching, the zoomed-in regions of B and C show decreased intensity. All images (256 x 256 pixels) were recorded using a CFI Apo LWD 25x/1.1 NA water immersion objective and an exposure time of 400 μs per pixel. The bar represents 25 μm. (A) Excitation power of 9 mW, rectangular box measures 50 x 50 μm. (B) and (C) Excitation power of 17 mW, rectangular box measures 25 x 25 μm.

To obtain spectral images, the fluorescence emission was projected onto a well-defined region of the 128 x 128 pixel EMCCD chip. For each image-pixel of the nonlinear spectral image, three regions (defined as

tracks in the Multi-Track mode) of the EMCCD chip were read out: A region for parallel and perpendicular polarized fluorescence, respectively, and one non-illuminated region for background subtraction. Each region consisted of 7 lines (perpendicular to the dispersion direction, from now on referred to as the vertical direction) of 128 pixels (in the dispersion direction, from now on referred to as the horizontal direction). The regions were first hardware binned in the vertical direction and then read out. The Vertical Pixel Shift Speed was set at 0.0875 μs and the Vertical Clock Voltage was set at 2 V. The read out parameters in the horizontal direction were set as follows: Readout Rate at 10 MHz at 14-bit and Pre-Amplifier Gain at 4.5 x.

Nonlinear spectral images (256 x 256 pixels) were acquired with an exposure time of 400 μs per pixel and a power ranging from 1 to 27 mW at the specimen. For imaging, a CFI S Fluor 20x air objective (NA 0.75, Nikon Instruments Europe) and a CFI Apo LWD 25x water immersion objective (NA 1.1, Nikon Instruments Europe) were used. Emission spectra were recorded for excitation wavelengths ranging from 720 nm to 940 nm. It should be noted that it is crucial to adjust the imaging parameters in such a way that bleaching of the endogenous fluorophores is avoided. Figure 4 shows an example of nonlinear spectral images of a freshly harvested *A. bisporus* mushroom cap imaged under different conditions. Here, for visualization purposes the spectral images are represented in real color, meaning that the spectral information of each pixel was transformed into RGB values that resemble the color of the fluorescence emission as it would be perceived by the human eye (Palero et al. 2006). Prior to acquisition of the images in Figure 4, a zoomed-in region was imaged, depicted by the rectangles. In Figure 4A an excitation power of 9 mW was used to first image a 50 x 50 μm and then a 100 x100 μm region of the mushroom cap. As there was no decrease in intensity, there had been no bleaching. In Figure 4B and C, an image of 25 x 25 μm, followed by a 100 x 100 μm image, was recorded at an excitation power of 17 mW. In these cases a clear drop in intensity was found in the area that had been scanned twice. Especially endogenous fluorophores emitting in the blue spectral range bleached fast, when compared to those emitting in the green spectral range. To summarize, this experiment illustrates that at a constant exposure time there are two major parameters that impact

bleaching, the field of view and the excitation power, both of which can be adjusted.

DATA ANALYSIS AND APPLICATIONS

Spectral phasor analysis introduced by (Fereidouni et al. 2012) has been used throughout this Thesis to analyze spectral data. The phasor approach is based on a Fourier transform of the spectra, where the amplitude and phase of the first harmonic of the Fourier transform of a normalized emission spectrum are used as coordinates in a phasor plot. Effectively, the position in the phasor plot is determined by the emission maximum and the spectral width (Figure 5). Depending on the emission maximum, this position is moving along the semicircle from the top, representing blue emission, in a counterclockwise direction to green and finally red emission. Increasing the spectral width results in moving of the phasor point closer to the center. A constant background signal is mapped to the center of the plot (Figure 5).

As an example, an experimental data set of 2 mg×ml^{-1} FAD (Sigma-Aldrich Chemie) in H_2O and 2.3 mM NADH (Sigma-Aldrich Chemie) in 100 mM 3-(N-morpholino)propanesulfonic acid (MOPS) (Sigma-Aldrich Chemie) buffer (pH 7.4) is discussed. Figure 5 shows the phasor plot of separately measured spectral images of pure FAD and NADH mapped in the same phasor plot. In addition, the average spectra of these fluorophores are shown (emission peak of NADH at 460 nm and FAD at 530 nm). It should be noted that the NADH spectrum was also used as a reference for NADPH, as both are spectrally indistinguishable (Huang et al. 2002). Emission spectra of pure FAD and NADH showed little variation; therefore they show up as a small cloud of points in the spectral phasor plot. Noise free constant spectra of pure components show up as single points in the plot. These data are employed as reference measurements of pure NADH and FAD throughout this Thesis.

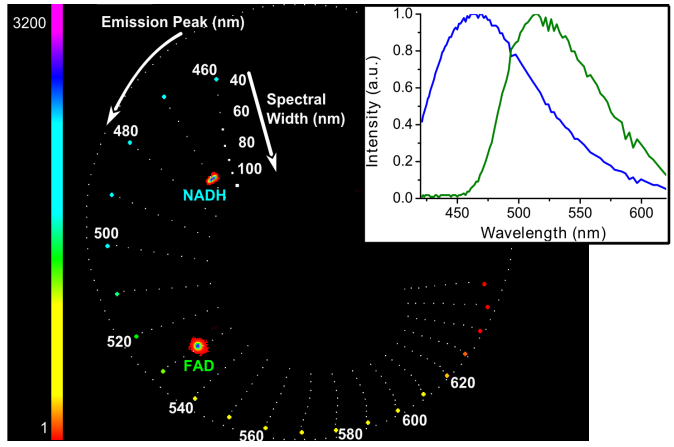

Figure 5. The spectral phasor plot is a polar representation of spectral data, where each emission spectrum is represented as a single point and its position is determined by the emission maximum and the spectral width. The spectral phasor plot of solubilized NADH and FAD is shown with their corresponding fluorescence emission spectra (blue curve for NADH, green curve for FAD). Color bar represents counts (number of pixels with a certain phasor value).

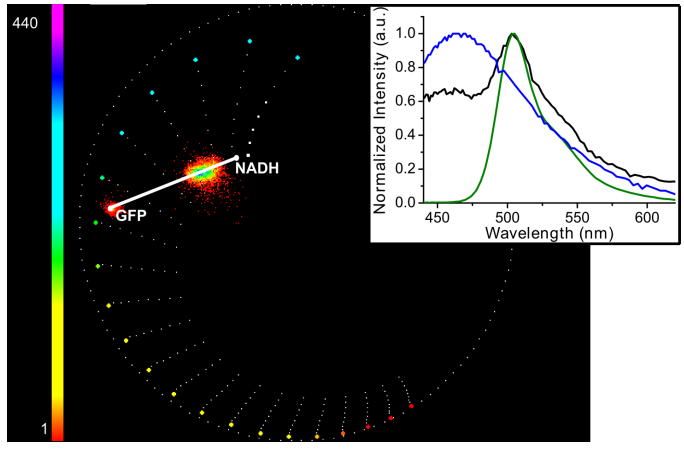

Figure 6. Spectral phasor plot of mycelium of an *A. niger* strain expressing GFP in mitochondria and their corresponding emission spectra (black curve excitation at 740 nm, green curve excitation at 925 nm). The spectrum of pure NADH (blue curve) is marked as a white dot in the phasor plot. In the phasor plot the scatter cloud of GFP-expressing strain (excited at 740 nm), is lying on the line connecting the phasors of pure NADH and pure GFP. Color bar represents counts (number of pixels with a certain phasor value).

An *Aspergillus niger* strain (derivative of AB4.1) (van Hartingsveldt et al. 1987) expressing a reporter construct of mitochondrial targeted GFP was used to demonstrate spectral unmixing applying the phasor approach. Its mitochondria contain NAD(P)H and GFP as two major fluorescent compounds. Data were acquired at a laser wavelength of 740 nm (preferential NAD(P)H excitation) and 925 nm (preferential GFP excitation), were background subtracted, and superimposed in one spectral phasor plot (Figure 6). The average spectrum obtained at 740 nm excitation (black curve) showed a combination of peaks at 460 nm (NADH) and 505 nm (GFP). Spectra of pure NADH (excitation 740 nm) and pure GFP (excitation at 925 nm) are shown in the Figure as blue and green curves respectively. The phasor plot of the GFP-expressing *A. niger* strain excited at 740 nm falls on a line connecting pure NADH (white point in phasor plot, from reference measurement in Figure 5) and pure GFP (GFP-expressing strain excited at 925 nm). This demonstrates the linear behavior of phasors, which is important for spectral decomposition. The phasor of a mixture of two different fluorophores falls on the line connecting the pure components, and the distances between this phasor position of the mixture and those of the pure components represent the relative contribution of the individual components in the mixture. Applied to the GFP-expressing strain excited at 740 nm (Figure 6) this results in relative contributions of 75 % for NADH and 25 % for GFP.

DISCUSSION

Spectral measurements of endogenous fluorophores revealed that spectral changes can be utilized to identify fungal spores exposed to UV-B irradiation (Arcangeli et al. 2000). Later, it was shown that endogenous spectra in combination with simple RGB-unmixing, achieved by using optical filters, can be used to distinguish between different fungal species encountered in the clinic (Lin et al. 2009). Motivated by these results, the spectrally resolved microscope described in this Chapter has been adapted for advanced imaging of mycelium and reproductive structures of fungi. The spectral range of the setup had to be compatible with the endogenous fluorophores present in fungi. These fluorophores have their emission maximum between 440

and 620 nm (Knaus et al. 2013). Optical components assuring a high spectral resolution and sensitivity were chosen inspired by previous setups (Palero et al. 2006, Esposito et al. 2011, Frederix et al. 2001) and calibration protocols were established, enabling comparison with measurements recorded by other systems. The experiments presented in this Chapter demonstrate that the microscope reliably acquires spectrally resolved images of fungi. How well spectral imaging can be used to characterize fungi and mushrooms is shown by a variety of applications discussed in Chapters 3 and 4.

The combination of multi-photon microscopy and spectroscopy in one system is not entirely new. However, so far mainly laboratory solutions, like customer built setups on optical tables, exist. These require advanced skills in optics, though being flexible as optical components can be exchanged to optimize the system for specific applications. Within the spectrally resolved anisotropy microscope both is combined. The commercial confocal laser-scanning microscope ensures user-friendly operation, while the home-build spectrograph provides flexibility of the detection by allowing adjusting the optics according to the applications. Another advantage is the presence of a binocular and the possibility for bright-field and 1p fluorescence imaging. This gives the opportunity to make an overlay of the spectral image with the bright-field image. It also ensures easy navigation through the sample towards the region of interest. The design of the microscope allows guiding of the emission to the anisotropy resolved spectrograph or to any other fiber coupled detector, e.g. a PMT or a fluorescence lifetime imaging module. This gives access to complementary information found in spectrum, polarization, and lifetime.

Living biological specimens contain multiple endogenous fluorophores that contribute to the measured fluorescence emission. Identification of the individual fluorophores is important for biological applications, e.g. metabolic monitoring. To this end, various decomposition techniques, such as linear unmixing (Garini et al. 2006), blind source separation or non-negative matrix factorization (Neher et al. 2009), and phasor analysis (Verveer and Hanley 2009, Fereidouni et al. 2012) can be applied. In this chapter, spectra were decomposed using the spectral phasor approach. Decomposition was done using two components

but it can be done with up to three components. In the latter case the phasor of the mixture falls inside a triangle spanned between the vertices determined by the positions of the three individual phasor positions (pure components). The spectral phasor approach offers several advantages over other techniques for spectral decomposition. It is a graphical method based on a single point representation of complex spectral data. It allows for unmixing without fitting and is therefore very fast. Potentially, it allows for (semi) blind unmixing of the spectra. Importantly, regions in the phasor plot can be mapped back onto the spatial image, thus yielding information about the spatial distribution of a specific component, or highlighting regions with similar chemical composition. However, in case of mixtures with more than three components unmixing is, at the present, not possible. Spectral unmixing can be difficult when emission spectra exhibit large overlap (e.g. free and protein bound NADH). Fluorescence anisotropy imaging complements spectral analysis. In particular it can provide information about viscosity or changes in rotational mobility related to free to bound conformations. The first steps towards simultaneous spectral and anisotropy imaging were made in this Chapter by carrying out calibration measurements and first attempts to separate different fluorophores by their anisotropy. In the next step the representation of multi-dimensional data sets will be explored. Moreover, the applicability for single hyphae measurements has to be tested, as anisotropy is very sensitive to noise.

REFERENCES

Ameloot M, van de Ven M, Acuña AU, Valeur B (2013) Fluorescence anisotropy measurements in solution: Methods and reference materials (IUPAC Technical Report). Pure Appl Chem 85: 589-608

Arcangeli C, Yu W, Cannistraro S, Gratton E (2000) Two-photon autofluorescence microscopy and spectroscopy of Antarctic fungus: New approach for studying effects of UV-B irradiation. Biopolymers 57: 218-225

Axelrod D (1979) Carbocyanine dye orientation in red cell membrane studied by microscopic fluorescence polarization. Biophys J 26: 557-573

Bader AN, Hofman EG, van Bergen en Henegouwen, P.M.P., Gerritsen HC (2007) Imaging of protein cluster sizes by means of confocal time-gated fluorescence anisotropy microscopy. Opt Express 15: 6934-6945

Bader AN, Pena AM, Johan van Voskuilen C, Palero JA, Leroy F, Colonna A, Gerritsen HC (2011) Fast nonlinear spectral microscopy of in vivo human skin. Biomed Opt Express 2: 365-373

Bader AN, Hofman EG, Voortman J, Van Bergen En Henegouwen, Paul MP, Gerritsen HC (2009) Homo-FRET imaging enables quantification of protein cluster sizes with subcellular resolution. Biophys J 97: 2613-2622

Bestvater F, Spiess E, Stobrawa G, Hacker M, Feurer T, Porwol T, Berchner-Pfannschmidt U, Wotzlaw C, Acker H (2002) Two-photon fluorescence absorption and emission spectra of dyes relevant for cell imaging. J Microsc 208: 108-115

Butler M, Gardiner R, Day A (2005) Fungal melanin detection by the use of copper sulfide-silver. Mycologia 97: 312-319

Denk W, Strickler JH, Webb WW (1990) Two-photon laser scanning fluorescence microscopy. Science 248: 73-76

Eisenman HC, Nosanchuk JD, Webber JBW, Emerson RJ, Camesano TA, Casadevall A (2005) Microstructure of cell wall-associated melanin in the human pathogenic fungus *Cryptococcus neoformans*. Biochemistry 44: 3683-3693

Esposito A, Bader AN, Schlachter SC, van den Heuvel DJ, Schierle GSK, Venkitaraman AR, Kaminski CF, Gerritsen HC (2011) Design and application of a confocal microscope for spectrally resolved anisotropy imaging. Opt Express 19: 2546-2555

Fereidouni F, Bader AN, Gerritsen HC (2012) Spectral phasor analysis allows rapid and reliable unmixing of fluorescence microscopy spectral images. Opt Express 20: 12729-12741

Frederix P, Asselbergs MAH, van Sark W, van den Heuvel, D J, Hamelink W, de Beer EL, Gerritsen HC (2001) High sensitivity spectrograph for use in fluorescence microscopy. Appl Spectrosc 55: 1005-1012

Gardecki J, Maroncelli M (1998) Set of secondary emission standards for calibration of the spectral responsivity in emission spectroscopy. Appl Spectrosc 52: 1179-1189

Garini Y, Young IT, McNamara G (2006) Spectral imaging: principles and applications. Cytometry A 69: 735-747

Gerritsen HC, De Grauw CJ (1999) Imaging of optically thick specimen using two-photon excitation microscopy. Microsc Res Tech 47: 206-209

Gu M, Gan X, Kisteman A, Xu MG (2000) Comparison of penetration depth between two-photon excitation and single-photon excitation in imaging through turbid tissue media. Appl Phys Lett 77: 1551-1553

Harris DM, Diderich JA, Van der Krogt ZA, Luttik MAH, Raamsdonk LM, Bovenberg RAL, Van Gulik WM, Van Dijken JP, Pronk JT (2006) Enzymic analysis of NADPH metabolism in β-lactam-producing *Penicillium chrysogenum*: presence of a mitochondrial NADPH dehydrogenase. Metab Eng 8: 91-101

Hickey PC, Swift SR, Roca MG, Read ND (2004) Live-cell imaging of filamentous fungi using vital fluorescent dyes and confocal microscopy, Microbial Imaging. In: Savidge T and Pothoulakis C (eds) Methods in Microbiology. Elsevier, pp 63-87

Hua SST, Brandl MT, Hernlem B, Eng JG, Sarreal SBL (2011) Fluorescent viability stains to probe the metabolic status of aflatoxigenic fungus in dual culture of *Aspergillus flavus* and *Pichia anomala*. Mycopathologia 171: 133-138

Huang S, Heikal AA, Webb WW (2002) Two-photon fluorescence spectroscopy and microscopy of NAD(P)H and flavoprotein. Biophys J 82: 2811-2825

Kentner D, Sourjik V (2010) Use of fluorescence microscopy to study intracellular signaling in bacteria. Annu Rev Microbiol 64: 373-390

Kierdaszuk B, Malak H, Gryczynski I, Callis P, Lakowicz JR (1996) Fluorescence of reduced nicotinamides using one-and two-photon excitation. Biophys Chem 62: 1-13

Kuhn D, Balkis M, Chandra J, Mukherjee P, Ghannoum M (2003) Uses and limitations of the XTT assay in studies of *Candida* growth and metabolism. J Clin Microbiol 41: 506-508

Lakowicz JR (2006) Principles of fluorescence spectroscopy. Springer Science & Business Media LLC, New York, USA

Lakowicz JR, Gryczynski I, Malak H, Schrader M, Engelhardt P, Kano H, Hell SW (1997) Time-resolved fluorescence spectroscopy and imaging of DNA labeled with DAPI and Hoechst 33342 using three-photon excitation. Biophys J 72: 567-578

Levitt JM, McLaughlin-Drubin ME, Münger K, Georgakoudi I (2011) Automated biochemical, morphological, and organizational assessment of precancerous changes from endogenous two-photon fluorescence images. PloS one 6: e24765

Lin SJ, Tan HY, Kuo CJ, Wu RJ, Wang SH, Chen WL, Jee SH, Dong CY (2009) Multiphoton autofluorescence spectral analysis for fungus imaging and identification. Appl Phys Lett 95: 043703

Moss BJ, Kim Y, Nandakumar M, Marten MR (2008) Quantifying metabolic activity of filamentous fungi using a colorimetric XTT assay. Biotechnol Prog 24: 780-783

Neher RA, Mitkovski M, Kirchhoff F, Neher E, Theis FJ, Zeug A (2009) Blind source separation techniques for the decomposition of multiply labeled fluorescence images. Biophys J 96: 3791-3800

Palero JA, Bader AN, de Bruijn HS, van den Heuvel A, Sterenborg HJCM, Gerritsen HC (2011) In vivo monitoring of protein-bound and free NADH during ischemia by nonlinear spectral imaging microscopy. Biomed Opt Express 2: 1030-1039

Palero JA, de Bruijn HS, Sterenborg HJCM, van Weelden H, Gerritsen HC (2008) In vivo nonlinear spectral imaging microscopy of visible and ultraviolet irradiated hairless mouse skin tissues. Photochem Photobiol Sci 7: 1422-1425

Palero JA, de Bruijn HS, van der Ploeg-van den Heuvel A, Sterenborg HJCM, Gerritsen HC (2006) In vivo nonlinear spectral imaging in mouse skin. Opt Express 14: 4395-4402

Stringari C, Sierra R, Donovan PJ, Gratton E (2012) Label-free separation of human embryonic stem cells and their differentiating progenies by phasor fluorescence lifetime microscopy. J Biomed Opt 17: 046012-1-046012-11

Theer P, Denk W (2006) On the fundamental imaging-depth limit in two-photon microscopy. J Opt Soc Am A Opt Image Sci Vis 23: 3139-3149

van Hartingsveldt W, Mattern IE, van Zeijl CM, Pouwels PH, van den Hondel, Cees AMJJ (1987) Development of a homologous transformation system for *Aspergillus niger* based on the pyrG gene. Mol Gen Genet 206: 71-75

Verveer PJ, Hanley QS (2009) Frequency domain FLIM theory, Instrumentation and data analysis. In: Gadella TWJ (ed) FRET and FLIM Techniques. Elsevier, Amsterdam, pp 59-94

Vishwasrao HD, Heikal AA, Kasischke KA, Webb WW (2005) Conformational dependence of intracellular NADH on metabolic state revealed by associated fluorescence anisotropy. J Biol Chem 280: 25119-25126

Volkmer A, Subramaniam V, Birch DJ, Jovin TM (2000) One-and two-photon excited fluorescence lifetimes and anisotropy decays of green fluorescent proteins. Biophys J 78: 1589-1598

Xu C and Webb W W (1996) Measurement of two-photon excitation cross sections of molecular fluorophores with data from 690 to 1050 nm. JOSA B 13: 481

Zipfel WR, Williams RM, Webb WW (2003) Nonlinear magic: multiphoton microscopy in the biosciences. Nat Biotechnol 21: 1369-1377

CHAPTER 3

Monitoring the metabolic state of fungal hyphae and the presence of melanin by nonlinear spectral imaging

This chapter has been published as: Helene Knaus, Gerhard A. Blab, Alexandra V. Agronskaia, Dave J. van den Heuvel, Hans C. Gerritsen, Han A. B. Wösten. Applied and Environmental Microbiology 79: 6345-6350

ABSTRACT

Label-free nonlinear spectral imaging microscopy (NLSM) records two-photon excited fluorescence emission spectra of endogenous fluorophores within the specimen. Here, NLSM is introduced as a novel minimally-invasive method to analyze the metabolic state of fungal hyphae by monitoring the autofluorescence of NAD(P)H and FAD. Moreover, the presence of melanin was analyzed by NLSM. NAD(P)H, FAD and melanin were used as biomarkers for freshness of mushrooms of *Agaricus bisporus* (the white button mushroom) that had been stored at 4 °C for 0-17 days. During this period the mushrooms did not show changes in morphology or color as detectable by eye. In contrast, FAD / NAD(P)H and melanin / NAD(P)H ratios increased over time. For instance, these ratios increased from 0.92 to 2.02 and from 0.76 to 1.53, respectively, at the surface of mushroom caps that had been harvested by cutting the stem. These ratios were lower under the skin than at the surface of fresh mushrooms (0.78 vs 0.92 and 0.41 vs 0.76, respectively), indicative of higher metabolism and lower pigment formation within the fruiting body. Signals were not only different between tissues of the mushroom but also between neighboring hyphae. These data show that NLSM can be used to determine freshness of mushrooms and to follow postharvest browning at an early stage. Moreover, it demonstrates the potential of NLSM to address a broad range of fundamental and applied microbiological processes.

INTRODUCTION

Worldwide the annual production of edible mushrooms amounts to approximately 7.7 million tons. The white button mushroom *Agaricus bisporus* is one of the most important commercial species. It is low in fat and rich in fiber, vitamins, minerals, linoleic acid, and bioactive compounds such as anti-cancer polysaccharides (Mattila et al. 2001, Kozarski et al. 2011, Jeong et al. 2010). Moreover, the button mushroom contains more digestible proteins than most vegetables, and only slightly less than meat products and milk (Wani et al. 2010, Kurtzman Jr 1997). Mushrooms are a perishable product. Therefore, there is a need for tools to monitor freshness of fruiting bodies. These tools could also be applied in breeding programs and to improve storage conditions.

The metabolic state and melanin formation could be used as indicators for freshness of mushrooms. The presence of melanin can be detected by various microscopic techniques (Butler et al. 2005, Eisenman et al. 2005, Hegnauer et al. 1985). There are also several methods to quantify the metabolic activity of fungi. They are often based on fluorescence assays monitoring the activity of NADH-dependent dehydrogenases (Harris et al. 2006), or NADH-dependent oxidoreductases (Moss et al. 2008, Kuhn et al. 2003) or by viability stains that are metabolized in the presence of ATP and intracellular esterases (Hua et al. 2011). Most of these assays require cell extracts, tissue sectioning and incorporation of marker molecules into cells. Nonlinear spectral microscopy (NLSM) is a potent non-invasive (Gu et al. 2000, Theer and Denk 2006, Gerritsen and de Grauw 1999, Masters et al. 1998, Zipfel et al. 2003) alternative to monitor the metabolic state and the presence of melanin in fungi. NLSM maps (auto)fluorescence emission spectra within the specimen (Huang et al. 2002, Laiho et al. 2005, Palero et al. 2007). Phototoxicity of this technique is low because excitation is limited to the focal volume. The recorded emission spectrum of a specimen is a combination of the spectra of the individual fluorophores. NAD(P)H, FAD, and melanin are autofluorescent molecules that occur in fungi (Knaus et al. 2013). These compounds have maximum emission in the blue (460 nm), green (530 nm), and red (620 nm) wavelength range, respectively (Huang et al. 2002, Teuchner et al. 2000). Quantification of

the contribution of each fluorophore is possible by decomposition of the measured emission spectrum. Such unmixing methods mostly rely on reference spectra or pre-assumptions of the components (Garini et al. 2006, Neher et al. 2009), but recently "blind unmixing" – not requiring a priori knowledge of the autofluorescent components – has been introduced (Fereidouni et al. 2013).

We here show that NLSM can be used to monitor freshness of *Agaricus bisporus* mushrooms using NAD(P)H, FAD and melanin as biomarkers. These results illustrate that NLSM has potential use in fundamental and applied microbiological research, for instance in monitoring fungal activity in bioreactors.

MATERIALS AND METHODS

Growth and storage of *A. bisporus*.

Plastic containers (17.5 x 27.5 x 22.5 cm) were filled with 3.5 kg phase-III compost colonized with *A. bisporus* strain Sylvan A15 (CNC Grondstoffen, Milsbeek, The Netherlands) and topped with 1 kg of casing soil (CNC Grondstoffen). The cultures were incubated at 24 °C and 95 % relative humidity (RH) in Economic Premium Climate chambers (Snijders Scientific, Tilburg, The Netherlands). Water (200 ml) was added to each of the containers during the first 4 days of incubation. Growth was prolonged at 20 °C and 88 % RH when aggregates had formed on the casing layer (i.e. after 14 days of culturing). Mushroom caps with a diameter of about 5.5 cm were selected for NLSM. Mushrooms were harvested either by picking or by cutting the stem. They were stored in plastic bags at 4 °C.

Nonlinear spectral imaging.

A schematic diagram of the nonlinear spectral imaging setup is shown in Figure 1. An Eclipse Ti-U inverted microscope (Nikon Instruments Europe, Amsterdam, The Netherlands) was used with a CFI S Fluor 20x air objective (NA 0.75, Nikon Instruments Europe). The excitation source was a tunable Chameleon Ultra II mode-locked titanium-sapphire laser (Coherent Europe, Utrecht, The Netherlands). It was

coupled directly into a C1 confocal scan-head (Nikon Instruments Europe), in which the fiber coupling unit was removed. The emission was reflected by a T680dcspxr multiphoton dichroic mirror (Chroma Technology, Olching, Germany) within the scan-head. The emission was guided via a high reflectance MaxMirror (Semrock, Rochester, NY, USA) and a FF01-680/SP-25 BrightLine multiphoton short-pass emission filter (Semrock) through a periscope (containing two high reflectance MaxMirrors) to the spectrograph. The spectrograph consisted of a Quartz 0.5 degrees Wollaston prism (MWQ25-05-HEAR 450-750 nm; Karl Lambrecht, Chicago, USA), a 056-0120 BK7 Equilateral Prism (OptoSigma, Santa Ana, CA, USA), a 026-0770 achromatic doublet lens (diameter 25 mm, focal length 119.8 mm, broadband antireflection 425-675 nm; OptoSigma) and an IxonEM 860 electron multiplication CCD camera (Andor, Belfast, UK).

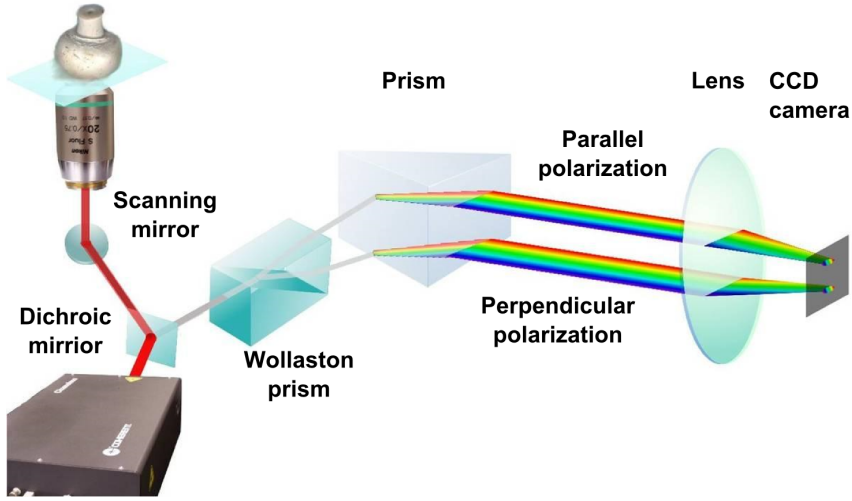

Figure 1. Schematic representation of the nonlinear spectral imaging setup.

The wavelength calibration of the spectrograph was carried out by measuring two-photon (2p) spectra of Lucifer Yellow (Life Technologies Europe, Bleiswijk, The Netherlands), 7-Methoxycoumarin-4-acetic acid (Sigma-Aldrich Chemie, Zwijndrecht, The Netherlands) and Coumarin120 (Aldrich) with and without the following optical filters: the 390/482/563/640 nm BrightLine filter (Semrock), the 633 nm, 514 nm, and 442 nm RazorEdge (Semrock) filters, the HQ 585/40m

and the HQ 510/50m (Chroma Technology) filters, and the Ex 450-490 and the BA 420 Nikon Fluorescence Filter Cube filters. The spectral response correction of the instrument was determined by using secondary emission standards as described (Gardecki and Maroncelli 1998). As secondary emission standards Lucifer Yellow and Coumarin120 were chosen.

Nonlinear spectral images (256 x 256 pixels, 400 x 400 μm) were acquired with an exposure time of 400 μs per pixel and a power of 14 mW at the specimen. Emission spectra were recorded for excitation wavelengths ranging from 720 nm to 940 nm (in 20 nm steps), while keeping the power at the specimen constant. All other images were recorded with an excitation wavelength of 765 nm. The storage experiment was performed in duplo. For each condition (cut and picked mushrooms, and peeled and unpeeled caps) five mushrooms were examined at five randomly chosen spots. For the heat-treatment experiment a freshly harvested mushroom was imaged before and after incubation in water at 65 °C for 10 min.

Data analysis.

All data was background subtracted before further analysis. For visualization purposes the spectral images are represented in "real color". To this end, the spectral information of each pixel is transformed into RGB values that resemble the color of the fluorescence emission as perceived by eye (Palero et al. 2006). Spectral decomposition was performed using the spectral phasor analysis (Fereidouni et al. 2012) yielding the fractional intensities of NAD(P)H, FAD and melanin. The reference signatures of FAD and NADH were obtained by acquiring 2p excited spectra of 2 mg×ml^{-1} FAD (Sigma-Aldrich Chemie) in H_2O and 2.3 mM NADH (Sigma-Aldrich Chemie) in 100 mM 3-(N-morpholino)propanesulfonic acid (Sigma-Aldrich Chemie) buffer (pH 7.4) yielding emission peaks of 460 nm and 530 nm, respectively. The emission peak of melanin (620 nm) was taken from (Teuchner et al. 2000). For every nonlinear spectral image the fractional intensities of NAD(P)H, FAD and melanin were used to calculate the average ratios of FAD / NAD(P)H and melanin / NAD(P)H. Error bars represent error of the mean of 50 measurements. Statistical analysis was per-

formed using OriginPro 8 SR2 (OriginLab, Northampton, USA) using Two-sample-t-Tests (unequal variance) with a p-value ≤ 0.05.

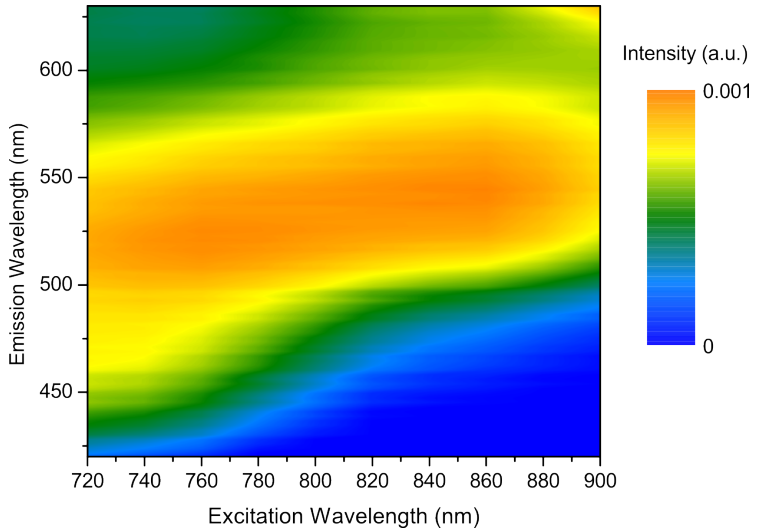

Figure 2. Excitation-emission matrix of a peeled cap of a freshly cut *A. bisporus* mushroom. The colormap represents intensity. Data were measured in 20 nm bins and smoothed with OriginLab.

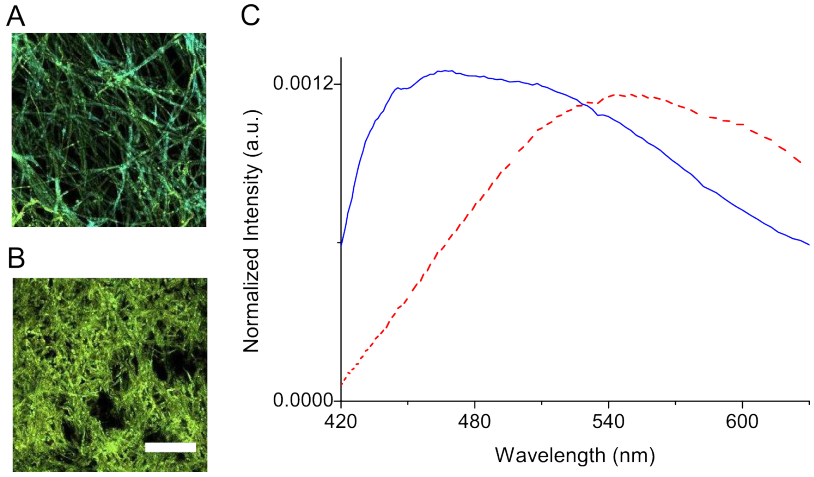

Figure 3. Nonlinear spectral images of the cap of a freshly harvested *A. bisporus* mushroom before (A) and after (B) incubation for 10 min at 65 °C. (C) shows the average spectrum of (A) as a solid line (high level of NAD(P)H) and (B) as a dashed line (no NAD(P)H, melanin formation). Bar represents 100 μm.

RESULTS

Spectral characterization of the specimen.

Emission spectra of a peeled cap of a freshly cut mushroom were recorded between 425 nm and 650 nm using excitation wavelengths ranging from 720 nm to 940 nm. The resulting excitation-emission matrix (Figure 2) shows that 2p excitation should be between 720 and 780 nm to excite all endogenous fluorophores emitting between 425 and 650 nm (i.e. NAD(P)H, FAD, and melanin).

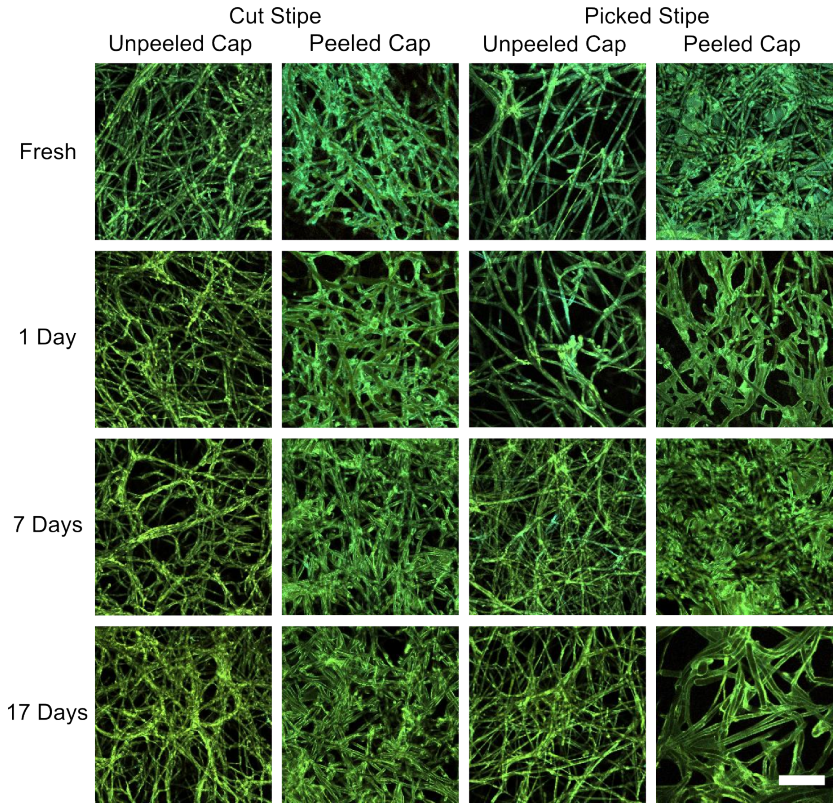

Figure 4. Nonlinear spectral images of *A. bisporus* caps showing the effect of storage at 4 °C (excitation at 765 nm). Mushroom caps were imaged after picking (picked stipe) or cutting the stipe (cut stipe) and after removing (peeled) the skin layer or not (unpeeled). Images represent freshly harvested mushrooms and mushrooms stored for 1, 7, and 17 days. Bar represents 100 μm.

Monitoring the metabolic state and aging of fungal hyphae.

Nonlinear spectral images of freshly cut mushroom caps of *A. bisporus* were recorded using an excitation wavelength of 765 nm (Figure 3). The broad emission spectrum (Figure 3 C) showed a high intensity between 450 and 500 nm, indicative for the presence of NAD(P)H. The spectrum was clearly red shifted when the mushroom had been incubated for 10 min at 65 °C (Figure 3 C). Note that the spectra were recorded at the same imaging conditions. The shoulder-peak in the blue spectral range, mainly attributed to the presence of NAD(P)H (Huang et al. 2002, Palero et al. 2007), had disappeared. At the same time the red part of the spectrum (> 600 nm) had increased, which is likely due to the presence of melanin. Indeed, browning of the mushroom after the heat treatment was detectable even by eye. Thus, inactivation of *A. bisporus* hyphae by a heat treatment was accompanied by a blue- to red-shifted spectrum.

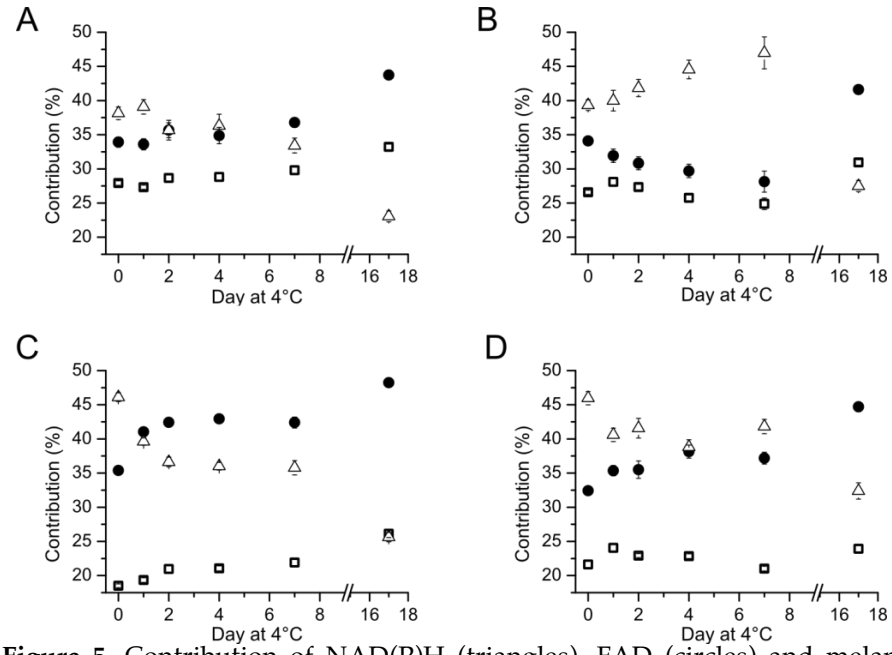

Figure 5. Contribution of NAD(P)H (triangles), FAD (circles) and melanin (squares) in the emission spectra of *A. bisporus* caps that had been stored for 0-17 days at 4 °C. NLSM images were acquired for (A) cut-stipe and unpeeled caps, (B) picked-stipe and unpeeled caps, (C) cut-stipe and peeled caps, and (D) picked-stipe and peeled caps using an excitation at 765 nm.

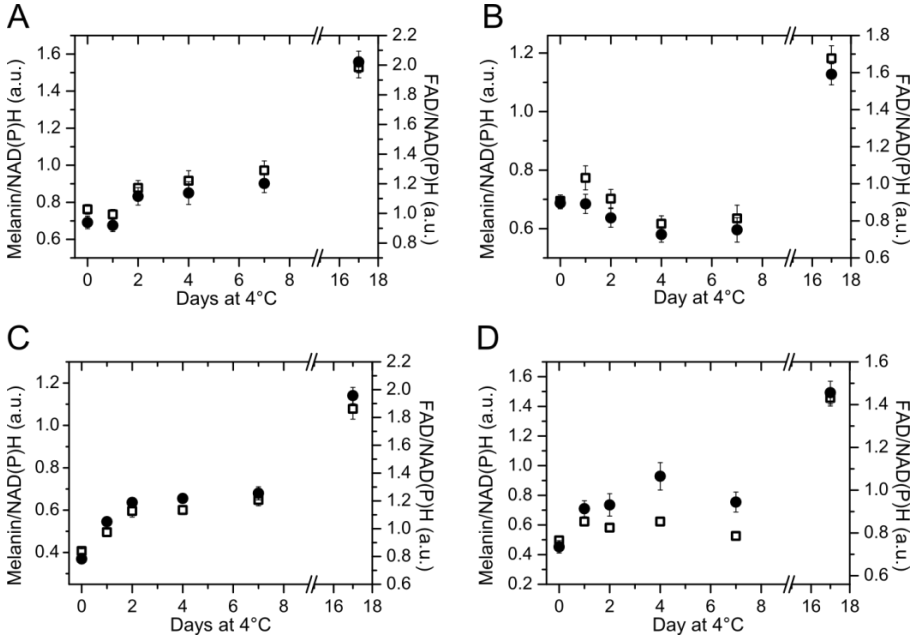

Figure 6. Changes in FAD / NAD(P)H (circles) and melanin / NAD(P)H (squares) ratios in the 2p excited emission spectra during storage of *A. bisporus* mushrooms at 4 °C. NLSM images were acquired for (A) cut-stipe and unpeeled caps, (B) picked-stipe and unpeeled caps, (C) cut-stipe and peeled caps, and (D) picked-stipe and peeled caps using an excitation at 765 nm.

In the next set of experiments it was examined whether a blue- to red-shifted spectrum can be also observed upon storage of *A. bisporus* mushrooms at 4 °C. To this end, the surface of mushroom caps was imaged directly or after peeling off the skin tissue. The mushrooms were harvested by either cutting the stipe (mimicking the harvesting process in commercial mushroom farming) or by gently picking them from the bed. In the latter case, casing soil and vegetative mycelium remained attached to the lower part of the stipe. In all cases, morphology and color of the mushrooms did not change during the 17-days-storage period as detected by eye. Nonlinear spectral images of hyphae of unpeeled caps were more heterogeneous than those exposed after peeling of the skin (Figure 4). Generally, fresh mushrooms exhibited spectra peaking in the blue (Figure 4). This was most obvious for peeled mushroom caps. Mushrooms stored for 1 day had already a red-shifted spectrum and thus appear greener in the RGB images (Fig-

ure 4). This red-shift was even more pronounced by extending the storage time. To quantify these spectral differences, the emission spectra were decomposed into the main components by the spectral phasor analysis, resulting in the spectral contributions of NAD(P)H, FAD, and melanin (Figure 5). With increasing storage times, the relative melanin and FAD contributions are increasing, while the NAD(P)H contribution is decreasing. The metabolic state expressed as the FAD / NAD(P)H ratio changed from 0.94 to 1.12 after two days of storage in the case of cut-stipe unpeeled mushrooms (Figure 6 A, Table 1). This ratio remained unchanged between 2 and 7 days, but had increased to 2.02 after 17 days of storage. Notably, the FAD / NAD(P)H ratio had increased already after one day from 0.78 to 1.05 in peeled cut-stipe caps. This ratio had further increased to 1.19 after two days of storage. No changes were detected between 2-7 days of storage, but after 17 days the FAD / NAD(P)H ratio had increased to 1.96 (Figure 6 C, Table 1). Unpeeled picked mushrooms showed a slight, if at all, decrease in the FAD / NAD(P)H ratio between harvesting and 7-days of storage. Only after 17 days the ratio had increased from 0.89 to 1.59 (Figure 6 B, Table 1). This ratio is lower than that of cut-stipe mushrooms after 17 days (Figure 6 A). When the skin layer was removed, picked mushrooms followed the same trend as cut-stipe mushrooms. Similar to peeled cut-stipe caps, a significant increase in the FAD / NAD(P)H ratio from 0.73 to 0.91 was found after 1 day of storage. Between 1 and 7 days of storage at 4 °C no significant changes were detected. Only after 17 days of storage, the FAD / NAD(P)H ratio had raised to 1.46 (Figure 6 D, Table 1). Taken together, The FAD / NAD(P)H ratios found at the surface of picked-stipe caps were generally lower when compared to those at the surfaces of cut-stipe caps. This was less clear after removing the peel. Data also show that the FAD / NAD(P)H ratio at the surface of freshly cut or picked mushrooms is about 0.92 (Figure 6 A, B), while it is about 0.76 after removing the peel (Figure 6 C, D). This indicates that the hyphae under the skin of *A. bisporus* mushroom caps are more metabolically active than on the surface.

Table 1. P-values of the statistical analysis of the differences in the FAD / NAD(P)H ratios of different storage days using a Two-sample-t-Test for unequal variance. Shaded boxes indicate significant differences (p-value ≤ 0.05).

Days compared	Cut stem, unpeeled	Cut stem, peeled	picked stem, unpeeled	picked stem, peeled
1 & 0	0.73	<0.01	0.94	<0.01
2 & 0	0.02	<0.01	0.18	<0.01
2 & 1	0.01	<0.01	0.30	0.78
4 & 0	0.03	<0.01	<0.01	<0.01
4 & 1	0.01	<0.01	0.01	0.04
4 & 2	0.82	0.54	0.17	0.11
7 & 0	<0.01	<0.01	0.05	<0.01
7 & 1	<0.01	<0.01	0.10	0.60
7 & 2	0.31	0.26	0.44	0.85
7 & 4	0.51	0.52	0.75	0.13
17 & 0	<0.01	<0.01	<0.01	<0.01
17 & 1	<0.01	<0.01	<0.01	<0.01
17 & 2	<0.01	<0.01	<0.01	<0.01
17 & 4	<0.01	<0.01	<0.01	<0.01
17 & 7	<0.01	<0.01	<0.01	<0.01

Cut-stipe unpeeled mushrooms exhibited an increase in the melanin / NAD(P)H ratio from 0.76 to 0.88 after two days of storage. No changes were observed between 2 and 7 days of storage but the value had increased to 1.53 after 17 days of storage (Figure 6 A, Table 2). Significant differences in the melanin / NAD(P)H ratio were detected (from 0.41 to 0.50) after 1 day of storage when the skin layer was removed from the cap. Similar to unpeeled cut-stipe mushrooms, no differences were observed between 2 and 7 days of storage, while after 17 days the melanin / NAD(P)H ratio increased to 1.08 (Figure 6 C, Table 2). Unpeeled picked-stipe mushrooms showed no changes in the melanin / NAD(P)H ratio between the first 7 storage days but it had increased from 0.63 to 1.18 after 17 days of storage (Figure 6 C, D, Table 2). Freshly picked peeled mushrooms had a lower melanin / NAD(P)H ratio when compared to those that had been stored. In addition, picked peeled mushrooms that had been stored for 17 days had a higher melanin / NAD(P)H ratio when compared to 1-7-days stored

mushrooms (Figure 6 D, Table 2). Taken together, the melanin / NAD(P)H ratio is generally lower in picked mushrooms (Figure 6 B, D) when compared to cut-stipe mushrooms (Figure 6 A, C). This was less clear after removing the peel. Data also show that the melanin / NAD(P)H ratio at the surface of freshly cut or picked mushrooms is about 0.73 (Figure 6 A, B), while it is about 0.45 after removing the peel (Figure 6 C, D). This and the data presented in Figure 5 show that there is more melanin formation within the surface layer of *A. bisporus* fruiting bodies and that the layer under the skin is more metabolically active.

Table 2. P-values of the statistical analysis of the differences in the melanin / NAD(P)H ratios of different storage days using a Two-sample-t-Test for unequal variance. Shaded boxes indicate significant differences (p-value ≤ 0.05).

Days compared	Cut stem, unpeeled	Cut stem, peeled	picked stem, unpeeled	picked stem, peeled
1 & 0	0.47	<0.01	0.09	<0.01
2 & 0	0.02	<0.01	0.83	0.01
2 & 1	<0.01	<0.01	0.17	0.27
4 & 0	0.01	<0.01	0.02	<0.01
4 & 1	<0.01	<0.01	<0.01	0.99
4 & 2	0.57	0.90	0.04	0.27
7 & 0	<0.01	<0.01	0.23	0.38
7 & 1	<0.01	<0.01	0.03	0.01
7 & 2	0.15	0.19	0.22	0.06
7 & 4	0.46	0.17	0.73	0.01
17 & 0	<0.01	<0.01	<0.01	<0.01
17 & 1	<0.01	<0.01	<0.01	<0.01
17 & 2	<0.01	<0.01	<0.01	<0.01
17 & 4	<0.01	<0.01	<0.01	<0.01
17 & 7	<0.01	<0.01	<0.01	<0.01

DISCUSSION

This study combined NLSM with spectral phasor analysis as a novel minimally-invasive method to study the effect of storage on metabo-

lism and pigment formation in *A. bisporus* mushrooms. To this end, the endogenous fluorophores NAD(P)H, FAD and melanin were used as biomarkers directly at the surface of the mushroom and after removing the peel. Unpeeled caps showed in general a greater variation in their spectra when compared to peeled caps. This may be due to a higher variation in metabolism and melanin formation between hyphae that make up the surface layer of the mushroom. It may also be caused by bacteria that colonize the surface of the mushroom (Doores et al. 1987, Egbebi and Fakoya 2011). Nevertheless, changes in the spectra of unpeeled and peeled surface followed the same trend.

Spectra of *A. bisporus* mushroom caps change upon storage at 4 °C. The contribution of NAD(P)H to the total spectrum is decreasing, while the contribution of FAD and melanin is increasing over time. NAD(P)H is oxidized in the electron transport chain to non-fluorescent NAD(P) for ATP-production. Decreasing fluorescence emission of NAD(P)H indicates less or no new NAD(P)H formation within the glycolysis and the citric acid cycle. Non fluorescent $FADH_2$ is also produced in the citric acid cycle and is also oxidized in the electron transport chain yielding fluorescent FAD. Thus, none or little $FADH_2$ formation within the citric acid cycle coincides with increasing FAD emission. The FAD / NAD(P)H ratio can therefore be considered as an indicator of metabolic activity (Chance et al. 1979). This ratio increased upon storage of *A. bisporus* mushrooms, especially in the case of fruiting bodies that had been harvested by cutting. Vegetative mycelium and casing layer remain attached to the mushroom when fruiting bodies are harvested by picking. The vegetative mycelium may still have some feeding capacity and at the same time picking may prevent drying out of the fruiting body.

It is known that mechanical damage (Burton et al. 1993) or infection (Soler-Rivas et al. 2000, Soler-Rivas et al. 1999) of mushrooms results in the formation of melanin. Normally, tyrosinase and its phenol substrates are spatially separated, but when brought together melanin synthesis is initiated (Jolivet et al. 1998, Butler and Day 1998, Eisenman and Casadevall 2012). Melanin contribution to the total spectrum increased during storage, while the NAD(P)H contribution decreased (Figure 5). As a result, melanin / NAD(P)H ratios increased during

storage. In general, cut-stipe mushrooms exhibited higher melanin / NAD(P)H values than picked-stipe caps. In fact, FAD / NAD(P)H and melanin / NAD(P)H ratios follow the same trend. This suggests that reduction in metabolic activity is accompanied with melanin formation.

Freshly harvested mushrooms exhibited lower FAD / NAD(P)H and melanin / NAD(P)H ratios underneath the skin when compared to the surface layer. This can be explained by higher metabolic activity of the hyphae under the peel and at the same time by reduced melanin formation in this tissue. These data thus show that zones within the mushroom are heterogeneous with respect to metabolism and pigment formation. Previously, it has been shown that metabolism, gene expression, growth and secretion are heterogeneous between different zones of a vegetative mycelium (Masai et al. 2006, Masai et al. 2006, Kasuga and Glass 2008, Moukha et al. 1993, Levin et al. 2007, Krijgsheld et al. 2012, Wösten et al. 1991). In fact, these processes can even be heterogeneous between neighboring hyphae within a zone of a colony (de Bekker et al. 2011, Vinck et al. 2005, Vinck et al. 2011, van Veluw et al. 2012, Bleichrodt et al. 2012). Spectra of neighboring hyphae at the surface and under the peel of the mushroom were also heterogeneous (see Figure 4). These differences may be partly due to bacterial load in the case of the skin but can only be attributed to heterogeneity of metabolism and pigment formation under the peel.

To summarize, NLSM provides an excellent alternative to conventional methods that are used to monitor metabolic activity of cells. It is non-invasive, shows reduced phototoxicity compared to other imaging methods, does not depend on exogenous molecules, and provides spectral and spatial information down to the sub-cellular level. We have shown that NLSM can be used to predict freshness of mushrooms by monitoring their metabolism. Monitoring metabolism is also of interest for bioprocess modeling, controlling fermentations in bioreactors (Moss et al. 2008) and for cell biology studies of microbes.

REFERENCES

Bleichrodt RJ, Veluw GJ, Recter B, Maruyama J, Kitamoto K, Wösten HAB (2012) Hyphal heterogeneity in *Aspergillus oryzae* is the result of dynamic closure of septa by Woronin bodies. Mol Microbiol 86: 1334-1344

Burton K, Love M, Smith J (1993) Biochemical changes associated with mushroom quality in *Agaricus spp.*. Enzyme MicrobTechnol 15: 736-741

Butler M, Day A (1998) Fungal melanins: a review. Can J Microbiol 44: 1115-1136

Butler M, Gardiner R, Day A (2005) Fungal melanin detection by the use of copper sulfide-silver. Mycologia 97: 312-319

Chance B, Schoener B, Oshino R, Itshak F, Nakase Y (1979) Oxidation-reduction ratio studies of mitochondria in freeze-trapped samples. NADH and flavoprotein fluorescence signals. J Biol Chem 254: 4764-4771

de Bekker C, van Veluw GJ, Vinck A, Wiebenga LA, Wösten HAB (2011) Heterogeneity of *Aspergillus niger* microcolonies in liquid shaken cultures. Appl Environ Microbiol 77: 1263-1267

Doores S, Kramer M, Beelman R (1987) Evaluation and bacterial populations associated with fresh mushrooms (*Agaricus bisporus*). Developments in crop science. 10: 283-294

Egbebi A, Fakoya S (2011) Comparative studies on close button and open cup mushrooms of *Agaricus bisporus*. Int J Trop Med Public Health 1: 11-17

Eisenman HC, Casadevall A (2012) Synthesis and assembly of fungal melanin. Appl Microbiol Biotechnol 93: 931-940

Eisenman HC, Nosanchuk JD, Webber JBW, Emerson RJ, Camesano TA, Casadevall A (2005) Microstructure of cell wall-associated melanin in the human pathogenic fungus *Cryptococcus neoformans*. Biochemistry 44: 3683-3693

Fereidouni F, Bader AN, Gerritsen HC (2012) Spectral phasor analysis allows rapid and reliable unmixing of fluorescence microscopy spectral images. Opt Express 20: 12729-12741

Fereidouni F, Bader AN, Colonna A, Gerritsen HC (2013) Phasor analysis of multiphoton spectral images distinguishes autofluorescence components of in vivo human skin. J Biophotonics . DOI 10.1002/jbio.201200244

Gardecki J, Maroncelli M (1998) Set of secondary emission standards for calibration of the spectral responsivity in emission spectroscopy. Appl Spectrosc 52: 1179-1189

Garini Y, Young IT, McNamara G (2006) Spectral imaging: principles and applications. Cytometry A 69: 735-747

Gerritsen HC, de Grauw CJ (1999) Imaging of optically thick specimen using two-photon excitation microscopy. Microsc Res Tech 47: 206-209

Gu M, Gan X, Kisteman A, Xu MG (2000) Comparison of penetration depth between two-photon excitation and single-photon excitation in imaging through turbid tissue media. Appl Phys Lett 77: 1551-1553

Harris DM, Diderich JA, Van der Krogt ZA, Luttik MAH, Raamsdonk LM, Bovenberg RAL, Van Gulik WM, Van Dijken JP, Pronk JT (2006) Enzymic analysis of NADPH metabolism in β-lactam-producing *Penicillium chrysogenum*: presence of a mitochondrial NADPH dehydrogenase. Metab Eng 8: 91-101

Hegnauer H, Nyhlén LE, Rast DM (1985) Ultrastructure of native and synthetic *Agaricus bisporus* melanins - Implications as to the compartmentation of melanogenesis in fungi. Exp Mycol 9: 1-29

Hua SST, Brandl MT, Hernlem B, Eng JG, Sarreal SBL (2011) Fluorescent viability stains to probe the metabolic status of aflatoxigenic fungus in dual culture of *Aspergillus flavus* and *Pichia anomala*. Mycopathologia 171: 133-138

Huang S, Heikal AA, Webb WW (2002) Two-photon fluorescence spectroscopy and microscopy of NAD(P)H and flavoprotein. Biophys J 82: 2811-2825

Jeong SC, Jeong YT, Yang BK, Islam R, Koyyalamudi SR, Pang G, Cho KY, Song CH (2010) White button mushroom (*Agaricus bisporus*) lowers blood glucose and cholesterol levels in diabetic and hypercholesterolemic rats. Nutr Res 30: 49-56

Jolivet S, Arpin N, Wichers HJ, Pellon G (1998) *Agaricus bisporus* browning: a review. Mycol Res 102: 1459-1483

Kasuga T, Glass NL (2008) Dissecting colony development of *Neurospora crassa* using mRNA profiling and comparative genomics approaches. Eukaryotic cell 7: 1549-1564

Knaus H, Blab GA, van Veluw GJ, Gerritsen HC, Wösten HAB (2013) Label-free fluorescence microscopy in fungi. Fungal Biol Rev 27: 60-66

Kozarski M, Klaus A, Niksic M, Jakovljevic D, Helsper JP, Van Griensven LJ (2011) Antioxidative and immunomodulating activities of polysaccharide extracts of the medicinal mushrooms *Agaricus bisporus*, *Agaricus brasiliensis*, *Ganoderma lucidum* and *Phellinus linteus*. Food Chem 129: 1667-1675

Krijgsheld P, Altelaar AFM, Post H, Ringrose JH, Müller HW, Heck AJR, Wöstem HAB (2012) Spatially resolving the sectretome within the mycelium of the cell factory *Aspergillus niger*. J Proteome Res 11: 2807-2818

Kuhn D, Balkis M, Chandra J, Mukherjee P, Ghannoum M (2003) Uses and limitations of the XTT assay in studies of *Candida* growth and metabolism. J Clin Microbiol 41: 506-508

Kurtzman Jr RH (1997) Nutrition from mushrooms, understanding and reconciling available data. Mycoscience 38: 247-253

Laiho LH, Pelet S, Hancewicz TM, Kaplan PD, So PTC (2005) Two-photon 3-D mapping of ex vivo human skin endogenous fluorescence species based on fluorescence emission spectra. J Biomed Opt 10: 024016

Levin AM, De Vries RP, Conesa A, De Bekker C, Talon M, Menke HH, van Peij NNME, Wösten HAB (2007) Spatial differentiation in the vegetative mycelium of *Aspergillus niger*. Eukaryotic cell 6: 2311-2322

Masai K, Maruyama J, Sakamoto K, Nakajima H, Akita O, Kitamoto K (2006) Square-plate culture method allows detection of differential gene expression and screening of novel, region-specific genes in *Aspergillus oryzae*. Appl Microbiol Biotechnol 71: 881-891

Masters BR, So PTC, Gratton E (1998) Multiphoton Excitation Microscopy of In Vivo Human Skin: Functional and Morphological Optical Biopsy Based on Three-Dimensional Imaging, Lifetime Measurements and Fluorescence Spectroscopya. Ann N Y Acad Sci 838: 58-67

Mattila P, Könkö K, Eurola M, Pihlava J, Astola J, Vahteristo L, Hietaniemi V, Kumpulainen J, Valtonen M, Piironen V (2001) Contents of vitamins, mineral elements, and some phenolic compounds in cultivated mushrooms. J Agric Food Chem 49: 2343-2348

Moss BJ, Kim Y, Nandakumar M, Marten MR (2008) Quantifying metabolic activity of filamentous fungi using a colorimetric XTT assay. Biotechnol Prog 24: 780-783

Moukha SM, Wösten HAB, Mylius EJ, Asther M, Wessels JGH (1993) Spatial and temporal accumulation of mRNAs encoding two common lignin peroxidases in *Phanerochaete chrysosporium*. J Bacteriol 175: 3672-3678

Neher RA, Mitkovski M, Kirchhoff F, Neher E, Theis FJ, Zeug A (2009) Blind source separation techniques for the decomposition of multiply labeled fluorescence images. Biophys J 96: 3791-3800

Palero JA, de Bruijn HS, van der Ploeg van den Heuvel A, Sterenborg HJCM, Gerritsen HC (2007) Spectrally resolved multiphoton imaging of in vivo and excised mouse skin tissues. Biophys J 93: 992-1007

Palero JA, de Bruijn HS, van der Ploeg-van den Heuvel A, Sterenborg HJCM, Gerritsen HC (2006) In vivo nonlinear spectral imaging in mouse skin. Opt Express 14: 4395-4402

Soler-Rivas C, Arpin N, Olivier JM, Wichers HJ (2000) Discoloration and tyrosinase activity in *Agaricus bisporus* fruit bodies infected with various pathogens. Mycol Res 104: 351-356

Soler-Rivas C, Jolivet S, Arpin N, Olivier JM, Wichers HJ (1999) Biochemical and physiological aspects of brown blotch disease of *Agaricus bisporus*. FEMS Microbiol Rev 23: 591-614

Teuchner K, Ehlert J, Freyer W, Leupold D, Altmeyer P, Stücker M, Hoffmann K (2000) Fluorescence studies of melanin by stepwise two-photon femtosecond laser excitation. J Fluoresc 10: 275-275

Theer P, Denk W (2006) On the fundamental imaging-depth limit in two-photon microscopy. J Opt Soc Am A Opt Image Sci Vis 23: 3139-3149

van Veluw GJ, Teertstra WR, de Bekker C, Vinck A, van Beek N, Muller WH, Arentshorst M, van der Mei HC, Ram AFJ, Dijksterhuis J, Wösten HAB (2012) Heterogeneity in liquid shaken cultures of *Aspergillus niger* inoculated with melanised conidia or conidia of pigmentation mutants. Stud Mycol 74: 47-57

Vinck A, de Bekker C, Ossin A, Ohm RA, de Vries RP, Wösten HAB (2011) Heterogenic expression of genes encoding secreted proteins at the periphery of *Aspergillus niger* colonies. Environ Microbiol 13: 216-225

Vinck A, Terlou M, Pestman WR, Martens EP, Ram AF, Van Den Hondel CA, Wösten HAB (2005) Hyphal differentiation in the exploring mycelium of *Aspergillus niger*. Mol Microbiol 58: 693-699

Wani BA, Bodha R, Wani A (2010) Nutritional and medicinal importance of mushrooms. J Med Plant Res 4: 2598-2604

Wösten HAB, Moukha SM, Sietsma JH, Wessels JGH (1991) Localization of growth and secretion of proteins in *Aspergillus niger*. J Gen Microbiol 137: 2017-2023

Zipfel WR, Williams RM, Webb WW (2003) Nonlinear magic: multiphoton microscopy in the biosciences. Nat Biotechnol 21: 1369-1377

CHAPTER 4

Monitoring melanin and the metabolic state during development of *Agaricus bisporus* by nonlinear spectral microscopy

Helene Knaus, Gerhard A. Blab, Alexandra V. Agronskaia, Aurin M. Vos, Hans C. Gerritsen, Han A. B. Wösten.
In preparation

ABSTRACT

Label-free nonlinear spectral imaging microscopy (NLSM) acquires two-photon excited fluorescence emission spectra of endogenous fluorophores within a specimen. Here, NLSM was used to monitor the presence of melanin during development of the white button mushroom *Agaricus bisporus* and to determine the FAD / NAD(P)H ratios, which are indicative of the metabolic state. Mycelium had colonized the casing soil 9 days after it had been placed on top of colonized compost, while primordia and mushrooms had formed after 14 and 16-18 days, respectively. Mycelium in the compost and casing exhibited a FAD / NAD(P)H ratio between 1.32 ± 0.39 and 1.98 ± 0.98 at day 9 and 14, respectively. The FAD / NAD(P)H ratio of aerial structures was much lower, implying they were more metabolically active. For instance, the outer surface of mushrooms with a cap diameter of 1 - 4 cm exhibited the lowest FAD / NAD(P)H ratio (i.e. between 0.44 ± 0.23 and 0.58 ± 0.21), while those with a cap of 8 cm had a value of 0.78 ± 0.30. NLSM detected melanin in aerial structures and in the mycelium in the compost and in the casing, although this pigment was not visible by eye. Notably, melanin contribution was highest in the mycelium in the compost. These data imply that NLSM can be used to monitor the quality of the mycelium during colonization of compost and casing and to optimize harvesting for increased shelf life. Moreover, data indicate that melanin plays a role in colonization of substrates.

INTRODUCTION

The white button mushroom *Agaricus bisporus* is one of the most important commercial mushrooms. It offers a low amount of fat and is a good source of digestible protein. In addition, *A. bisporus* mushrooms contain vitamins, minerals and bio-active compounds like anti-oxidative and immuno-modulating polysaccharides (Kurtzman Jr 1997, Wani et al. 2010, Kozarski et al. 2011, Mattila et al. 2001). Commercial cultivation of *A. bisporus* makes use of a composted layer of lignocellulose rich material (Iiyami et al. 1996, Atkey and Wood 1984, Iiyama et al. 1994, Chen et al. 2000) that is topped with a casing layer. The casing layer provides high water activity (Bels-Koning 1950, Flegg 1956, Kalberer 1987) and a microbial flora (Eger 1961) that is important for induction of fruiting body formation. Activated charcoal (Eger 1961, Noble et al. 2003) or removal of volatile compounds (Noble et al. 2009) can replace the microbes in the casing soil. Air with a lower temperature, CO_2, and moisture content than the air during vegetative growth is also a prerequisite for mushroom formation of *A. bisporus*. Eastwood et al. (2013) proposed that the organic volatile 1-octen-3-ol would act as a repressor of early development, while high temperature would inhibit the transition from smooth to elongated differentiated primordia. On the other hand, CO_2 levels would impact the number of fruiting bodies.

Development of *A. bisporus* fruiting bodies starts with differentiation of fluffy mycelial cords in the casing layer when they are exposed to the reproduction stimulating environmental conditions. As a result, fluffy hyphal knots are formed (Eastwood et al. 2013, Umar and van Griensven 1997). Further growth and aggregation results in a 1–2 mm sized fluffy initial. These undifferentiated primordia develop into smooth undifferentiated primordia (Eastwood et al. 2013), of which 5–10 % develop into mature fruiting bodies (Noble et al. 2003). Stipe and cap tissue can be distinguished in 4 mm sized differentiated primordia. These tissues further develop when the mushroom is formed (Umar and van Griensven 1997). Gill tissue with basidiospore forming basidia is developed on the underside of the cap as the fruiting body enlarges.

Knowledge about the molecular mechanisms underlying fruiting body formation is still limited in the case of *A. bisporus*. Here the metabolic state of the vegetative mycelium and aerial structures was studied as well as the presence of melanin by using nonlinear spectral microscopy (NLSM) (Knaus et al. 2013a). NLSM provides a spatial distribution of (auto)fluorescence emission spectra within the specimen (Huang et al. 2002, Laiho et al. 2005, Palero et al. 2007). The emission spectrum is the sum of the spectra of the individual fluorophores. NAD(P)H, FAD, and melanin are autofluorescent molecules that are present in fungi (Knaus et al. 2013b). These compounds have maximum emission in the blue (460 nm), green (530 nm), and red (620 nm) wavelength range, respectively (Huang et al. 2002, Teuchner et al. 2000). The overall emission spectrum can be decomposed resulting in quantification of the contribution of each fluorophore. The FAD / NAD(P)H ratio is indicative for the metabolic state (Chapter 3, Knaus et al. 2013a, Chance et al. 1979). Using this ratio, we show that the vegetative mycelium is much less metabolically active than aerial hyphae, and the outer layers of primordia and mushrooms. Furthermore, it is shown for the first time that low levels of melanin are present in vegetative hyphae and aerial structures of *A. bisporus*.

MATERIALS AND METHODS

Development of *A. bisporus*.

Strain Sylvan A15 was grown as described by Knaus et al. (2013a). Plastic containers (17.5 x 27.5 x 22.5 cm) were filled with 3.5 kg phase-III compost colonized with *A. bisporus* A15 (CNC Grondstoffen, Milsbeek, The Netherlands) and topped with 1 kg of casing soil (CNC Grondstoffen). The cultures were incubated at 24 °C and 95 % relative humidity (RH) in Economic Premium Climate Chambers (Snijders Scientific, Tilburg, The Netherlands). Water (200 ml per day) was added to each of the containers during the first 4 days of incubation. Growth was prolonged at 20 °C and 88 % RH when aggregates had formed on the casing layer (i.e. after 9 days of culturing). *A. bisporus* was also grown on autoclaved compost agar. To this end, water was added to 150 gram wet weight Phase III compost to a final volume of 1 l and

homogenized in a Warring blender 6 times 1 min at high speed. The homogenized compost was sterilized at 123 °C for 3 times 20 min and mixed with 3 % agar in a 1:1 ratio.

Nonlinear spectral imaging.

The nonlinear spectral imaging setup is described in Chapter 2. Nonlinear spectral images (256 x 256 pixels, 100 x 100 μm) were acquired with an excitation wavelength of 740 nm using a CFI Apo LWD 25x water objective with NA 1.1 (Nikon Instruments Europe, Amsterdam, The Netherlands), an exposure time of 400 μs, and a power at the specimen of about 9 mW. Mycelium within the compost and in and on the casing layer was imaged 10 times using biological duplicates (i.e. 20 images per sample in total). In the case of primordia, 5 individuals were examined in duplicate, each at five randomly chosen spots. Mushrooms with a diameter of 1, 2, 4, and 8 cm were imaged at five random spots and for each class five individuals were taken from 3 independent cultures.

Data analysis.

For visualization, spectral images were represented in real color. To this end, spectral information of each pixel was transformed into RGB values that resemble the color of the fluorescence emission as perceived by eye (Palero et al. 2006). Data was background subtracted before spectral analysis. Spectral decomposition was carried out using the spectral phasor analysis (Fereidouni et al. 2012) yielding the contribution (fractional intensity) of NAD(P)H, FAD and melanin. The reference signatures of NADH and FAD were obtained as described (Chapter 2, Knaus et al. 2013a). The reference signature of melanin was determined by exciting melanin in spores present on a mushroom cap at 740 nm. To determine the absolute signal of each of the components, contribution was multiplied by the total intensity in each of the pixels. This was calculated for 6 NLSM images of vegetative mycelium in compost (9 days) and for mushroom caps with a diameter of 4 cm. Since imaging conditions were identical in all cases, the intensity was not normalized. Two-sample-t-Tests (unequal variance) with a p-value

of 0.05 were performed in OriginPro 8 SR2 (OriginLab Corporation, Northampton, USA).

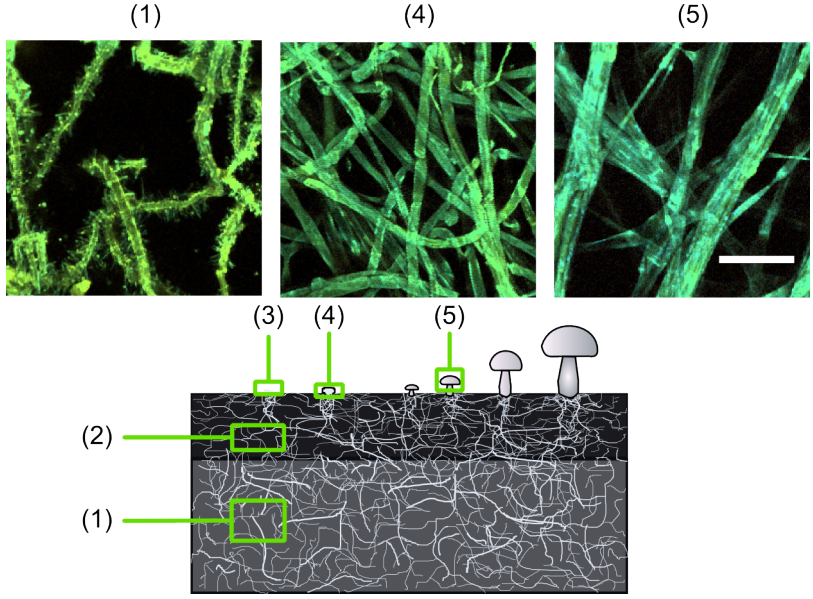

Figure 1. Samples used for NLSM analysis of *A. bisporus*. Compost and casing are indicated in gray and black, respectively. Vegetative mycelium growing in the compost (1), in casing (2), and on casing (3) were imaged 9 and 14 days after compost had been covered by casing. Primordia (4) were examined 14 days after applying the casing. Fruiting bodies with a cap diameter between 1 and 8 cm had formed after 16-18 days of culturing (5). Typical NLSM images of vegetative mycelium (1), primordia (4) and a mushroom with a cap diameter of 2 cm (5) are presented in RGB. NLSM was performed at 740 nm excitation wavelength and the color of each pixel in the images is the result of the relative contribution of RGB values of the total fluorescence intensity. Bar represents 30 μm.

RESULTS

Nonlinear spectral images were acquired 9 and 14 days after colonized compost had been covered with casing soil. After 9 days the mycelium had colonized the casing layer and aerial hyphae either or not in aggregates had been formed, while after 14 days primordia had developed. Mushrooms with caps between 1 and 8 cm had formed 16 - 18 days after topping the compost with casing. Figure 1 shows typical

examples of NLSM images of hyphae in the compost, of primordia and of a mushroom with a cap diameter of 2 cm. Here, the spectral information was transformed into RGB values that resemble the color of the fluorescence emission as perceived by eye. The color per pixel thus results from the relative contribution of RGB values of the total fluorescence intensity. Mycelium within the compost appeared green-yellow, while the spectrum of the surface of the mushroom cap is blue-shifted (Figure 1). The spectrum of the primordia is in between that of the mycelium in the compost and that of the mushroom.

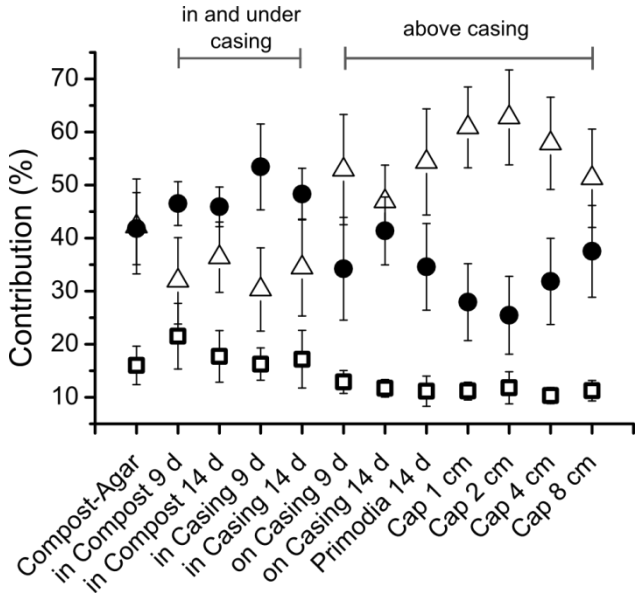

Figure 2. Contribution of NAD(P)H (triangles), FAD (circles) and melanin (squares) as a percentage of the emission spectrum of *A. bisporus* mycelium (in compost, in casing, on casing), and of primordia and 1-8 cm wide mushroom caps. Samples of mycelium and primordia were taken 9 or 14 days after colonized compost had been topped with casing soil. Mushrooms were collected after 16 – 18 days. Mycelium that had been grown on compost based agar was used as a reference. NLSM images were acquired at 740 nm excitation wavelength and the contributions of the autofluorescent components were determined by spectral decomposition. Bars indicate standard deviation.

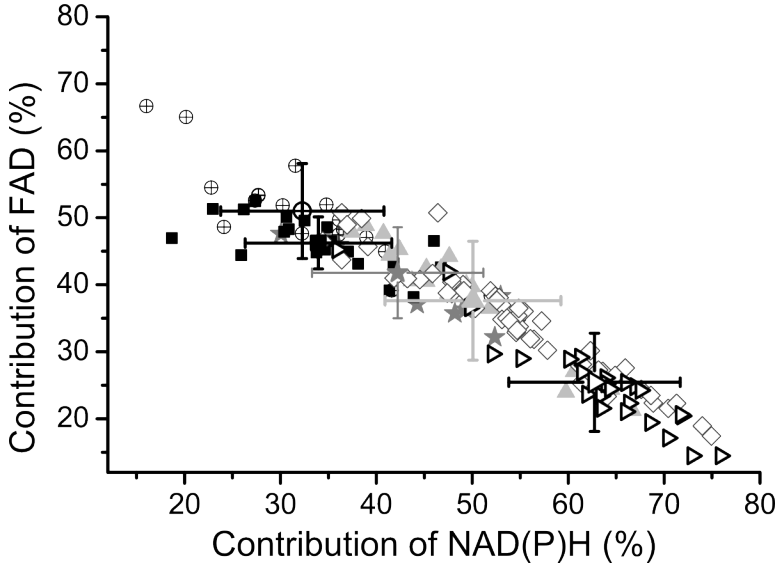

Figure 3. Contribution of FAD versus NAD(P)H during different stages of development in *A. bisporus*. Vegetative mycelium in the compost (squares), within the casing (circles), and on the casing (up triangle) were imaged 9 and 14 days after applying the casing onto the compost. Primordia (diamonds) were examined 14 days after applying the casing onto the compost. The mushroom caps (right triangle) were imaged at a size of 2 cm. Data points depict individual NLSM images, while the symbols with the standard deviation represents the mean value of each population. NLSM images were acquired at 740 nm excitation wavelength and the contributions of NAD(P)H and FAD were determined by spectral decomposition.

Total emission spectra were decomposed by spectral phasor analysis to quantify the spectral contribution of NAD(P)H, FAD and melanin during the development of *A. bisporus*. The time point (9 and 14 days after applying casing onto compost) had less impact on the contribution of these three components than the type of mycelium tested (Figure 2, Table 1). There were no significant changes in the contribution of FAD (compost 9 days: 46.52 ± 4.12 %; compost 14 days: 45.91 ± 3.74 %; casing 9 days: 53.42 ± 8.11 %; casing 14 days: 48.30 ± 4.86 %) and NAD(P)H (compost 9 days: 31.96 ± 8.14 %; compost 14 days: 36.40 ± 6.63 %; casing 9 days: 30.33 ± 8.14 %; casing 14 days: 34.45 ± 9.12 %) when vegetative mycelium in the compost and in the casing was compared. In contrast, *A. bisporus* growing on top of the casing (aerial hyphae, primordia and fruiting bodies) exhibited significant differences

when compared to the vegetative mycelium within the compost and the casing (Figure 2, Table 1). Contribution of NAD(P)H (52.91 ± 10.38 %) and FAD (34.21 ± 9.68 %) in aerial hyphae 9 days after topping the casing were similar to that of primordia (54.37 ± 10.00 % and 34.59 ± 8.16 %, respectively). However, the contribution of FAD was significantly higher and NAD(P)H significantly lower when compared to mushroom caps with a diameter of 1 or 2 cm. Young mushrooms (1 to 4 cm cap-diameter) exhibited the highest NAD(P)H and the lowest FAD contributions. For instance, the 2 cm mushroom caps had a NAD(P)H contribution of 62.74 ± 8.94 % and a FAD contribution of 25.44 ± 7.34 %. Mushrooms with a cap-diameter of 8 cm had a lower NAD(P)H contribution (51.27 ± 9.26 %) and a higher FAD contribution (37.50 ± 8.63 %) similar to primordia and aerial mycelium on casing. Mycelium growing on compost based agar had a NAD(P)H (42.21 ± 8.93 %) and FAD (41.79 ± 6.79 %) contribution similar to vegetative mycelium on casing (Figure 2, Table 1). Figure 3 shows a cluster plot of the contribution of NAD(P)H and FAD for every single NLSM image during the developmental stages (mycelium in compost, in casing, and on casing, and primordia and mushrooms with a cap diameter of 2 cm). The plot shows a linear relationship of NAD(P)H and FAD, implying that the rate of change was constant throughout *A. bisporus* development. Depending on the developmental state, the FAD / NAD(P)H ratio was changing from 1.60 ± 0.66 in mycelium within compost and casing (9 and 14 days) to 0.72 ± 0.30 for mycelium growing on top of the casing layer and primordia (Table 2). The lowest FAD / NAD(P)H ratio (0.50 ± 0.21) was found in mushrooms with a cap diameter of 1 – 4 cm. Mushrooms with a cap diameter of 8 cm had an increased FAD / NAD(P)H ratio of 0.78 ± 0.30, which is similar to that of mycelium growing on casing and of primordia (Table 2).

Table 1. P-values of the statistical analysis of differences in melanin, FAD, and NAD(P)H contribution in the spectra of different stages of development of *A. bisporus* using a Two-sample-t-Test for unequal variance. Shaded boxes indicate significant differences (p-value ≤ 0.05).

Comparison	Melanin	FAD	NAD(P)H
in Compost 9 d & Compost-Agar	0.02	0.07	0.01
in Compost 9 d & in Compost 14 d	0.14	0.73	0.2
in Compost 9 d & in Casing 9 d	0.02	0.03	0.65
in Compost 9 d & in Casing 14 d	0.11	0.4	0.53
in Compost 9 d & on Casing 9 d	<0.01	0	<0.01
in Compost 9 d & on Casing 14 d	<0.01	0.04	<0.01
in Compost 14 d & Compost-Agar	0.4	0.11	0.11
in Compost 14 d & in Casing 9 d	0.45	0.02	0.09
in Compost 14 d & in Casing 14 d	0.83	0.26	0.61
in Compost 14 d & on Casing 9 d	0.02	0	<0.01
in Compost 14 d & on Casing 14 d	0.01	0.08	0
in Casing 9 d & Compost-Agar	0.86	0	0
in Casing 9 d & in Casing 14 d	0.66	0.11	0.31
in Casing 9 d & on Casing 9 d	0.01	<0.01	<0.01
in Casing 9 d & on Casing 14 d	0	0	<0.01
in Casing 14 d & Compost-Agar	0.59	0.02	0.07
in Casing 14 d & on Casing 9 d	0.05	<0.01	<0.01
in Casing 14 d & on Casing 14 d	0.02	0.02	0
on Casing 9 d & Compost-Agar	0.03	0.04	0.02
on Casing 9 d & on Casing 14 d	0.17	0.06	0.13
on Casing 14 d & Compost-Agar	0	0.88	0.19
Primordia 14 d & Compost-Agar	0	0.01	0
Primordia 14 d & in Compost 9 d	<0.01	<0.01	<0.01
Primordia 14 d & in Compost 14 d	0	<0.01	<0.01
Primordia 14 d & in Casing 9 d	<0.01	<0.01	<0.01
Primordia 14 d & in Casing 14 d	0.03	<0.01	<0.01
Primordia 14 d & on Casing 9 d	0.03	0.9	0.67
Primordia 14 d & on Casing 14 d	0.41	0.01	0.01
Primordia 14 d & Cap 1 cm	0.98	<0.01	0
Primordia 14 d & Cap 2 cm	0.38	<0.01	<0.01
Primordia 14 d & Cap 4 cm	0.09	0.17	0.12
Primordia 14 d & Cap 8 cm	0.91	0.16	0.18
Cap 1 cm & Cap 2 cm	0.37	0.23	0.43
Cap 1 cm & Cap 4 cm	0.06	0.08	0.19
Cap 1 cm & Cap 8 cm	0.92	<0.01	<0.01
Cap 2 cm & Cap 4 cm	0.04	0	0.06
Cap 2 cm & Cap 8 cm	0.43	<0.01	<0.01
Cap 4 cm & Cap 8 cm	0.07	0.02	0.01

Table 2. FAD / NAD(P)H ratio during development. Error represents standard deviation.

Developmental State	FAD / NAD(P)H
Compost – Agar	1.07 ± 0.42
in Compost 9 d	1.56 ± 0.48
in Compost 14 d	1.32 ± 0.39
in Casing 9 d	1.98 ± 0.98
in Casing 14 d	1.52 ± 0.51
on Casing 9 d	0.70 ± 0.33
on Casing 14 d	0.91 ± 0.24
Primordia 14 d	0.69 ± 0.29
Cap 1 cm	0.48 ± 0.18
Cap 2 cm	0.44 ± 0.23
Cap 4 cm	0.58 ± 0.21
Cap 8 cm	0.78 ± 0.30

NLSM showed that melanin was present throughout development (Figure 2), although the pigment was not visible by eye. Mycelium within the compost exhibited significantly higher melanin contributions in the spectra when compared to *A. bisporus* above the casing, especially when compared to mushroom caps (Figure 2, Table 2). The relative contribution of melanin in mycelium within the compost, 9 and 14 days after topping, was 21.52 ± 6.18 % and 17.70 ± 4.86 %, respectively. Primordia and mushroom caps showed a melanin contribution between 10.32 ± 1.51 % and 11.80 ± 3.03 %. The absolute signal of melanin also changed during development. It was 6.5 ± 1.2 a.u. and

2.2 ± 0.9 a.u. in the case of mycelium in compost (9 days after topping) and at the surface of a 4 cm wide mushroom cap. FAD displayed a same behavior, albeit with a larger variability between pixels, resulting in 17.3 ± 16.4 a.u. for mycelium in the compost and 7.7 ± 5.6 a.u. for mushrooms with a 4 cm-wide cap. The ratio of NAD(P)H however was similar with 12.0 ± 10.2 a.u. and 13.0 ± 6.8 a.u., respectively.

DISCUSSION

Label-free nonlinear spectral imaging microscopy (NLSM) was introduced as a novel minimally-invasive method to analyze the metabolic state of fungal hyphae by monitoring the autofluorescence of NAD(P)H and FAD (Chapter 3, Knaus et al. 2013a). These signals combined with the presence of melanin were used to monitor freshness of *A. bisporus* mushrooms that had been stored at 4 °C. It was found that the FAD / NAD(P)H and melanin / NAD(P)H ratios increased from 0.92 to 2.02 and from 0.76 to 1.53, respectively, during a 17 day storage period. This indicated that NLSM can be used to determine the freshness of mushrooms and to follow the postharvest browning process at an early stage. Here, NLSM was used to study development of *A. bisporus*. It is shown that aerial structures are more metabolically active than mycelium in compost and casing. Moreover, we present evidence that vegetative hyphae and aerial structures of *A. bisporus* contain low levels of melanin even in the absence of bruising or infection.

Oxidative phosphorylation in mitochondria results in the production of ATP by transferring electrons to molecular oxygen. During this process fluorescent NAD(P)H is oxidized to non-fluorescent NAD and non-fluorescent $FADH_2$ is oxidized to fluorescent FAD. In the cytosol, NAD is reduced to NAD(P)H during glycolysis. The FAD / NAD(P)H ratio can therefore be considered as an indicator of the metabolic state of a cell (Chance et al. 1979, Chance 1989). For instance, the ratio decreases when cells become highly active, such as in cancer cells (Chance 1989). The mycelium in the compost and in the casing layer is characterized by a high FAD and low NAD(P)H contribution, while aerial structures (aerial hyphae, primordia, and mushrooms) exhibited

higher NAD(P)H and lower FAD contributions. The absolute signal of NAD(P)H did not change when mycelium in the compost and mushrooms with a 4-cm-wide-cap were compared. On the other hand, FAD contribution and absolute signals correlated. Together, this points to a shift within the energy metabolism between the vegetative mycelium and the aerial structures. This finding is supported by gene expression studies, showing that the carbohydrate metabolism is different in vegetative mycelium and fruiting bodies (Patyshakuliyeva et al. 2013, Morin et al. 2012). Expression profiling and analysis of soluble sugars indicated that the vegetative mycelium consumes a wide variety of monosaccharides, while mushrooms only exhibit hexose catabolism. It was concluded that C6 sugars or their conversion products are transported from the colonizing mycelium to the developing fruiting bodies, while C6 and C5 sugars would provide energy for growth and maintenance of the vegetative mycelium.

The lower metabolic activity of hyphae in the compost and the casing cannot be attributed to a lack of nutrients. On the contrary, mycelium in the non-nutritious casing layer and the aerial structures depend on the mycelium in the compost for their nutrients. There is a flow of these nutrients from the mycelium in the compost, via the mycelium in the casing, to the developing mushrooms (Woolston et al. 2011). The FAD / NAD(P)H ratio may well be affected by availability of oxygen (Mayevsky and Chance 1975, Papandreou et al. 2006, Palero et al. 2011). Oxygen in the compost and casing may be limiting and thus causes reduced metabolic activity. In this study material was sampled before imaging. The time needed for sampling and start of imaging (less than 5 min) most likely changed the oxygen conditions and therefore oxygen does not seem to be the cause for the change in the FAD / NAD(P)H ratio in this case. It would be interesting to test the effect of oxygen by growing the mycelium in a growth chamber at the microscope stage.

Only 5-10 % of the primordia develop into a mushroom (Noble et al. 2003). It would be highly interesting to be able to predict which primordium develops into a mature mushroom. Possibly, this can be done by monitoring the FAD / NAD(P)H ratio. Variation in this ratio was found in the primordia but the sample number was too low to

distinguish distinct populations of primordia based on this ratio. Hence, it would be interesting to examine a much higher number of individuals at different days of development.

Primordia grow out rapidly to form a mushroom. After the cap has reached a diameter of 1 cm, further increase in diameter is exponential (Straatsma et al. 2013). Fruiting bodies with a 1 – 4 cm wide cap exhibited the lowest FAD / NAD(P)H ratio, while mushrooms with a cap of 8 cm already had a higher ratio, thus being less metabolically active. This and the data of Knaus et al. (2013a) suggest that small mushrooms have a longer shelf life than large ones. Preliminary studies indeed point in this direction.

NLSM is also capable to monitor the presence of melanin. So far, melanin has been related to bruising and infection of the mushrooms (Burton et al. 1993, Soler-Rivas et al. 2000, Soler-Rivas et al. 1999). Melanin formation is initiated in *A. bisporus* fruiting bodies by polyphenol oxidase mediated oxidation of phenols into quinones, which spontaneously polymerize into melanin (Jolivet et al. 1998). Weijn et al. (2013) presented evidence that GHB melanin is the main melanin responsible for browning of mushrooms. This melanin is formed from the intermediates γ-L-glutaminyl-4-hydroxybenzene (GHB) and γ-L-glutaminyl-3,4-dihydroxybenzene (GDHB). NLSM showed that aerial hyphae, primordia and mushroom caps contained some level of melanin despite their white appearance (they had not been exposed to bruising or a pathogen). Notably, hyphae in the compost and the casing contained higher levels of melanin when compared to the aerial structures. This suggests that melanin plays a role during vegetative growth. Possibly, it functions in defense in the compost and the casing to protect against the microbial flora and oxidative compounds in these substrates. Such a role has been suggested in the case of other fungi (Soler-Rivas et al. 2000, Eisenman and Casadevall 2012, Hegnauer et al. 1985, Nosanchuk and Casadevall 2003, Butler and Day 1998, Butler et al. 2005, Dadachova et al. 2007, Rosas et al. 2000). Future studies should reveal the identity of the melanin in the vegetative mycelium. It may be of the GHB type but could also be of the PAP, DOPA or catechol type (Jolivet et al. 1998). All these melanins result from the action of polyphenol oxidase. A polyphenol oxidase deficient strain may no

longer produce brown spots on the cap (which is of commercial interest) but may also have hyphae that are more sensitive to the conditions in the compost and the casing.

REFERENCES

Atkey PT, Wood DA (1984) Electron microscopic study of wheat straw degradation during composting. Appl Biochem Biotechnol 9: 335-336

Bels-Koning H (1950) Experiments with casing soils, water supply and climate. Mushroom Science 1: 78-84

Burton K, Love M, Smith J (1993) Biochemical changes associated with mushroom quality in *Agaricus spp.*. Enzyme MicrobTechnol 15: 736-741

Butler M, Day A (1998) Fungal melanins: a review. Can J Microbiol 44: 1115-1136

Butler M, Gardiner R, Day A (2005) Fungal melanin detection by the use of copper sulfide-silver. Mycologia 97: 312-319

Chance B (1989) Metabolic heterogeneities in rapidly metabolizing tissues. J Appl Cardiol 4: 207-221

Chance B, Schoener B, Oshino R, Itshak F, Nakase Y (1979) Oxidation-reduction ratio studies of mitochondria in freeze-trapped samples. NADH and flavoprotein fluorescence signals. J Biol Chem 254: 4764-4771

Chen Y, Chefetz B, Rosario R, van Heemst J, Romaine C, Hatcher P (2000) Chemical nature and composition of compost during mushroom growth. Compost Sci Util 8: 347-359

Dadachova E, Bryan RA, Huang X, Moadel T, Schweitzer AD, Aisen P, Nosanchuk JD, Casadevall A (2007) Ionizing radiation changes the electronic properties of melanin and enhances the growth of melanized fungi. PLoS One 2: e457

Eastwood DC, Herman B, Noble R, Dobrovin-Pennington A, Sreenivasaprasad S, Burton KS (2013) Environmental regulation of reproductive phase change in *Agaricus bisporus* by 1-octen-3-ol, temperature and CO_2. Fungal Genet Biol 55: 54-66

Eger G (1961) Untersuchungen ueber die Funktion der Deckschicht bei der Fruechtkoerperbildung des Kulturchampignons, *Psalliota bispora* Lge. Archiv fuer Mikrobiologie 39: 313-334

Eisenman HC, Casadevall A (2012) Synthesis and assembly of fungal melanin. Appl Microbiol Biotechnol 93: 931-940

Fereidouni F, Bader AN, Gerritsen HC (2012) Spectral phasor analysis allows rapid and reliable unmixing of fluorescence microscopy spectral images. Opt Express 20: 12729-12741

Flegg P (1956) The casing layer in the cultivation of the mushroom (*Psalliota hortensis*). Eur J Soil Sci 7: 168-176

Hegnauer H, Nyhlén LE, Rast DM (1985) Ultrastructure of native and synthetic *Agaricus bisporus* melanins - Implications as to the compartmentation of melanogenesis in fungi. Exp Mycol 9: 1-29

Huang S, Heikal AA, Webb WW (2002) Two-photon fluorescence spectroscopy and microscopy of NAD(P)H and flavoprotein. Biophys J 82: 2811-2825

Iiyama K, Stone BA, Macauley BJ (1994) Compositional changes in compost during composting and growth of *Agaricus bisporus*. Appl Environ Microbiol 60: 1538-1546

Iiyami K, Lam TBT, Stone BA, Macauley BJ (1996) Characterisation of material generated on the surface of wheat straw during composting for mushroom production. J Sci Food Agric 70: 461-467

Jolivet S, Arpin N, Wichers HJ, Pellon G (1998) *Agaricus bisporus* browning: a review. Mycol Res 102: 1459-1483

Kalberer PP (1987) Water potentials of casing and substrate and osmotic potentials of fruit bodies of *Agaricus bisporus*. Scientia Horticulturae 32: 175-182

Knaus H, Blab GA, Agronskaia AV, van den Heuvel D J, Gerritsen HC, Wösten HAB (2013a) Monitoring the metabolic state of fungal hyphae and the presence of melanin by nonlinear spectral imaging. Appl Environ Microbiol 79: 6345-6350

Knaus H, Blab GA, van Veluw GJ, Gerritsen HC, Wösten HAB (2013b) Label-free fluorescence microscopy in fungi. Fungal Biol Rev 27: 60-66

Kozarski M, Klaus A, Niksic M, Jakovljevic D, Helsper JP, Van Griensven LJ (2011) Antioxidative and immunomodulating activities of polysaccharide extracts of the medicinal mushrooms *Agaricus bisporus*, *Agaricus brasiliensis*, *Ganoderma lucidum* and *Phellinus linteus*. Food Chem 129: 1667-1675

Kurtzman Jr RH (1997) Nutrition from mushrooms, understanding and reconciling available data. Mycoscience 38: 247-253

Laiho LH, Pelet S, Hancewicz TM, Kaplan PD, So PTC (2005) Two-photon 3-D mapping of ex vivo human skin endogenous fluorescence species based on fluorescence emission spectra. J Biomed Opt 10: 024016

Mattila P, Könkö K, Eurola M, Pihlava J, Astola J, Vahteristo L, Hietaniemi V, Kumpulainen J, Valtonen M, Piironen V (2001) Contents of vitamins, mineral elements, and some phenolic compounds in cultivated mushrooms. J Agric Food Chem 49: 2343-2348

Mayevsky A, Chance B (1975) Metabolic responses of the awake cerebral cortex to anoxia hypoxia spreading depression and epileptiform activity. Brain Res 98: 149-165

Morin E, Kohler A, Baker AR, Foulongne-Oriol M, Lombard V, Nagye LG, Ohm RA, Patyshakuliyeva A, Brun A, Aerts AL, Bailey AM, Billette C, Coutinho PM, Deakin G, Doddapaneni H, Floudas D, Grimwood J, Hildén K, Kües U, Labutti KM, Lapidus A, Lindquist EA, Lucas SM, Murat C, Riley RW, Salamov AA, Schmutz J, Subramanian V, Wösten HAB, Xu J, Eastwood DC, Foster GD, Sonnenberg AS, Cullen D, de Vries RP, Lundell T, Hibbett DS, Henrissat B, Burton KS, Kerrigan RW, Challen MP, Grigoriev IV M, F. (2012) Genome sequence of the button mushroom *Agaricus bisporu*s reveals mechanisms governing adaptation to a humic-rich ecological niche. Proc Natl Acad Sc USA 109: 17501-17506

Noble R, Fermor TR, Lincoln S, Dobrovin-Pennington A, Evered C, Mead A, Li R (2003) Primordia initiation of mushroom (*Agaricus bisporus*) strains on axenic casing materials. Mycologia 95: 620-629

Noble R, Dobrovin-Pennington A, Hobbs PJ, Pederby J, Rodger A (2009) Volatile C8 compounds and pseudomonads influence primordium formation of *Agaricus bisporus*. Mycologia 101: 583-591

Nosanchuk JD, Casadevall A (2003) The contribution of melanin to microbial pathogenesis. Cell Microbiol 5: 203-223

Palero JA, Bader AN, de Bruijn HS, van den Heuvel A, Sterenborg HJCM, Gerritsen HC (2011) In vivo monitoring of protein-bound and free NADH during ischemia by nonlinear spectral imaging microscopy. Biomed Opt Express 2: 1030-1039

Palero JA, de Bruijn HS, van der Ploeg van den Heuvel A, Sterenborg HJCM, Gerritsen HC (2007) Spectrally resolved multiphoton imaging of in vivo and excised mouse skin tissues. Biophys J 93: 992-1007

Palero JA, de Bruijn HS, van der Ploeg-van den Heuvel A, Sterenborg HJCM, Gerritsen HC (2006) In vivo nonlinear spectral imaging in mouse skin. Opt Express 14: 4395-4402

Papandreou I, Cairns RA, Fontana L, Lim AL, Denko NC (2006) HIF-1 mediates adaptation to hypoxia by actively downregulating mitochondrial oxygen consumption. Cell metabolism 3: 187-197

Patyshakuliyeva A, Jurak E, Kohler A, Baker A, Battaglia E, de Bruijn W, Burton KS, Challen MP, Coutinho PM, Eastwood DC, Gruben BS, Mäkelä MR, Martin F, Nadal M, van den Brink J, Wiebenga A, Zhou M, Henrissat B, Kabel M, Gruppen H and de Vries RP (2013) Carbohydrate utilization and metabolism is highly differentiated in *Agaricus bisporus*. BMC Genomics 14: 663-677

Rosas ÁL, Nosanchuk JD, Gómez BL, Edens WA, Henson JM, Casadevall A (2000) Isolation and serological analyses of fungal melanins. J Immunol Methods 244: 69-80

Soler-Rivas C, Arpin N, Olivier JM, Wichers HJ (2000) Discoloration and tyrosinase activity in *Agaricus bisporus* fruit bodies infected with various pathogens. Mycol Res 104: 351-356

Soler-Rivas C, Jolivet S, Arpin N, Olivier JM, Wichers HJ (1999) Biochemical and physiological aspects of brown blotch disease of *Agaricus bisporus*. FEMS Microbiol Rev 23: 591-614

Straatsma G, Sonnenberg ASM, van Griensven LJLD (2013) Development and growth of fruit bodies and crops of the button mushroom, *Agaricus bisporus*. Fungal Biology 117: 697-707

Teuchner K, Ehlert J, Freyer W, Leupold D, Altmeyer P, Stücker M, Hoffmann K (2000) Fluorescence studies of melanin by stepwise two-photon femtosecond laser excitation. J Fluoresc 10: 275-275

Umar MH, van Griensven LJLD (1997) Morphological studies on the life span, developmental stages, senescence and death of fruit bodies of *Agaricus bisporus*. Mycol Res 101: 1409-1422

Wani BA, Bodha R, Wani A (2010) Nutritional and medicinal importance of mushrooms. J Med Plant Res 4: 2598-2604

Weijn A, van den Berg-Somhorst, Dianne BPM, Slootweg JC, Vincken JP, Gruppen H, Wichers HJ, Mes JJ (2013) Main Phenolic Compounds of the Melanin Biosynthesis Pathway in Bruising-Tolerant and Bruising-Sensitive Button Mushroom (*Agaricus bisporus*) Strains. J Agric Food Chem 61: 8224-8231

Woolston BM, Schlagnhaufer C, Wilkinson J, Larsen J, Shi Z, Mayer KM, Walters DS, Curtis WR, Romaine CP (2011) Long-distance translocation of protein during morphogenesis of the fruiting body in the filamentous fungus, *Agaricus bisporus*. Plos One 6: e28412

CHAPTER 5

Fluorescence intensity enhancement of fungal melanin and its precursors

Helene Knaus, Frank J. J. Segers, Alexandra V. Agronskaia, Wieke R. Teertstra, Gerhard A. Blab, Jan Dijksterhuis, Hans C. Gerritsen, Han A. B. Wösten. In preparation.

ABSTRACT

Melanin protects fungi against microbial attack, host defense and environmental stresses such as oxidizing agents and UV light. Melanin can be synthesized via different pathways even in a single fungal species, making this a heterogeneous macromolecule. Human and *Sepia officinalis* eumelanin shows extraordinary behavior. Its emission is enhanced by several orders of magnitude after it is illuminated with a high level of near-infrared light. Here it is shown that this effect is irreversible and can also be observed in the case of synthetic melanin and melanin isolated from spores of *Aspergillus niger*. Also reproductive structures and vegetative mycelium of *A. niger* and *Agaricus bisporus* showed the same behavior. Moreover, spores of *A. niger* strains that are blocked in one of the steps in the melanin pathway displayed enhanced fluorescence intensity upon exposure to strong near-infrared light. Together, several types of melanin and melanin precursors (or their derived pigments) show the phenomenon of enhanced fluorescence intensity. This property can be used to monitor the presence of melanin or its precursors in a sensitive way. Our data suggest that melanin-like pigments form a structural component of the fungal cell wall next to cell wall polysaccharides and proteins.

INTRODUCTION

Fungi play important roles in nature. They are essential for conversion of dead organic material and they establish mutual beneficial and parasitic interactions. Fungi are also important for mankind. For instance, they are used as a food source and to process food (Mattila et al. 2001). Moreover, fungi are utilized as cell factories for the production of therapeutic compounds (Berends et al. 2009, Kozarski et al. 2011, Jeong et al. 2010), enzymes (Punt et al. 2002, Conesa et al. 2001, Krijgsheld et al. 2012), and metabolites such as organic acids (Andersen et al. 2011, Papagianni 2007). In the past, pigments of mushrooms were used as natural dyes for textiles (Bechtold and Mussak 2009). Apart from mushrooms and other sexual reproductive bodies, also vegetative mycelium, asexual reproductive structures and asexual and sexual spores can be pigmented. Pigmentation can change or be induced by infections or mechanical damaging (Burton et al. 1993, Soler-Rivas et al. 2000, Soler-Rivas et al. 1999, Knaus et al. 2013a). It is an important classification feature in fungal taxonomy (Guarro et al. 1999, Iwen 2011).

Many pigments contain phenolic and indolic compounds (Zhou and Liu 2010). Melanin is the best known representative of these pigments. It is a complex molecule that is involved in virulence and defense against environmental stresses such as oxidizing agents and UV light (Soler-Rivas et al. 2000, Eisenman and Casadevall 2012, Hegnauer et al. 1985, Nosanchuk and Casadevall 2003, Butler and Day 1998, Butler et al. 2005, Dadachova et al. 2007, Rosas et al. 2000, Cunha et al. 2010, Wang and Casadevall 1994). Many fungi, including *Aspergillus spp.* synthesize melanin by polymerization of 1,8- dihydroxynaphthalene (DHN) (Wheeler 1983, Bell and Wheeler 1986) (Figure 1). *Aspergillus fumigatus* also produces pyomelanin. Pyomelanin is synthesized from homogentisate (HGA), which is an intermediate in the tyrosine degradation pathway (Schmaler-Ripcke et al. 2009) (Figure 1). Four melanin synthesis pathways have been proposed in the case of the mushroom forming fungus *Agaricus bisporus* (Jolivet et al. 1998, Weijn et al. 2013a). Three of these pathways start from chorismate, which is enzymatically converted into L-DOPA, γ-L-glutaminyl-4-hydroxybenzene (GHB)

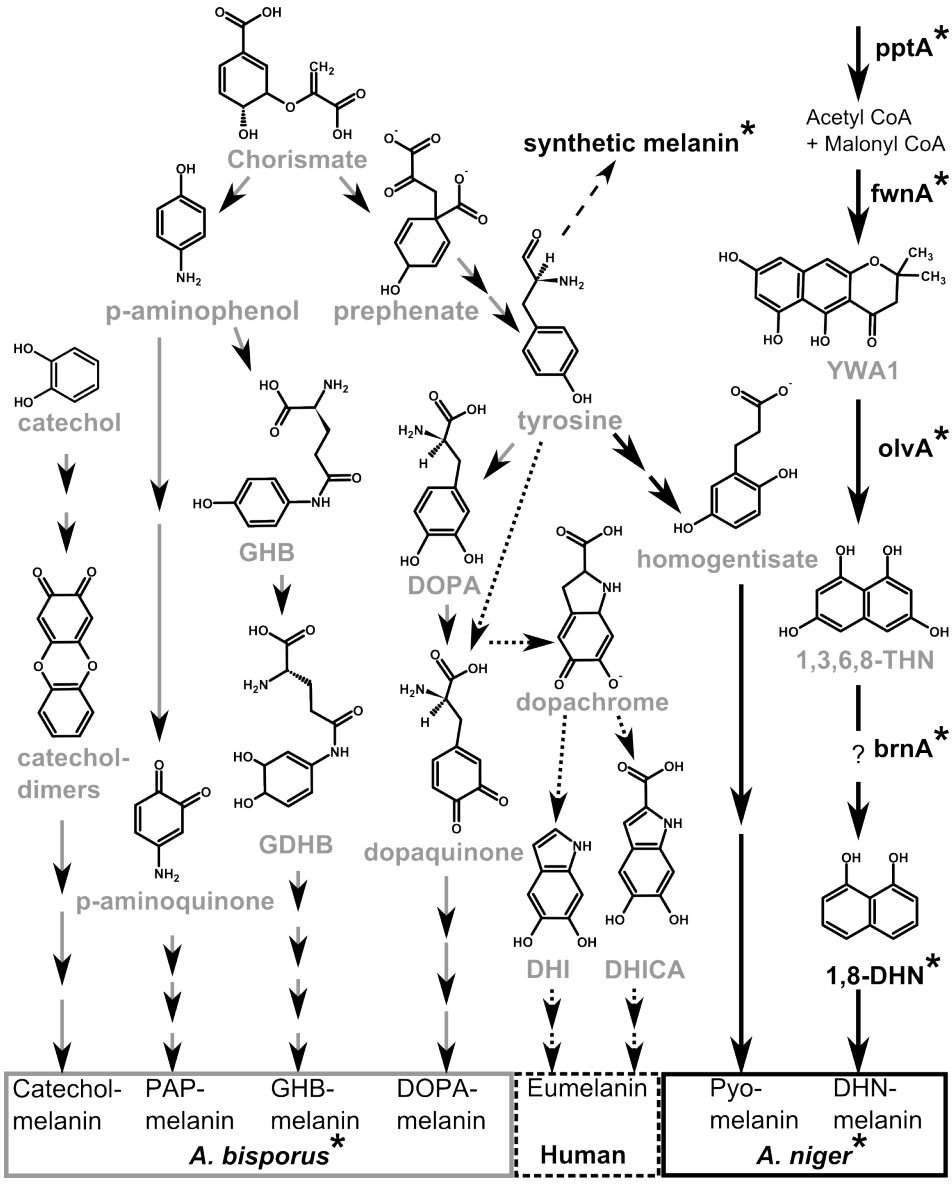

Figure 1. Proposed melanin synthesis pathways of *A. niger* (black, solid), *A. bisporus* (grey, solid) and of human eumelanin (black, dotted). Absence of genes encoding enzymes in the DHN-melanin pathway (*pptA, fwn, olvA, brnA*) leads to *A. niger* strains that produce spores with different colors when compared to the black spores of the wild-type. Strains or pigments with a star were examined during this study. YWA1, heptaketide naphtopyrone;

or p-aminoquinone, leading to the formation of DOPA-, GHB- and PAP-melanin, respectively. The fourth melanin pathway starts from catechol and leads to the formation of catechol-melanin (Figure 1). It should be noted that the understanding of the pathways leading to fungal melanin is still far from complete.

Nonlinear spectral microscopy (NLSM) has recently been introduced to study development and freshness of fruiting bodies of *A. bisporus* (Knaus et al. 2013a), Chapter 3 and 4). By using near-infrared excitation, NLSM monitors autofluorescence of NAD(P)H, FAD, and melanin in a non-invasive way. NLSM combines biochemical and spatial information by mapping emission spectra comprised of the individual spectra of the endogenous fluorophores that are present in the specimen (Huang et al. 2002, Laiho et al. 2005, Palero et al. 2007). The contribution of these fluorophores can be distinguished by their spectral characteristics (spectral width and maximum emission). For instance, NAD(P)H and FAD have maximum emissions in the blue (460 nm) and green (530 nm) wavelength range, respectively (Huang et al. 2002). Amongst other endogenous fluorophores in fungi (Knaus et al. 2013b), NAD(P)H and FAD are spectrally well characterized and show a photophysical behavior similar to other common fluorophores. This means they can be brought into an excited state and emit fluorescence when falling back to the ground state. Excitation light can also induce permanent changes in the structure of a fluorophore. As a result, the molecule can no longer be excited and thus is photobleached. How often a fluorophore can be brought in an excited state depends on the molecular structure and environment of the fluorophore (Lakowicz 2006). Eumelanin in black human hair or isolated from ink sacs of the cuttlefish *Sepia officinalis* behaves photophysically very differently (Kerimo et al. 2011). Fluorescence emission is enhanced by several orders of magnitude after it is illuminated with a high level of near-

1,3,6,8-THN, 1,3,6,8-tetrahydroxynaphtalene; 1,8-DHN, 1,8-dihydroxynaphthalene; GHB, γ-L-glutaminyl-4-hydroxybenzene; GDHB, γ-L-glutaminyl-3,4-dihydroxybenzene; DOPA, L-3,4-dihyroxyphenylalanine; DHI, 5,6-dihydroxyindole; DIHCA, 5,6-dihydroxyindole-2-carboxylic acid (adapted from Jolivet et al. 1998, Weijn et al. 2013a, Jørgensen et al. 2011, Krijgsheld et al. 2013, Borovansky and Riley 2011).

infrared light. This remarkable photophysics is probably due to the molecular structure of melanin. However, the eumelanin structure is still not known, as it is a highly insoluble and heterogeneous macromolecule (Watt et al. 2009). Two secondary structures of eumelanin have been proposed but they are still controversial. One model assumes that monomers form a large extended heteropolymer (Longuet-Higgins 1960, Pullman and Pullman 1961), while the other model suggests that 5 to 6 monomers are arranged in planar sheets (graphite like stacking) to form oligomeric nanostructures that make up eumelanin (Watt et al. 2009, Zajac et al. 1994). NLSM showed that melanin could have a contribution of up to 30% of the total autofluorescence (Knaus et al. 2013a, Chapter 4). We here show that melanin of *A. bisporus* and *A. niger* also shows intensity enhancement as was described for eumelanin (Kerimo et al. 2011). By using pigmentation mutants of *A. niger* (Jørgensen et al. 2011) and melanin precursors, it is shown that the intermediates in the melanin pathway (or their derived pigments) also show intensity enhancement.

MATERIALS AND METHODS

Strains and growth conditions.

A. bisporus (Sylvan A15) was grown on a polycarbonate membrane (0.1 μm pore size, 76 mm in diameter, Maine Manufacturing, LLC, Sanford, USA) on autoclaved compost agar. Compost agar was prepared by homogenizing 150 gram wet weight phase III A15 pre-colonized compost (CNC Grondstoffen, Milsbeek, The Netherlands) in a Waring blender 6 times 1 min at high speed. The homogenized compost was sterilized at 123 °C for 3 times 20 min and mixed with 3 % agar in a 1:1 ratio. Mushrooms of *A. bisporus* (Sylvan A15) were grown as described (Knaus et al. 2013a). Plastic containers (17.5 x 27.5 x 22.5 cm) were filled with 3.5 kg phase-III A15 pre-colonized compost and topped with 1 kg of casing soil (CNC Grondstoffen). The cultures were incubated at 24 °C and 95 % relative humidity (RH) in Economic Premium Climate Chambers (Snijders Scientific, Tilburg, The Netherlands). They were watered during the first 4 days of cultivation with 200 ml per container per day. Growth was prolonged at 20 °C and

88 % RH at the moment aggregates had formed (i.e. after 9 days of culturing). Intact and bruised mushrooms of *A. bisporus* were harvested right before imaging. Bruising was induced by applying a moderate pressure to the skin of the mushroom caps 24 h before imaging. *A. bisporus* spores were obtained by placing a mushroom cap on a coverslip, until the spores were released. Mycelium was imaged after placing a 0.5 cm x 1 cm piece of a colony on a coverslip. Mycelium was fixed with 4 % paraformaldehyde for 30 min on ice and washed 3 times 2 min in demi water while gently shaking.

A. niger strains (Table 1) were grown on solid complete medium (CM) with 2 % glucose (van Veluw et al. 2012). For imaging *A. niger* spores were stamped from a piece of a 4 day old colony onto a coverslip.

Table 1. Strains used in this study.

Strains	Parent	Genotype	Reference
N402			(Bos et al. 1988)
JP1.1	AB4.1	*pptA::AopyrG*	(Jørgensen et al. 2011)
MA93.1	N402	*fwnA::hygB*	(Jørgensen et al. 2011)
AW8.4	MA169.4	*olvA::AopyrG*	(Jørgensen et al. 2011)
AW6.1	MA169.4	*brnA::AopyrG*	(Jørgensen et al. 2011)

Chemicals and isolation of melanin.

Synthetic melanin (M8631-100MG, purity ≥ 97 %, prepared by oxidation of tyrosine with hydrogen peroxide) and 1,8-dihydroxynaphthalene (DHN, 740683-1G, purity ≥ 94.5 %) were purchased from Sigma-Aldrich Chemie (Schnelldorf, Germany). Melanin of *A. niger* was isolated from spores of strain N402. To this end, spores were harvested with 40 ml water from 10-day-old colonies (i.e. about 1×10^{10} conidia) and 40 µl 10 M NaOH was added to dissociate melanin (Wargenau et al. 2011). Spores were pelleted by centrifuging twice at 6000 rpm for 10 min. The supernatant was adjusted to pH 1 with 1 M HCl allowing the melanin to precipitate during a 30 min incubation at

room temperature. The melanin was pelleted at 12000 rpm for 10 min and resuspended in water. The pellet resulting from a 10 min centrifugation step at 12000 rpm was dried over night at 65 °C resulting in 30.6 mg melanin. Melanin was stored in a desiccator containing silica gel.

Nonlinear spectral imaging.

Nonlinear spectral images were acquired with the imaging setup described in Chapter 2. The laser had a repetition rate of 80 MHz and a pulse width of 140 fs. An excitation wavelength of 740 nm and a CFI Apo LWD 25x water objective with NA 1.1 (Nikon Instruments Europe, Amsterdam, The Netherlands) were used. The pixel dwell time was 400 μs. All samples were imaged dry. Areas of 100 x 100 μm (256 x 256 pixels) of mycelium or mushroom were imaged followed by imaging part of this area (25 x 25 μm; 256 x 256 pixels) several times to obtain the peak power density resulting in enhancement of melanin fluorescence intensity. Images were then taken again with a field of view of 100 x 100 μm (256 x 256 pixels). Spores were imaged in a series of four sequential scans of 25 x 25 μm (128 x 128 pixels), each taking 6.6 s.

Data analysis.

For visualization, spectral images were represented in real color. To this end, spectral information of each pixel was transformed into RGB values that resemble the color of the fluorescence emission as perceived by eye (Palero et al. 2006). Data was background subtracted before spectral analysis. Peak power density, $P_{Density}$, was calculated as: $P_{Density} = P_{avr} \times (f \times \Delta t)^{-1} \times (\pi \times R^2)^{-1}$. With P_{avr} being the average laser power, f the repetition rate of the laser, Δt the pulse width of the laser and R the laser beam radius. R was derived from the airy disk (Gaussian approximation for open pinhole) as $R = 0.21 \times \lambda_{em} \times NA^{-1}$ with λ_{em} being the emission wavelength and NA the numerical aperture of the objective (Thomann et al. 2002).

RESULTS

Fluorescence enhancement of human eumelanin has been previously reported (Kerimo et al. 2011). A time series of nonlinear spectral images was made to assess whether the same effect could be observed in the case of *A. bisporus* spores (Figure 2A). Samples were exposed to 4 scans of 4.75×10^8 kW/cm^2. Autofluorescence of a spore (blue circle) was relatively low in the first scan, increased to its maximum in the second scan, and decreased again in the third and fourth scan (Figure 2B, filled circles). During these last two scans this spore had been destroyed. Notably, sufficient laser power focused on part of the spore led to enhanced fluorescence intensity over the whole spore. Additionally, the difference in intensity before and during the enhancement was extremely large (about 15,000 fold), meaning that at first the signal was close to the detection limit and then increased instantly to saturate the detector. The latter caused that NLSM images of spores often appeared yellow-green during the enhanced state and not orange-red (Figure 2D). The same enhancement behavior was observed with synthetic melanin and melanin isolated from *A. niger* N402 spores upon exposure to 4 scans of 1.70×10^8 kW/cm^2 and 23.40×10^8 kW/cm^2, respectively (Figure 2B). The *A. bisporus* spore and the two melanins showed the same emission spectrum (Figure 2C). In contrast, dry solid DHN monomers emitted in the blue spectral range (emission maximum outside of the detection range, Figure 2C, grey dashed curve). Yet, after absorbing high powers, dendritic structures had formed around the solid DHNs (Figure 3). These structures also showed enhanced fluorescence intensity and a red emission after exposure to a high level of near-infrared light (Figure 2B, C).

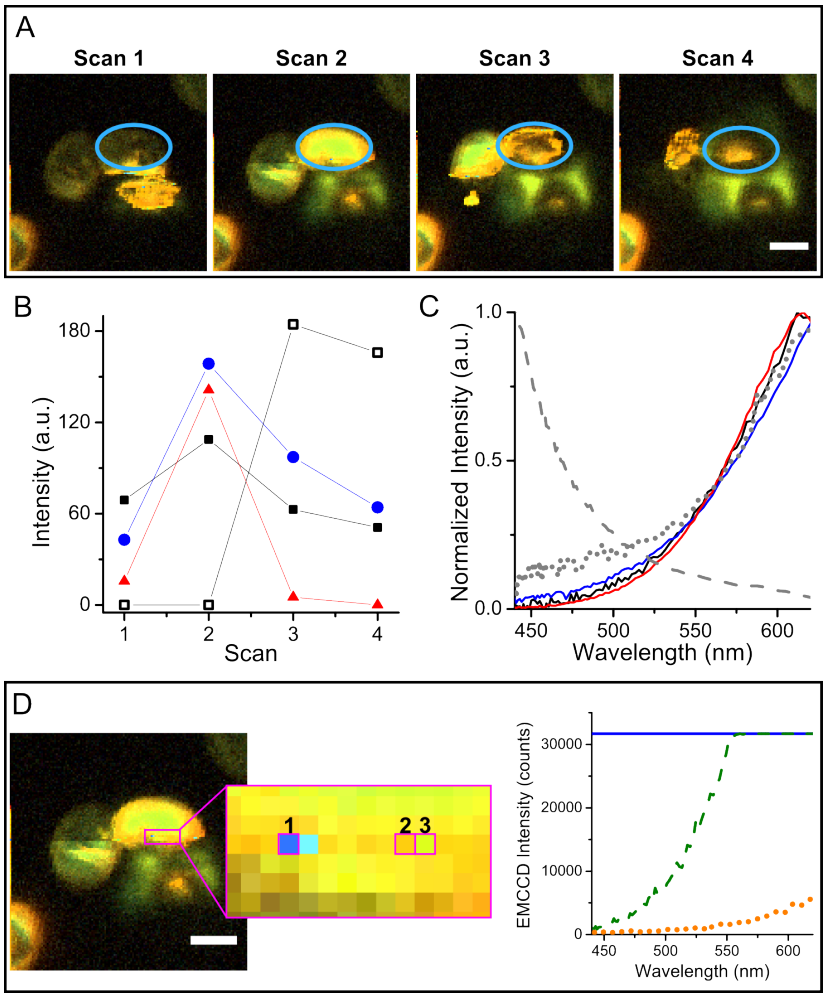

Figure 2. Fluorescence enhancement of melanin when exposed to near-infrared light. (**A**) Nonlinear spectral images of a spore of *A. bisporus* (blue circle) imaged sequentially four times at an average power of 2.8 mW (peak power density = 4.75×10^8 kW/cm^2). Bar represents 5 μm. (**B**) Average intensity of the *A. bisporus* spore (filled circles; see A), melanin isolated from *A. niger* N402 spores (filled triangles), synthetic melanin (filled squares), and DHN dendritic structures resulting from strong laser radiation (empty squares). (**C**) Normalized spectra after intensity enhancement of an *A. bisporus* spore (blue solid curve), melanin isolated from *A. niger* N402 spores (solid red curve), synthetic melanin (solid black curve), DHN (dashed grey curve) and

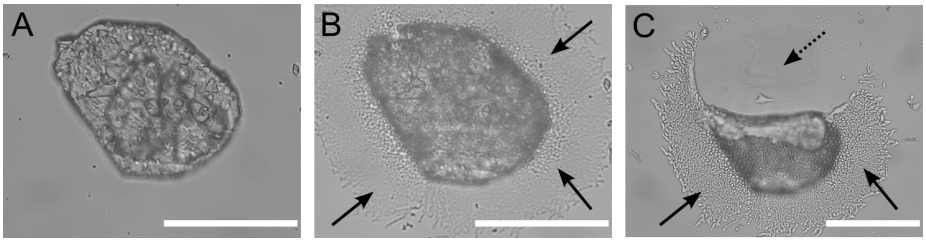

Figure 3. Images of solid, dry, synthetic DHN before (**A**) and after (**B-C**) absorbing high level near-infrared light. Solid arrows indicate dendritic structures, which are formed upon strong laser radiation. These dendritic structures show fluorescence enhancement and spectra in the red spectral range (Figure 2B, C). Dotted arrow indicates area where dendritic structures were destroyed due to strong laser radiation. Bar represents 50 μm.

Spectral unmixing of NLSM images indicated for the first time that melanin was present in vegetative mycelium that appeared white by eye (Chapter 4). Fresh and paraformaldehyde-fixed *A. bisporus* mycelium did not show enhancement of fluorescence at a peak power density of 4.75×10^8 kW/cm^2 like observed with spores of *A. bisporus*. Yet, a 2-fold enhanced fluorescence was measured when fresh and fixed mycelium was exposed to three scans of 37.30×10^8 kW/cm^2 and 45.78×10^8 kW/cm^2, respectively (Figure 4). Notably, in this case the yellow-orange emission is not a detection artifact, but a result of the low pigment concentration (when compared to spores) and the contribution of other endogenous fluorophores emitting in the green spectral wavelength range (data not shown). Intensity enhancement was only detected in the cell wall of hyphae and not in the cytoplasm. Most importantly, this experiment demonstrates that high level of near-

DHN dendritic structures resulting from strong laser radiation (dotted grey curve). (**D**) RGB-representation artifact of spectra saturating the detector. Nonlinear spectral image (left side) of an *A. bisporus* spore after fluorescence enhancement. Zoomed-in region shows RGB representation of single oversaturated pixels (1-3). On the right, spectra of the pixels highlighted in the left image, where position 1 is the blue solid curve, 2 the orange dotted curve and 3 the green dashed curve. Positions 1 and 3 were saturating the detector. The shorter the wavelength at which the saturation takes place, the more blue-shifted the artifact in the RGB-representation occurs. Position 2 shows a spectrum, which is not saturating the detector and thus appears in the correct color. Bar represents 5 μm.

infrared light does not induce enzymatic melanin formation in *A. bisporus* mycelium, as similar results were found for fresh and paraformaldehyde-fixed mycelium (Figure 4).

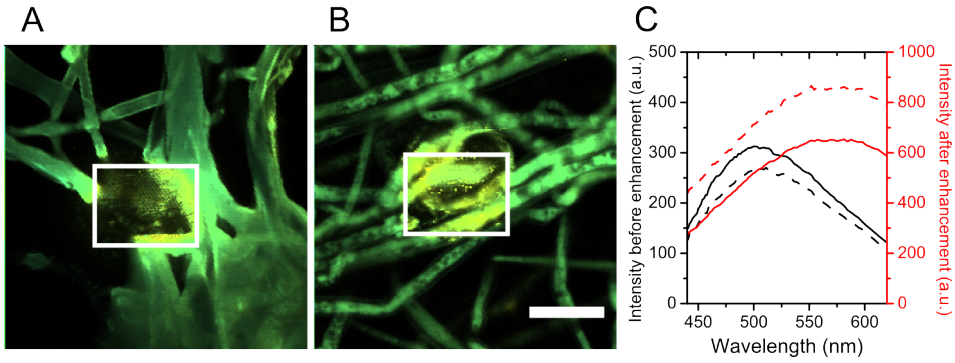

Figure 4. Nonlinear spectral images of fresh (**A**) and fixed (**B**) *A. bisporus* mycelium grown on compost based agar. Prior to acquisition, an area of 25 x 25 μm (red square) was three times exposed to a power of (A) 22 mW (peak power density = 37.30×10^8 kW/cm^2) and (B) 27 mW (peak power density = 45.78×10^8 kW/cm^2). (**C**) Spectra of the areas in the white squares. Solid curves represent fixed mycelium and dashed curves fresh mycelium. Black and red curves represent the spectra before and after exposure to high powers, respectively. Bar represents 25 μm.

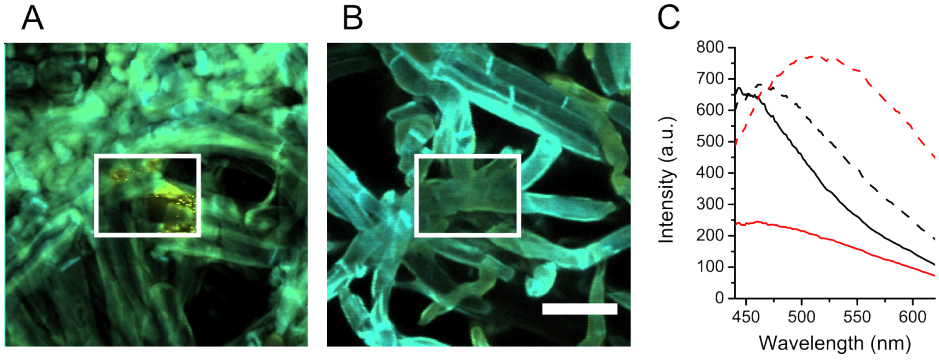

Figure 5. Nonlinear spectral images of a bruised (**A**) and intact (**B**) *A. bisporus* mushroom cap. Prior to acquisition, an area of 25 x 25 μm (red square) was five times exposed to a power of 17 mW (peak power density = 28.82×10^8 kW/cm^2). (**C**) Spectra of the areas in the white squares. Solid curves represent the intact cap, dashed curves the bruised cap. Black and red curves represent the spectra before and after exposure to high powers, respectively. Bar represents 25 μm.

An area of 25 x 25 μm of intact (white cap) and bruised (brown cap) mushrooms was exposed to 17 mW for five scans (i.e. peak power density of 28.82×10^8 kW/cm^2). The bruised spots that are characterized by increased levels of melanin showed red-shifted fluorescence spectra. The intact mushroom caps only showed bleaching of the blue spectral part (Figure 5). However, intensity enhancement was observed after 2 scans when the peak power density on intact caps was increased to 37.30×10^8 kW/cm^2 (data not shown). These results indicate that fluorescence enhancement of mushroom pigment (i.e. melanin) is concentration and peak power density dependent.

In the next set of experiments spores of the wild-type *A. niger* strain N402 were imaged as well as those of *A. niger* deletion strains affected in pigmentation. While the wild-type produces black spores, spores of the deletion strains are white (Δ*pptA*), fawn (Δf*wn*), olive (Δ*olv*) and brown (Δ*brn*). In all cases enhancement of fluorescence emission was observed (Figure 6). Yet, the darker the pigment, the less laser power was needed to observe enhanced fluorescence. Enhancement of fluorescence was only observed when laser light was focused on the cell wall. Spores, which didn't show enhanced fluorescence appeared to have a blue emission in the cytosol, which can be attributed to NAD(P)H (Figure 6, sum of all scans). This is most obvious for spores formed by Δ*pptA* and Δ*fwn*. The NAD(P)H signal was shown to be very stable since its fluorescence was still observed after storage of the spores for 6 days at room temperature. The NAD(P)H signal was not clear in RGB images of darker spores as those of N402 due to the impact of the pigment (e.g. absorption of excitation light, reabsorption of NAD(P)H emission, autofluorescence of the pigment).

Not only spores, but also vegetative mycelium of wild-type *A. niger* N402 and Δ*pptA* was examined by NLSM. In both cases enhancement of fluorescence intensity and a red-shift in spectrum was detected after 2 scans at a peak power density of 28.82×10^8 kW/cm^2 (Figure 7). These data indicate that both mycelia contain melanin or a related precursor pigment despite its white appearance by eye.

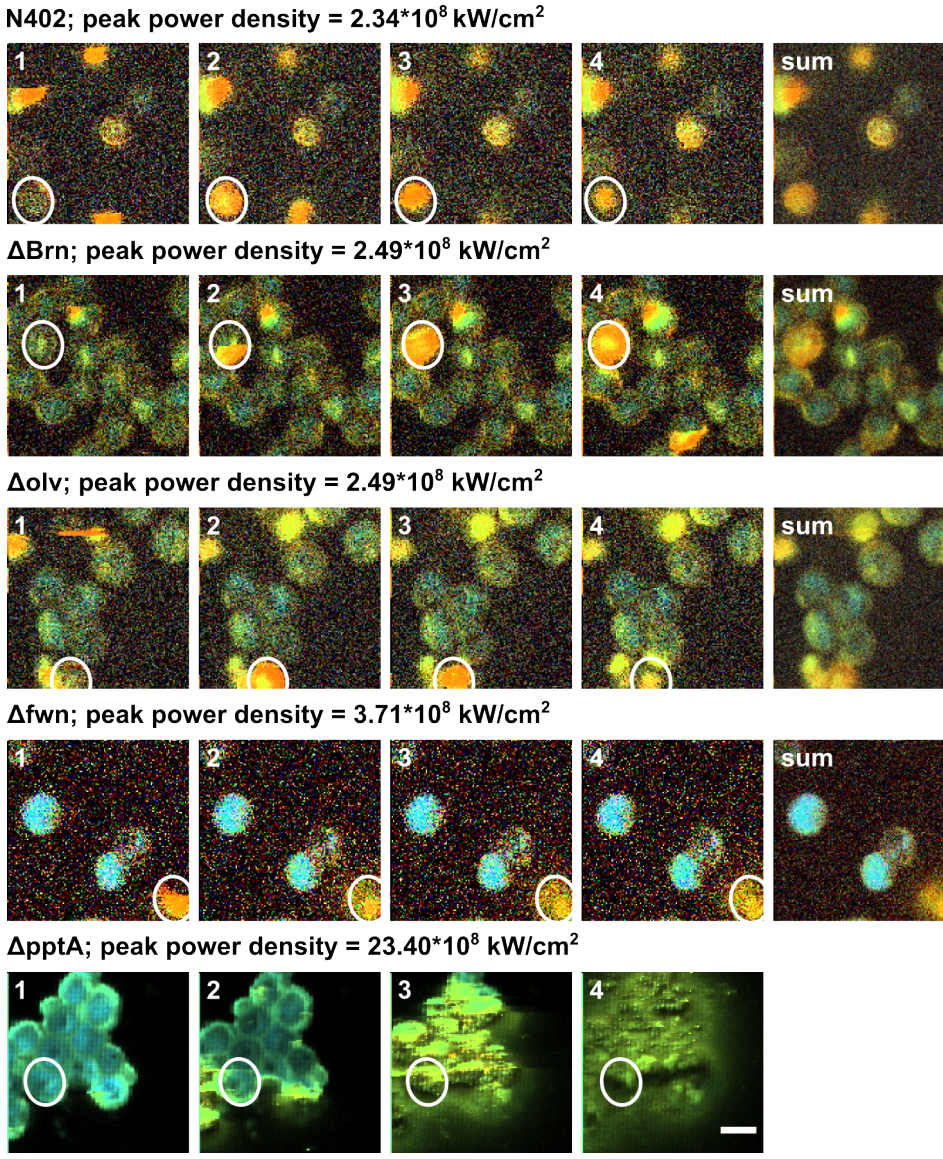

Figure 6. Nonlinear spectral images of spores of wild-type *A. niger* and its pigmentation mutants imaged sequentially four times (1-4) at the given peak power density. Sum column represents the sum of all four images. Spores were harvested from the conidiophores right before imaging. White circles highlight spores undergoing fluorescence intensity enhancement. Bar represents 5 μm.

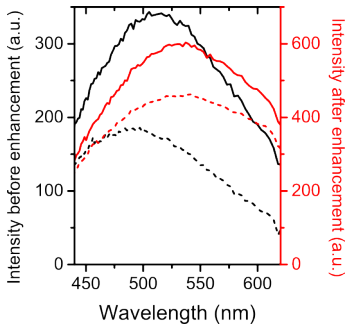

Figure 7. Emission spectra of *A. niger* mycelium taken from a 25 x 25 µm area, which was two times exposed to 17 mW (peak power density = 28.82×10^8 kW / cm^2). Solid curves represent strain Δ*pptA* and dashed curves strain N402. Black and red curves represent the spectra before and after exposure to high powers, respectively.

DISCUSSION

Many fungi synthesize melanin for protection against microbial enzymatic lysis in natural soils (Butler and Day 1998, Bull 1970), oxidative stress (Cunha et al. 2010, Wang and Casadevall 1994) and UV-radiation or gamma-radiation (Schweitzer et al. 2009,Felix et al. 1978). The latter is changing the electronic properties of melanin and leads to an enhanced growth of fungi, suggesting that fungal melanin converts radiation into a metabolically useful energy source (Dadachova et al. 2007). Moreover, melanin is important for virulence (Nosanchuk and Casadevall 2003, Salas et al. 1996, Heinekamp et al. 2012). For instance, it is instrumental in building up a turgor pressure of 80 bar in appressoria. This turgor pressure allows the fungus to mechanically invade plants (Howard et al. 1991). Melanin formation is induced in *A. bisporus* by infections or storage and handling (Soler-Rivas et al. 2000, Jolivet et al. 1998, Berendsen et al. 2010). Browning of the mushrooms causes a decrease in commercial value, which one tries to overcome by either blocking melanin formation or by selecting bruising-insensitive strains (Weijn et al. 2013b).

Different types of melanin exist, but they have common photophysical properties like an extremely low fluorescence quantum yield (weak emitter) (Meredith and Riesz 2004) and a broad absorption spectrum, decaying exponentially from the UV to the near-infrared (Teuchner et al. 2000). Enhancement of fluorescence intensity caused by illumina-

tion of a high level of near-infrared light was demonstrated for eumelanin (Kerimo et al. 2011). We observed the same behavior with synthetic melanin and melanin isolated from spores of *A. niger*. The effect of fluorescence enhancement was irreversible and noncumulative. This contrasts with the observations of (Kerimo et al. 2011). It is still unclear what happens at the molecular level. Kerimo et al. (2011) speculated that the heat generated by light absorption induces molecular changes leading to an increased fluorescence emission. Another explanation could be free radical production upon electromagnetic radiation (Dadachova et al. 2007).

Spores of *A. bisporus* and *A. niger* also showed enhanced fluorescence upon exposure to strong infrared light. Data indicate that this is due to the melanin contained in the cell wall of these spores. Even spores of the pigmentation mutants of *A. niger* showed the phenomenon of enhanced fluorescence. These spores have different colors because these mutants accumulate each a different melanin precursor or a pigment derived of these precursors. It is so far unclear if the precursors are present as monomers or assemble in a pigment with melanin-like properties. However, our experiments show that melanin and its precursors (or their derived pigments) have a similar autofluorescence spectrum. The peak power density needed to induce enhanced fluorescence is increased when the pigment is less dark. Fluorescence enhancement in spores of the Δ*pptA* mutant was unexpected. The Δ*pptA* mutant lacks the gene encoding phosphopantetheinyl transferase necessary to synthetize melanin via the DHN pathway. Although some of the genes involved in DHN-melanin synthesis are missing, *A. niger* is assumed to form DHN-melanin (Jørgensen et al. 2011). *A. fumigatus* produces DHN-melanin as well as pyomelanin, the latter being less abundant (Schmaler-Ripcke et al. 2009, Heinekamp et al. 2012). Pyomelanin results from the activity of the proteins encoded by *hmgA* and *hppD* (Schmaler-Ripcke et al. 2009). The genome of *A. niger* contains homologs for both genes. We therefore propose that the enhanced fluorescence intensity as observed in the Δ*pptA* mutant originates, at least partly, from low levels of pyomelanin. The amount of this second type of melanin would be too low to detect by eye explaining the white appearance of the Δ*pptA* spores. Similarly, mycelium of *A. niger* and *A. bisporus* have a white appearance but their cell walls do

show enhanced fluorescence intensity. Presence of low levels of melanin in the cell wall would agree with the finding that genes involved in the melanin synthesis pathway are expressed in *A. bisporus* mycelium (Weijn et al. 2013a). Together it is proposed that melanin-like pigments form a structural component of the cell wall next to cell wall polysaccharides and proteins. Our results indicate that enhancement of melanin fluorescence can be used to screen for the presence of melanins or its precursors in a sensitive way, without staining or complicated purification techniques. As the fluorescence enhancement is peak power density and concentration dependent, it can be used as a semi-quantitative method.

REFERENCES

Andersen MR, Salazar MP, Schaap PJ, van de Vondervoort PJ, Culley D, Thykaer J, Frisvad JC, Nielsen KF, Albang R, Albermann K, Berka RM, Braus GH, Braus-Stromeyer SA, Corrochano LM, Dai Z, van Dijck PW, Hofmann G, Lasure LL, Magnuson JK, Menke H, Meijer M, Meijer SL, Nielsen JB, Nielsen ML, van Ooyen AJ, Pel HJ, Poulsen L, Samson RA, Stam H, Tsang A, van den Brink JM, Atkins A, Aerts A, Shapiro H, Pangilinan J, Salamov A, Lou Y, Lindquist E, Lucas S, Grimwood J, Grigoriev IV, Kubicek CP, Martinez D, van Peij NN, Roubos JA, Nielsen J, Baker SE (2011) Comparative genomics of citric-acid-producing *Aspergillus niger* ATCC 1015 versus enzyme-producing CBS 513.88. Genome Res 21: 885-897

Bechtold T, Mussak R (2009) Handbook of natural colorants. John Wiley & Sons Ltd., Chichester, UK

Bell AA, Wheeler MH (1986) Biosynthesis and functions of fungal melanins. Annu Rev Phytopathol 24: 411-451

Berends E, Scholtmeijer K, Wösten HAB, Bosch D, Lugones LG (2009) The use of mushroom-forming fungi for the production of N-glycosylated therapeutic proteins. Trends Microbiol 17: 439-443

Berendsen RL, Baars JJP, Kalkhove SIC, Lugones LG, Wösten HAB, Bakker PAHM (2010) *Lecanicillium fungicola*: causal agent of dry bubble disease in white-button mushroom. Mol Plant Pathol 11: 585-595

Borovansky J, Riley PA (2011) Melanins and Melanosomes: Biosynthesis, Structure, Physiological and Pathological Functions. Wiley-VCH & Co. KGaA, Weinheim, Germany

Bos C, Debets A, Swart K, Huybers A, Kobus G, Slakhorst S (1988) Genetic analysis and the construction of master strains for assignment of genes to six linkage groups in *Aspergillus niger*. Curr Genet 14: 437-443

Bull AT (1970) Inhibition of polysaccharases by melanin: enzyme inhibition in relation to mycolysis. Arch Biochem Biophys 137: 345-356

Burton K, Love M, Smith J (1993) Biochemical changes associated with mushroom quality in *Agaricus spp.*. Enzyme MicrobTechnol 15: 736-741

Butler M, Day A (1998) Fungal melanins: a review. Can J Microbiol 44: 1115-1136

Butler M, Gardiner R, Day A (2005) Fungal melanin detection by the use of copper sulfide-silver. Mycologia 97: 312-319

Conesa A, Punt PJ, van Luijk N, van den Hondel, Cees AMJJ (2001) The secretion pathway in filamentous fungi: a biotechnological view. Fungal Genet Biol 33: 155-171

Cunha MM, Franzen AJ, Seabra SH, Herbst MH, Vugman NV, Borba LP, de Souza W, Rozental S (2010) Melanin in *Fonsecaea pedrosoi*: a trap for oxidative radicals. BMC Microbiol 10: 80-2180-10-80

Dadachova E, Bryan RA, Huang X, Moadel T, Schweitzer AD, Aisen P, Nosanchuk JD, Casadevall A (2007) Ionizing radiation changes the electronic properties of melanin and enhances the growth of melanized fungi. PLoS One 2: e457

Eisenman HC, Casadevall A (2012) Synthesis and assembly of fungal melanin. Appl Microbiol Biotechnol 93: 931-940

Felix C, Hyde J, Sarna T, Sealy R (1978) Melanin photoreactions in aerated media: electron spin resonance evidence for production of superoxide and hydrogen peroxide. Biochem Biophys Res Commun 84: 335-341

Guarro J, GeneJ, Stchigel AM (1999) Developments in fungal taxonomy. Clin Microbiol Rev 12: 454-500

Hegnauer H, Nyhlén LE, Rast DM (1985) Ultrastructure of native and synthetic *Agaricus bisporus* melanins - Implications as to the compartmentation of melanogenesis in fungi. Exp Mycol 9: 1-29

Heinekamp T, Thywißen A, Macheleidt J, Keller S, Valiante V, Brakhage AA (2012) *Aspergillus fumigatus* melanins: interference with the host endocytosis pathway and impact on virulence. Front Microbiol 3: 440-1-440-7

Howard RJ, Ferrari MA, Roach, D.H. and Money, N.P. (1991) Penetration of hard substrates by a fungus employing enormous turgor pressures. Proc Natl Acad Sci USA 88: 11281-11284

Huang S, Heikal AA, Webb WW (2002) Two-photon fluorescence spectroscopy and microscopy of NAD(P)H and flavoprotein. Biophys J 82: 2811-2825

Iwen PC (2011) Nomenclature, Taxonomy, and Fungal Morphology. In: Mc Pherson RA and Pincus MR (eds) Henry's clinical diagnosis and management by laboratory methods, 22nd edn. Elsevier Health Sciences

Jeong SC, Jeong YT, Yang BK, Islam R, Koyyalamudi SR, Pang G, Cho KY, Song CH (2010) White button mushroom (*Agaricus bisporus*) lowers blood glucose and cholesterol levels in diabetic and hypercholesterolemic rats. Nutr Res 30: 49-56

Jolivet S, Arpin N, Wichers HJ, Pellon G (1998) *Agaricus bisporus* browning: a review. Mycol Res 102: 1459-1483

Jørgensen TR, Park J, Arentshorst M, van Welzen AM, Lamers G, van Kuyk PA, Damveld RA, van den Hondel, Cees AM, Nielsen KF, Frisvad JC (2011) The molecular

and genetic basis of conidial pigmentation in *Aspergillus niger*. Fungal Genet Biol 48: 544-553

Kerimo J, Rajadhyaksha M, DiMarzio CA (2011) Enhanced Melanin Fluorescence by Stepwise Three-photon Excitation. Photochem Photobiol 87: 1042-1049

Knaus H, Blab GA, Agronskaia AV, van den Heuvel D J, Gerritsen HC, Wösten HAB (2013a) Monitoring the metabolic state of fungal hyphae and the presence of melanin by nonlinear spectral imaging. Appl Environ Microbiol 79: 6345-6350

Knaus H, Blab GA, van Veluw GJ, Gerritsen HC, Wösten HAB (2013b) Label-free fluorescence microscopy in fungi. Fungal Biol Rev 27: 60-66

Kozarski M, Klaus A, Niksic M, Jakovljevic D, Helsper JP, Van Griensven LJ (2011) Antioxidative and immunomodulating activities of polysaccharide extracts of the medicinal mushrooms *Agaricus bisporus*, *Agaricus brasiliensis*, *Ganoderma lucidum* and *Phellinus linteus*. Food Chem 129: 1667-1675

Krijgsheld P, Altelaar AFM, Post H, Ringrose JH, Müller WH, Heck AJR, Wösten HAB (2012) Spatially resolving the secretome within the mycelium of the cell factory *Aspergillus niger*. J Proteome Res 11: 2807-2818

Krijgsheld P, Bleichrodt R, van Veluw GJ, Wang F, Müller WH, Dijksterhuis J, Wösten HAB (2013) Development in *Aspergillus*. Stud Mycol 74:1-29

Laiho LH, Pelet S, Hancewicz TM, Kaplan PD, So PTC (2005) Two-photon 3-D mapping of ex vivo human skin endogenous fluorescence species based on fluorescence emission spectra. J Biomed Opt 10: 024016

Lakowicz JR (2006) Principles of fluorescence spectroscopy. Springer Science & Business Media LLC, New York, USA

Longuet-Higgins H (1960) On the origin of the free radical property of melanins. Arch Biochem Biophys 86: 231-232

Mattila P, Könkö K, Eurola M, Pihlava J, Astola J, Vahteristo L, Hietaniemi V, Kumpulainen J, Valtonen M, Piironen V (2001) Contents of vitamins, mineral elements, and some phenolic compounds in cultivated mushrooms. J Agric Food Chem 49: 2343-2348

Meredith P, Riesz J (2004) Radiative Relaxation Quantum Yields for Synthetic Eumelanin¶. Photochem Photobiol 79: 211-216

Nosanchuk JD, Casadevall A (2003) The contribution of melanin to microbial pathogenesis. Cell Microbiol 5: 203-223

Palero JA, de Bruijn HS, van der Ploeg van den Heuvel A, Sterenborg HJCM, Gerritsen HC (2007) Spectrally resolved multiphoton imaging of in vivo and excised mouse skin tissues. Biophys J 93: 992-1007

Palero JA, de Bruijn HS, van der Ploeg-van den Heuvel A, Sterenborg HJCM, Gerritsen HC (2006) In vivo nonlinear spectral imaging in mouse skin. Opt Express 14: 4395-4402

Papagianni M (2007) Advances in citric acid fermentation by *Aspergillus niger*: Biochemical aspects, membrane transport and modeling. Biotechnol Adv 25: 244-263

Pullman A, Pullman B (1961) The band structure of melanins. Biochim Biophys Acta 54: 384-385

Punt PJ, van Biezen N, Conesa A, Albers A, Mangnus J, van den Hondel C (2002) Filamentous fungi as cell factories for heterologous protein production. Trends Biotechnol 20: 200-206

Rosas ÁL, Nosanchuk JD, Gómez BL, Edens WA, Henson JM, Casadevall A (2000) Isolation and serological analyses of fungal melanins. J Immunol Methods 244: 69-80

Salas SD, Bennett JE, Kwon-Chung KJ, Perfect JR, Williamson PR (1996) Effect of the laccase gene CNLAC1, on virulence of *Cryptococcus neoformans*. J Exp Med 184: 377-386

Schmaler-Ripcke J, Sugareva V, Gebhardt P, Winkler R, Kniemeyer O, Heinekamp T, Brakhage AA (2009) Production of pyomelanin, a second type of melanin, via the tyrosine degradation pathway in *Aspergillus fumigatus*. Appl Environ Microbiol 75: 493-503

Schweitzer AD, Howell RC, Jiang Z, Bryan RA, Gerfen G, Chen CC, Mah D, Cahill S, Casadevall A, Dadachova E (2009) Physico-chemical evaluation of rationally designed melanins as novel nature-inspired radioprotectors. PloS one 4: e7229

Soler-Rivas C, Arpin N, Olivier JM, Wichers HJ (2000) Discoloration and tyrosinase activity in *Agaricus bisporus* fruit bodies infected with various pathogens. Mycol Res 104: 351-356

Soler-Rivas C, Jolivet S, Arpin N, Olivier JM, Wichers HJ (1999) Biochemical and physiological aspects of brown blotch disease of *Agaricus bisporus*. FEMS Microbiol Rev 23: 591-614

Teuchner K, Ehlert J, Freyer W, Leupold D, Altmeyer P, Stücker M, Hoffmann K (2000) Fluorescence studies of melanin by stepwise two-photon femtosecond laser excitation. J Fluoresc 10: 275-275

Thomann D, Rines DR, Sorger PK, Danuser G (2002) Automatic fluorescent tag detection in 3D with super-resolution: application to the analysis of chromosome movement. J Microsc 208: 49-64

van Veluw GJ, Teertstra WR, de Bekker C, Vinck A, van Beek N, Muller WH, Arentshorst M, van der Mei HC, Ram AFJ, Dijksterhuis J, Wösten HAB (2012) Heterogeneity in liquid shaken cultures of *Aspergillus niger* inoculated with melanised conidia or conidia of pigmentation mutants. Stud Mycol 74: 47-57

Wang Y, Casadevall A (1994) Susceptibility of melanized and nonmelanized *Cryptococcus neoformans* to nitrogen- and oxygen-derived oxidants. Infect Immun 62: 3004-3007

Wargenau A, Fleißner A, Bolten CJ, Rohde M, Kampen I, Kwade A (2011) On the origin of the electrostatic surface potential of *Aspergillus niger* spores in acidic environments. Res Microbiol 162: 1011-1017

Watt AA, Bothma JP, Meredith P (2009) The supramolecular structure of melanin. Soft Matter 5: 3754-3760

Weijn A, Bastiaan-Net S, Wichers HJ, Mes JJ (2013a) Melanin biosynthesis pathway in *Agaricus bisporus* mushrooms. Fungal Genet Biol 55: 42-53

Weijn A, van den Berg-Somhorst, Dianne BPM, Slootweg JC, Vincken JP, Gruppen H, Wichers HJ, Mes JJ (2013b) Main Phenolic Compounds of the Melanin Biosynthesis Pathway in Bruising-Tolerant and Bruising-Sensitive Button Mushroom (*Agaricus bisporus*) Strains. J Agric Food Chem 61: 8224-8231

Wheeler MH (1983) Comparisons of fungal melanin biosynthesis in ascomycetous, imperfect and basidiomycetous fungi. Transactions of the British Mycological Society 81: 29-36

Zajac G, Gallas J, Cheng J, Eisner M, Moss S, Alvarado-Swaisgood A (1994) The fundamental unit of synthetic melanin: a verification by tunneling microscopy of X-ray scattering results. Biochim Biophys Acta 1199: 271-278

Zhou Z, Liu J (2010) Pigments of fungi (macromycetes). Nat Prod Rep 27: 1531-1570

CHAPTER 6

Summary and general discussion

Fungi fulfill a wide variety of functions in nature. They are essential for recycling of organic material and establish mutual beneficial interactions with organisms such as algae (lichens), plants (mycorrhizae) and animals. Humans consume fungi (e.g. mushrooms) and they have been used to produce food, feed, and drinks. Moreover, fungi are used as cell factories for the production of enzymes, pharmaceuticals and organic acids. However, they can also be pathogenic, produce toxins, and are an important cause of spoilage of food and buildings. Given their impact, it is crucial to understand fungal growth and development and to be able to monitor their presence and physiology. In this Thesis I used *Agaricus bisporus* and *Aspergillus niger* as model organisms. The former makes fruiting bodies known as white button mushrooms (champignon), the most cultivated mushroom, whereas the latter is an important cell factory used by the industry. The aim of this Thesis was to introduce nonlinear spectral imaging microscopy (NLSM) to study growth and development of fungi and to monitor their physiology. This non-invasive technique makes use of autofluorescent molecules within cells that are monitored by two-photon (2p) excitation. Compared to one-photon (1p) excitation the overall phototoxicity for the biological specimen is reduced as excitation is limited to the focal volume. Additionally, near infrared excitation wavelengths lead to an increased penetration depth, as scattering by the specimen is low (Gu et al. 2000, Theer and Denk 2006, Gerritsen and de Grauw 1999, Denk et al. 1990). NAD(P)H, flavins, and melanin are autofluorescent molecules in fungi (Chapter 1, Knaus et al. 2013b). These molecules function in metabolism (NAD(P)H, flavins) and in defense and pathogenesis (melanin). Monitoring these molecules spatially and over time by NLSM provides information about the status of cells in a non-destructive way (Stringari et al. 2012, Vishwasrao et al. 2005, Palero et al. 2011).

NLSM IN FUNGI

Spectral imaging has been used to distinguish between different fungal species by detecting the red, green, and blue parts of the spectrum using optical filters (Lin et al. 2009). In contrast, a NLSM setup is described in Chapter 2 that acquires complete spectra. Thus, data analy-

sis is not restricted to the bandwidth of the optical filters and different data analysis methods can be applied, improving the spectral unmixing capacity. The setup is based on a commercial multiphoton microscope that was equipped with a binocular and offered bright-field and 1p fluorescence imaging as well. This ensures user-friendly operation and easy navigation towards the region of interest. The scope of applications was increased by e.g. giving the option to generate an overlay of spectral images with bright-field images or by providing an additional fiber-output facilitating e.g. lifetime measurements. The homebuild spectrograph can be flexibly adjusted depending on the application and offers a detection range between 440 and 620 nm enabling measurements of endogenous fluorophores in fungi in vivo. Although being user-friendly compared to laboratory solutions (customer built setups on optical tables) this is still an expensive research setup. It was shown in Chapter 3 and 4 that detection of the blue, red and / or green spectral range can be applied to monitor shelf life of mushrooms (see below). Considering the technical development of near-UV wavelength diode lasers, it would be worthwhile to explore whether in the near future 1p excitation could gives similar results at lower cost. In that case an array of diode lasers or LEDs for excitation can be combined with two or three emission channels and an array of photomultipliers as detector. As mentioned, 1p excitation can induce phototoxicity. This would not be a problem for applications like monitoring freshness of mushrooms. Miniaturized portable nonlinear microscopy systems would be another improvement. They are currently being developed for biomedical applications. They are based on resonant-scanned optical-fiber systems (Brown et al. 2012) or miniaturized fiber coupled detection units (Helmchen et al. 2001).

The emission spectrum is the result of the contribution of all fluorophores present in the cell or tissue. Each fluorophore is characterized by its emission spectrum. Therefore, the emission can be decomposed into the contributions of the individual components. To this end, various algorithms have been developed modeling the superimposition of different components. Some of these algorithms, like linear unmixing (Garini et al. 2006), require reference spectra, which are not always easy to retrieve in case of endogenous fluorophores. In contrast, nonnegative matrix factorization (Neher et al. 2009) only relies on an

initial estimate of the spectra of the individual components, but is a rather slow algorithm. Another mathematically quite complicated way is to use principal component analysis (Chorvat Jr et al. 2005) by finding the minimally necessary number of orthogonal coordinates that describe the experimental data. In this case, orthogonal coordinates mean generated estimates of spectra of individual autofluorescent components. In this Thesis, the phasor analysis was employed to unmix spectral imaging data (Fereidouni et al. 2012). This algorithm is based on a Fourier transform of the spectra, where each emission spectrum is represented as a point in a complex number plane. The polar coordinates of a pure component are determined by its emission maximum and the spectral width. The composition of a mixture is solely determined by its distance to the position of the pure components, which makes the spectral unmixing fast as no fitting is necessary. Semi-blind unmixing is also possible. Moreover, the spectral phasor approach offers graphical representation of complex spectral data as regions in the phasor plot can be retraced in the spatial image. In that way it depicts the spatial distribution of a certain component. However, endogenous fluorophores often have broad emission spectra resulting in large spectral overlaps. Hence, spectral unmixing can be challenging. Besides, for some applications spectral imaging is incapable of retrieving all the necessary information for unmixing and a complementary method is required. For instance, if the interaction of a fluorophore with its environment needs to be characterized, anisotropy resolved imaging is a good option. Anisotropy detects changes in rotational mobility and can therefore quantify the contribution of free and bound state molecules. Moreover, it provides information about viscosity. To exploit these new opportunities, simultaneous spectral and anisotropy imaging was implemented (Chapter 1, 2). However, especially when relying on autofluorescence for signal, anisotropy is very sensitive to noise, because the low total intensity is split into two channels for the detection of parallel and perpendicular polarization. This makes the simultaneous analysis of spectral and anisotropy data still challenging. Recently, it was demonstrated that the phasor analysis can be applied for blind unmixing of fluorophores in spectrally resolved lifetime images (Fereidouni et al. 2013). Therefore, it is worth

testing if the spectral phasor analysis is also suitable for the analysis of spectrally resolved anisotropy images.

MONITORING THE METABOLIC STATE BY NLSM USING THE FAD / NAD(P)H RATIO

Several methods can be used to quantify the metabolic activity of fungi. Commonly these assays use exogenous fluorescent labels to monitor the activity of NADH-dependent oxidoreductases (Moss et al. 2008, Kuhn et al. 2003) or NADH-dependent dehydrogenases (Harris et al. 2006). Others rely on fluorescent viability markers that are metabolized in presence of intracellular esterases and ATP (Hua et al. 2011). Cell extracts or tissue sectioning and incorporation of marker molecules into cells is a prerequisite for the majority of these assays. This Thesis introduces NLSM as a potent minimally invasive alternative to monitor the metabolic state in fungi (Chapter 2, 3, 4).

Oxidative phosphorylation in mitochondria converts fluorescent NAD(P)H to non-fluorescent NAD, while non-fluorescent $FADH_2$ is oxidized to fluorescent FAD. In the cytosol, NAD is reduced to NAD(P)H during glycolysis and $FADH_2$ is produced. Therefore, the FAD / NAD(P)H ratio is regarded as an indicator of the metabolic state of a cell (Chance et al. 1979, Chance 1989). A decrease in ratio means that cells are more active, as found in cancer cells (Chance 1989). A two-fold increase of the FAD / NAD(P)H ratio was observed during a 17 day postharvest storage period of white button mushrooms at 4 °C (cap diameter about 5.5 cm) (Knaus et al. 2013a, Chapter 3). Notably, changes in color and morphology were not detected by eye during this period. These data show that NLSI can be used to quantify freshness of mushrooms and to predict shelf life. It is tempting to speculate that this method can also be used for other fresh products such as vegetables. The FAD / NAD(P)H ratio was about 1.3 fold lower for mushrooms harvested by picking than for those harvested by cutting. This may be due to the feeding capacity of the vegetative mycelium and casing layer that remain attached to the stipe of picked mushrooms. They also may prevent drying out of the fruiting body.

Fluorescence intensity of FAD was 2.3 fold higher in vegetative mycelium in compost than in the fruiting bodies (cap diameter 4 cm). In contrast, intensity of NAD(P)H stayed constant during development (Chapter 4). As a consequence, the FAD / NAD(P)H ratio of mycelium growing in the compost and the casing layer was higher than in aerial structures (aerial hyphae, primordia and mushrooms), implying they were less metabolically active. These data indicate that energy metabolism shifts when hyphae grow into the air. This is supported by gene expression studies, where vegetative mycelium and fruiting bodies exhibit a different carbohydrate metabolism (Patyshakuliyeva et al. 2013). Mushrooms with a cap diameter of 1 – 4 cm had a 1.6 fold lower FAD / NAD(P)H ratio than 8 cm caps. These preliminary studies indicate that smaller mushrooms have a longer shelf life than large ones.

Only 5-10 % of the primordia develop into mature mushrooms (Noble et al. 2003). It would be of high interest to be able to predict which primordia will proceed development. The sample number in Chapter 4 was too low to distinguish distinct populations of primordia based on the FAD / NAD(P)H ratio. It would be interesting to increase sample size to see whether there is a correlation between primordial outgrowth and the FAD / NAD(P)H ratio.

To summarize, the FAD / NAD(P)H ratio is indicative for the metabolic state of cells and tissues. It can be used to monitor the quality of the mycelium during colonization of compost and casing and to optimize harvesting for increased shelf life. Monitoring metabolism is also of interest for bioprocess modeling, controlling fermentations in bioreactors, and for cell biology studies of microbes.

SCREENING FOR PRESENCE OF MELANIN(-LIKE) PIGMENTS BY FLUORESCENCE ENHANCEMENT

Many fungi produce melanin. This high molecular weight heterogeneous molecule is involved in virulence (Nosanchuk and Casadevall 2003, Salas et al. 1996, Heinekamp et al. 2012), defense against environmental stresses such as UV- and gamma-radiation (Schweitzer et al. 2009, Felix et al. 1978), and the protection against microbial enzymatic lysis in natural soils (Butler and Day 1998, Bull 1970) and oxida-

tive stress in or outside a host (Cunha et al. 2010, Wang and Casadevall 1994).

Eumelanin in human hair and extracted from *Sepia officinalis* shows remarkable photosphysical behavior (Kerimo et al. 2011). Fluorescence emission is enhanced by several orders of magnitude upon illumination with a high level of near-infrared light. The same behavior was found with synthetic melanin and melanin isolated from spores of *A. niger* (Chapter 5). Also spores of *A. niger* and *A. bisporus*, though synthesizing melanin via different pathways, showed enhanced fluorescence. These signals were localized in the cell wall, where melanin is deposited. Notably, enhanced fluorescence was also observed when strains of *A. niger* were used that are blocked in different steps of the melanin synthesis pathway. These spores differ in color resulting from accumulation of a particular melanin precursor or a pigment derived of these precursors. Even the white spores of the Δ*pptA* strain showed fluorescence enhancement. This was surprising as this pigmentation mutant lacks the gene encoding phosphopantetheinyl transferase that is necessary to start melanin synthesis via the DHN pathway. *A. niger* is assumed to form DHN-melanin, although some of the genes involved in this pathway are missing (Jørgensen et al. 2011). *A. fumigatus* produces pyomelanin apart from DHN-melanin, the latter being most abundant (Heinekamp et al. 2012, Schmaler-Ripcke et al. 2009). Pyomelanin results from the activity of the HmgA and HppD proteins (Schmaler-Ripcke et al. 2009). *A. niger* may also form this type of melanin since its genome contains homologs for *hmgA* and *hppD*. Pyomelanin was synthesized by the *pksP* pigmentation mutant of *A. fumigatus* (homologous to the Δ*pptA* mutant in *A. niger*) when tyrosine was present in the medium (Schmaler-Ripcke et al. 2009). The Δ*pptA* mutant of *A. niger* was grown on tyrosine containing CM (Chapter 5). Together, this suggests that enhanced fluoresence of the Δ*pptA* mutant of *A. niger* is due to pyomelanin. This form may also be present in the cell wall of vegetative hyphae.

Melanin formation is known to be induced by bruising and infection In *A. bisporus.* This causes browning of the mushrooms (Berendsen et al. 2010, Soler-Rivas et al. 2000, Jolivet et al. 1998). Our results indicate that melanin is also present in white caps (Chapter 4). As expected, the

pigment concentration in bruised mushrooms was higher, because lower peak power densities were needed to observe fluorescence enhancement (Chapter 5). In white mushroom caps an increasing melanin contribution was measured during a 17 day storage period at 4 °C (Knaus et al. 2013a, Chapter 3). The melanin / NAD(P)H ratio and the FAD / NAD(P)H ratio, used to determine the degree of freshness, followed the same trend. Thus, it is possible to use the melanin / NAD(P)H ratio to follow postharvest browning before it is visible by eye.

NLSM in combination with spectral unmixing also revealed that contribution of melanin to the total autofluorescence emission of *A bisporus* mycelium from compost and casing layer, as well as aerial hyphae and primordia could be up to 20 %, despite their white or hyaline appearance (Chapter 4, 5). The same behavior was found in vegetative mycelium of *A. niger*. These data suggest that melanin-like pigments form a structural component of the cell wall. This would agree with the finding that genes involved in melanin synthesis are expressed in *A. bisporus* mycelium (Weijn et al. 2013a). Notably, hyphae in the compost and the casing contained higher levels of melanin when compared to the aerial structures (Chapter 4), suggesting that melanin is important during vegetative growing. It may protect against the microbial flora and oxidative compounds in compost and casing. As postharvest browning of mushrooms decreases commercial value, attempts are made to block melanin formation or to select bruising-insensitive strains (Weijn et al. 2013b). However, this may weaken the vegetative mycelium when melanin produced in mushroom and mycelium are produced by similar pathways.

REFERENCES

Berendsen RL, Baars JJP, Kalkhove SIC, Lugones LG, Wösten HAB, Bakker PAHM (2010) *Lecanicillium fungicola*: causal agent of dry bubble disease in white-button mushroom. Mol Plant Pathol 11:585-595

Brown CM, Rivera DR, Pavlova I, Ouzounov DG, Williams WO, Mohanan S, Webb WW, Xu C (2012) In vivo imaging of unstained tissues using a compact and flexible multiphoton microendoscope. J Biomed Opt 17: 040505-1-040505-3

Bull AT (1970) Inhibition of polysaccharases by melanin: enzyme inhibition in relation to mycolysis. Arch Biochem Biophys 137: 345-356

Butler M, Day A (1998) Fungal melanins: a review. Can J Microbiol 44: 1115-1136

Chance B (1989) Metabolic heterogeneities in rapidly metabolizing tissues. J Appl Cardiol 4: 207-221

Chance B, Schoener B, Oshino R, Itshak F, Nakase Y (1979) Oxidation-reduction ratio studies of mitochondria in freeze-trapped samples. NADH and flavoprotein fluorescence signals. J Biol Chem 254: 4764-4771

Chorvat Jr D, Kirchnerova J, Cagalinec M, Smolka J, Mateasik A, Chorvatova A (2005) Spectral unmixing of flavin autofluorescence components in cardiac myocytes. Biophys J 89: L55-L57

Cunha MM, Franzen AJ, Seabra SH, Herbst MH, Vugman NV, Borba LP, de Souza W, Rozental S (2010) Melanin in *Fonsecaea pedrosoi*: a trap for oxidative radicals. BMC Microbiol 10: 80-2180-10-80

Denk W, Strickler JH, Webb WW (1990) Two-photon laser scanning fluorescence microscopy. Science 248: 73-76

Felix C, Hyde J, Sarna T, Sealy R (1978) Melanin photoreactions in aerated media: electron spin resonance evidence for production of superoxide and hydrogen peroxide. Biochem Biophys Res Commun 84: 335-341

Fereidouni F, Bader AN, Gerritsen HC (2012) Spectral phasor analysis allows rapid and reliable unmixing of fluorescence microscopy spectral images. Opt Express 20: 12729-12741

Fereidouni F, Blab GA, Gerritsen HC (2013) Blind unmixing of spectrally resolved lifetime images. J Biomed Opt 18: 086006

Garini Y, Young IT, McNamara G (2006) Spectral imaging: principles and applications. Cytometry A 69: 735-747

Gerritsen HC, de Grauw CJ (1999) Imaging of optically thick specimen using two-photon excitation microscopy. Microsc Res Tech 47: 206-209

Gu M, Gan X, Kisteman A, Xu MG (2000) Comparison of penetration depth between two-photon excitation and single-photon excitation in imaging through turbid tissue media. Appl Phys Lett 77: 1551-1553

Harris DM, Diderich JA, Van der Krogt ZA, Luttik MAH, Raamsdonk LM, Bovenberg RAL, Van Gulik WM, Van Dijken JP, Pronk JT (2006) Enzymic analysis of NADPH metabolism in β-lactam-producing *Penicillium chrysogenum*: presence of a mitochondrial NADPH dehydrogenase. Metab Eng 8: 91-101

Heinekamp T, Thywißen A, Macheleidt J, Keller S, Valiante V, Brakhage AA (2012) *Aspergillus fumigatus* melanins: interference with the host endocytosis pathway and impact on virulence. Front Microbiol 3: 440-1-440-7

Helmchen F, Fee MS, Tank DW, Denk W (2001) A miniature head-mounted two-photon microscope: high-resolution brain imaging in freely moving animals. Neuron 31: 903-912

Hua SST, Brandl MT, Hernlem B, Eng JG, Sarreal SBL (2011) Fluorescent viability stains to probe the metabolic status of aflatoxigenic fungus in dual culture of *Aspergillus flavus* and *Pichia anomala*. Mycopathologia 171: 133-138

Jolivet S, Arpin N, Wichers HJ, Pellon G (1998) *Agaricus bisporus* browning: a review. Mycol Res 102: 1459-1483

Jørgensen TR, Park J, Arentshorst M, van Welzen AM, Lamers G, van Kuyk PA, Damveld RA, van den Hondel, Cees AM, Nielsen KF, Frisvad JC (2011) The molecular

and genetic basis of conidial pigmentation in *Aspergillus niger*. Fungal Genet Biol 48: 544-553

Kerimo J, Rajadhyaksha M, DiMarzio CA (2011) Enhanced Melanin Fluorescence by Stepwise Three-photon Excitation. Photochem Photobiol 87: 1042-1049

Knaus H, Blab GA, Agronskaia AV, van den Heuvel D J, Gerritsen HC, Wösten HAB (2013a) Monitoring the metabolic state of fungal hyphae and the presence of melanin by nonlinear spectral imaging. Appl Environ Microbiol 79: 6345-6350

Knaus H, Blab GA, van Veluw GJ, Gerritsen HC, Wösten HAB (2013b) Label-free fluorescence microscopy in fungi. Fungal Biol Rev 27: 60-66

Kuhn D, Balkis M, Chandra J, Mukherjee P, Ghannoum M (2003) Uses and limitations of the XTT assay in studies of *Candida* growth and metabolism. J Clin Microbiol 41: 506-508

Lin SJ, Tan HY, Kuo CJ, Wu RJ, Wang SH, Chen WL, Jee SH, Dong CY (2009) Multiphoton autofluorescence spectral analysis for fungus imaging and identification. Appl Phys Lett 95: 043703

Moss BJ, Kim Y, Nandakumar M, Marten MR (2008) Quantifying metabolic activity of filamentous fungi using a colorimetric XTT assay. Biotechnol Prog 24: 780-783

Neher RA, Mitkovski M, Kirchhoff F, Neher E, Theis FJ, Zeug A (2009) Blind source separation techniques for the decomposition of multiply labeled fluorescence images. Biophys J 96: 3791-3800

Noble R, Fermor TR, Lincoln S, Dobrovin-Pennington A, Evered C, Mead A, Li R (2003) Primordia initiation of mushroom (*Agaricus bisporus*) strains on axenic casing materials. Mycologia 95: 620-629

Nosanchuk JD, Casadevall A (2003) The contribution of melanin to microbial pathogenesis. Cell Microbiol 5: 203-223

Palero JA, Bader AN, de Bruijn HS, van den Heuvel A, Sterenborg HJCM, Gerritsen HC (2011) In vivo monitoring of protein-bound and free NADH during ischemia by nonlinear spectral imaging microscopy. Biomed Opt Express 2: 1030-1039

Patyshakuliyeva A, Jurak E, Kohler A, Baker A, Battaglia E, de Bruijn W, Burton KS, Challen MP, Coutinho PM, Eastwood DC, Gruben BS, Mäkelä MR, Martin F, Nadal M, van den Brink J, Wiebenga A, Zhou M, Henrissat B, Kabel M, Gruppen H and de Vries RP (2013) Carbohydrate utilization and metabolism is highly differentiated in *Agaricus bisporus*. BMC Genomics 14: 663-677

Salas SD, Bennett JE, Kwon-Chung KJ, Perfect JR, Williamson PR (1996) Effect of the laccase gene CNLAC1, on virulence of *Cryptococcus neoformans*. J Exp Med 184: 377-386

Schmaler-Ripcke J, Sugareva V, Gebhardt P, Winkler R, Kniemeyer O, Heinekamp T, Brakhage AA (2009) Production of pyomelanin, a second type of melanin, via the tyrosine degradation pathway in *Aspergillus fumigatus*. Appl Environ Microbiol 75: 493-503

Schweitzer AD, Howell RC, Jiang Z, Bryan RA, Gerfen G, Chen CC, Mah D, Cahill S, Casadevall A, Dadachova E (2009) Physico-chemical evaluation of rationally designed melanins as novel nature-inspired radioprotectors. PloS one 4: e7229

Soler-Rivas C, Arpin N, Olivier JM, Wichers HJ (2000) Discoloration and tyrosinase activity in *Agaricus bisporus* fruit bodies infected with various pathogens. Mycol Res 104: 351-356

Stringari C, Sierra R, Donovan PJ, Gratton E (2012) Label-free separation of human embryonic stem cells and their differentiating progenies by phasor fluorescence lifetime microscopy. J Biomed Opt 17: 046012-1-046012-11

Theer P, Denk W (2006) On the fundamental imaging-depth limit in two-photon microscopy. J Opt Soc Am A Opt Image Sci Vis 23: 3139-3149

Vishwasrao HD, Heikal AA, Kasischke KA, Webb WW (2005) Conformational dependence of intracellular NADH on metabolic state revealed by associated fluorescence anisotropy. J Biol Chem 280: 25119-25126

Wang Y, Casadevall A (1994) Susceptibility of melanized and nonmelanized *Cryptococcus neoformans* to nitrogen- and oxygen-derived oxidants. Infect Immun 62: 3004-3007

Weijn A, Bastiaan-Net S, Wichers HJ, Mes JJ (2013a) Melanin biosynthesis pathway in *Agaricus bisporus* mushrooms. Fungal Genet Biol 55: 42-53

Weijn A, van den Berg-Somhorst, Dianne BPM, Slootweg JC, Vincken JP, Gruppen H, Wichers HJ, Mes JJ (2013b) Main Phenolic Compounds of the Melanin Biosynthesis Pathway in Bruising-Tolerant and Bruising-Sensitive Button Mushroom (*Agaricus bisporus*) Strains. J Agric Food Chem 61: 8224-8231

APPENDIX

Samenvatting

Zusammenfassung

Curriculum vitae

Publications

Acknowledgements

SAMENVATTING

Schimmels vervullen een belangrijke rol in de natuur. Zij zijn essentieel voor de recycling van organisch materiaal en gaan wederzijds voordelige interacties aan met organismen zoals algen (korstmossen), planten (mycorrhiza's) en dieren. De mens consumeert de paddenstoelen van schimmels en gebruikt schimmels voor de productie van voedsel (zoals brood, tofu, en kaas), diervoeder en dranken (bier, sake). Schimmels worden ook grootschalig door de industrie gebruikt voor de productie van enzymen, medicijnen, en organische zuren zoals citroenzuur. Schimmels kunnen echter ook ziekteverwekkend zijn voor planten (waaronder alle voedingsgewassen), dieren en de mens. Daarnaast kunnen ze toxische stoffen produceren en zijn zij een belangrijke oorzaak van bederf van voedsel en aantasting van gebouwen. Gezien hun impact is het van belang om schimmels te kunnen detecteren en hun groei, celactiviteit en ontwikkeling te kunnen volgen en bestuderen. In dit proefschrift gebruikte ik *Agaricus bisporus* en *Aspergillus niger* als modelsystemen. Eerstgenoemde maakt de meest geproduceerde paddenstoel, de champignon, terwijl laatstgenoemde gebruikt wordt door de industrie als productiesysteem van enzymen, medicijnen en zuren. Het doel van dit proefschrift was om niet-lineare spectrale beeldvormende microscopie (NLSM) te introduceren als techniek om groei en ontwikkeling van schimmels te bestuderen en hun celactiviteit te volgen. Deze niet-invasieve methode maakt gebruik van autofluorescente moleculen in cellen die middels 2-foton excitatie worden gedetecteerd. Het voordeel van 2-foton excitatie boven 1-foton excitatie is dat het minder schade geeft aan de cel omdat excitatie zich beperkt tot het brandpunt van de laser. Daarnaast kan men dieper in het organisme kijken doordat de verstrooiing van het licht laag is. NAD(P)H, flavines (o.a. FAD), en melanine zijn autofluorescente moleculen in schimmels (Hoofdstuk 1). NAD(P)H, en flavines zijn betrokken bij metabolisme, terwijl melanine beschermt tegen milieuomstandigheden (UV, oxidatieve stress) en betrokken is bij het infectieproces van ziekteverwekkende schimmels.

NLSM in schimmels

De NLSM-opstelling wordt beschreven in Hoofdstuk 2. Het detecteert alle golflengten die worden uitgezonden als gevolg van fluorescente moleculen binnen het organisme. Het apparaat is gebaseerd op een commercieel verkrijgbare multifoton-microscoop met binoculair dat ook gebruikt kan worden voor helderveld- en 1-foton fluorescentiemicroscopie. Het apparaat is gebruiksvriendelijk en men kan eenvoudig navigeren. Daarnaast kan men fluorescentiespectra combineren met anisotropie (zie later). De zelfgebouwde spectrograaf kan golflengten detecteren tussen 440 en 620 nm, wat het gebied is van het licht dat autofluorescente moleculen in schimmels vrijgeven. In hoofdstukken 3 en 4 werd aangetoond dat emissie in het blauwe, rode en groen spectrale gebied gebruikt kan worden om houdbaarheid van champignons te voorspellen (zie later). Het apparaat is op dit moment echter erg duur. Om kosten van een apparaat te reduceren die houdbaarheid kan meten zou men mogelijk 1-foton excitatie kunnen gebruiken omdat fototoxiciteit hier geen rol speelt. Als dit dezelfde resultaten geeft als de 2-foton excitatie dan zou men gebruik kunnen maken van een array van diode lasers of LEDs gecombineerd met 2 of 3 emissiekanalen en een array van fotomultipliers als detector. Het gebruik van kleine draagbare NLSM systemen zou een andere verbetering zijn. Dergelijke systemen worden nu ontwikkeld om gebruikt te worden voor medische diagnostiek.

Het emissiespectrum van een cel of weefsel is de optelsom van de emissie van elk van de fluorescente moleculen in de cel of in het weefsel. Elk fluorescent molecuul heeft een eigen karakteristieke emissie. Daarom kan het totale emissiespectrum worden ontleed in de bijdrage van elk van de fluorescente moleculen. Ik heb de fasor-analyse gebruikt om de spectra te ontleden. Dit algoritme is gebaseerd op een Fouriertransformatie van de spectra, waarbij elk emissie spectrum gerepresenteerd wordt als een punt in een vlak. De coördinaten worden bepaald door het emissiemaximum en de breedte van de emissie. De samenstelling van een mengsel kan worden afgeleid door de afstand in het vlak tot de positie van de pure componenten.

Spectrale beeldvorming kan worden gecombineerd met anisotropie. Anisotropie meet de bewegelijkheid van moleculen als gevolg van de

stroperigheid van zijn omgeving of de binding aan een ander molecuul zoals een enzym. Anisotropie is erg gevoelig voor ruis, zeker in het geval van NLSM omdat de emissie zo zwak is. Dit maakt gelijktijdige analyse van spectrale en anisotropie data moeilijk.

Het volgen van de metabolische staat middels NLSM

Er zijn verschillende methoden die de metabolische staat van een cel of weefsel kunnen bepalen. Echter, deze methoden maken gebruik van celextracten of het opdelen van het weefsel of van de introductie van moleculen die worden omgezet of die fluoresceren afhankelijk van de activiteit van de cellen. Dit proefschrift introduceert NLSM als een niet-invasieve methode om cel- en weefselactiviteit van schimmels te bepalen (Hoofdstuk 2, 3 en 4). Er wordt gebruikgemaakt van de autofluorescentie van NAD(P)H en FAD. De FAD / NAD(P)H autofluorescentieverhouding wordt genomen als maat voor de activiteit. Een verlaging van deze verhouding betekent dat de cellen actiever zijn. Champignons werden gedurende 17 dagen bij 4 °C opgeslagen. Tijdens deze periode kon ik geen veranderingen in kleur en vorm van de champignons waarnemen. De FAD / NAD(P)H verhouding steeg met een factor 2 tijdens de opslag van de champignons (Hoofdstuk 3). De FAD / NAD(P)H verhouding was ongeveer 1,3 keer lager wanneer champignons waren geplukt in plaats van geoogst door te snijden. Mogelijk blijft het mycelium en de dekaarde die bij het plukken aan de champignon verbonden blijven de paddenstoel voeden of voorkomen zij uitdroging (Hoofdstuk 3).

De fluorescentie-intensiteit van FAD was 2,3 keer hoger in het mycelium van de compost en de dekaarde vergeleken met die in champignons met een hoedgrootte van 4 cm. De intensiteit van NAD(P)H bleef onveranderd (Hoofdstuk 4). Hierdoor was de FAD / NAD(P)H verhouding van het mycelium hoger dan die van de champignons. Dit betekent dat de paddenstoelen actiever zijn. Ook bleek dat champignons met een hoedgrootte van 1 - 4 cm een 1,6 keer lagere FAD / NAD(P)H verhouding hebben dan paddenstoelen met een hoed van 8 cm. Dit suggereert dat kleinere paddenstoelen langer houdbaar zijn.

Slechts 5-10% van de primordia groeien uit tot champignons. Het zou heel interessant zijn om middels NLSM te kunnen voorspellen welke

priomorida gaan uitgroeien. Het aantal primoridia dat werd gebruikt voor de metingen was echter te laag om hierover een uitspraak te kunnen doen. Samenvattend kan worden gesteld dat de FAD / NAD(P)H verhouding een maat is voor de metabolische staat van schimmelcellen en weefsels. Het kan worden gebruikt om de kwaliteit van mycelium te volgen en om de versheid van champignons te meten en hun houdbaarheid te bepalen. NLSM studies zouden oogstprocessen kunnen optimaliseren met als doel het afleveren van langer houdbare champignons. Deze methode is ook interessant om mycelium te monitoren in industriële fermentaties en voor fundamenteel celbiologisch onderzoek aan schimmels. NLSM is mogelijk ook interessant voor kwaliteitsstudies van andere versproducten zoals groenten en fruit.

Fluorescentie enhancement van melanine(-achtige) pigmenten

Veel schimmels vormen melanine. Dit hoogmoleculaire heterogene pigment is betrokken bij infectie van gastheren, afweer tegen ziekteverwekkers van schimmels, en tegen UV en zuurstofradicalen. Het zogenaamde eumelanine uit menselijk haar en uit de inktvis vertoont opmerkelijk gedrag. Zijn fluorescentie wordt sterk verhoogd wanneer het wordt blootgesteld aan een hoge dosis nabij-infrarood licht. Ik vond hetzelfde gedrag met synthetisch melanine en met melanine dat geïsoleerd was uit sporen van *A. niger* (Hoofdstuk 5). Dit gedrag kon ook rechtstreeks worden gemeten gebruikmakend van sporen van *A. niger* en van de champignon. De verhoogde fluorescentie was gelokaliseerd in de celwand, daar waar het melanine zich bevindt. Verhoogde fluorescentie werd ook waargenomen in stammen van *A. niger* die geblokkeerd zijn in één van de stappen van de melanine biosynthese. Deze sporen zijn steeds anders van kleur en hopen dus steeds andere pigmenten op. Zelfs de witte sporen van de Δ*pptA* stam vertoonde verhoogde fluorescentie. Dit was verrassend omdat ik ervan uit ging dat deze stam geheel geen melanine of voorloperpigment zou produceren. *A. niger* wordt verondersteld DHN-melanine te vormen. Het zou kunnen zijn dat deze schimmel net als *Aspergillus fumigatus* ook pyomelanine vormt. Deze kleine hoeveelheden zouden niet zichtbaar zijn met het oog maar wel een verhoogde fluorescentie kunnen geven. Uit deze resultaten kan worden geconcludeerd dat melanine resulte-

rend van verschillende biosynthese routes verhoogde fluorescentie vertonen na aanstralen met licht van een golflengte in het gebied nabij-infrarood. Zelfs voorlopermoleculen of hun afgeleiden pigmenten vertonen dit gedrag.

Vorming van melanine wordt geïnduceerd in de champignon door beschadiging en door infectie. Hierdoor krijgen de champignons bruine plekken. Onze resultaten wijzen er op dat melanine ook aanwezig is in de hoed van witte champignons maar wel in mindere hoeveelheden als beschadigde of geïnfecteerde champignons, dit omdat er meer energie nodig was om de verhoogde fluorescentie waar te nemen vergeleken met de bruine hoeden (Hoofdstuk 5). De hoeveelheid melanine in de witte hoeden nam toe gedurende de 17 dagen dat champignons werden opgeslagen bij 4 °C (Hoofdstuk 3)). Hieruit kan geconcludeerd worden dat zowel de melanine / NAD(P)H verhouding als de FAD / NAD(P)H verhouding gebruikt kan worden om versheid en houdbaarheid van champignons te volgen.

NLSM toonde aan dat de bijdrage van melanine in het emissiespectrum van mycelium, primordia en champignons wel kon oplopen tot 20% van de totale fluorescentie. Dit ondanks hun witte of kleurloze voorkomen (Hoofdstuk 4 en 5). NLSM detecteerde ook melanine in het mycelium van *A. niger*. Deze data suggereren dat melanine(-achtige) pigmenten een structureel onderdeel uitmaken van de schimmelcelwand. De hoeveelheid melanine lijkt in het mycelium van de champignon hoger te zijn dan in de paddenstoel zelf. Mogelijk speelt dit melanine een rol in de verdediging van het mycelium tegen andere microben of oxiderende verbindingen in de compost. Dit werpt een kritisch licht op de poging niet-bruinende paddenstoelen te ontwikkelen. Het mycelium van champignons die geen melanine meer kunnen vormen is mogelijk verzwakt, waardoor groei en ontwikkeling negatief wordt beïnvloed.

ZUSAMMENFASSUNG

Pilze spielen eine wichtige Rolle im Ökosystem. Sie wiederaufbereiten organische Verbindungen und können in Symbiose mit Algen (Flechten), Pflanzen (Mykorrhizae) und Tieren leben. Auch der Mensch nutzt Pilze auf vielerlei Weise: direkt als Speisepilz, aber auch in der Herstellung von Lebensmitteln (Brot, Tofu, Käse), von Tierfutter und von Getränken (Bier, Sake). Außerdem werden Schimmelpilze auch industriell in großem Maßstab zur Gewinnung von Enzymen, Medikamenten (z.B. Penicillin) und organischen Säuren (z.B. Zitronensäure) eingesetzt. Die Kehrseite der Medaille ist, dass Schimmelpilze auch Krankheitserreger sind, die Tiere, Menschen und insbesondere Nahrungsplanzen befallen. Darüberhinaus können sie toxische Stoffe produzieren, verderben Lebensmittel und Schädigen die Bausubstanz. Angesichts ihrer Bedeutung ist es wichtig Schimmelpilze nachweisen zu können und ihrem Wachstum, Stoffwechsel, sowie ihrer Entwicklung zu folgen und diese zu erforschen. In dieser Dissertation habe ich *Agaricus bisporus* und *Aspergillus niger* als Modellsysteme eingesetzt. *A. bisporus*, der Champignon, ist der weltweit am meisten produzierte Speisepilz, während *A. niger* zur biotechnologischen Herstellung von Enzymen, Medikamenten und Säuren zum Einsatz kommt. Das Ziel dieser Arbeit war es spektral aufgelöste Multiphotonenmikroskopie (aus dem Englischen als NLSM abgekürzt) als Methode einzuführen um das Wachstum und die Entwicklung von Schimmelpilzen zu untersuchen, sowie deren Stoffwechselaktivität zu folgen. Dabei wird die biochemischen Charakterisierung (Spektroskopie) mit einem bildgebenden Verfahren (Fluoreszenzmikroskopie) kombiniert. Bei der Fluoreszenzmikroskopie absorbieren bestimmte Moleküle (Fluorophore) Licht und werden dadurch in den angeregten Zustand überführt. Fallen diese wieder in den Grundzustand zurück, emittieren sie Licht charakteristischer Farbe, die Fluoreszenz. Bei der herkömmlichen Fluoreszenzmikroskopie (Ein-Photonen-Fluoreszenz) das emittierte Licht energieärmer, d.h. langwelliger als das absorbierte. Dies verhält sich genau umgekehrt bei der Multiphotonenmikroskopie (meist Zwei-Photonen-Fluoreszenzmikro-skopie). Da das Anregungslicht im nahen Infrarotbereich deutlich energieärmer ist, müssen zwei Photonen fast

zeitgleich vom Fluorophor absorbiert werden. Dies ist nur mit sehr hohen Lichtintensitäten zu erreichen. Verglichen mit der Ein-Photonen-Fluoreszenzmikroskopie, werden dadurch nur Fluorophore im Fokus angeregt und das umliegendes Gewebe wird geschont. Außerdem streuen die meisten biologischen Gewebe Licht im nahen Infrarotbereich weniger stark als kurzwelliges Licht, wodurch auch tieferliegende Schichten abgebildet werden können. Nichtinvasiv wird Multiphotonenmikroskopie, wenn man sich, wie in dieser Arbeit, autofluoreszenter Biomoleküle bedient. Diese sogenannten Autofluorophore kommen natürlich in biologischen Organismen vor und sind bei Schimmelpilzen unter anderem NAD(P)H, Flavine und Melanin (Kapitel 1). Dabei sind NAD(P)H und Flavine als Elektronenüberträger an zahlreichen Redoxreaktionen des Stoffwechsels beteiligt, während Melanin ein Pigment ist, welches sowohl zum Schutz vor UV-Strahlung und oxidativem Stress dient, als auch an Infektionsprozessen beteiligt ist. Jeder (Auto)fluorophor hat ein charakteristisches Emissionsspektrum, welches durch das Emissionsmaximum, sowie durch den Verlauf des Spektrums gekennzeichnet ist und mit einem Spektrometer gemessen werden kann (Spektroskopie). Auch für die Absorption und die Emission von Licht haben (Auto)fluorophore eine Vorzugsrichtung. Werden unbewegliche (Auto)fluorophore mit polarisiertem Licht angeregt (z. B. Laserlicht) emittieren sie polarisiertes Licht. Können die (Auto)fluorophore higegen frei rotieren, hat das einen Einfluss auf die Fluoreszenzpolarisation und sie emittieren depolarisiertes Licht. In welchem Maße die Orientierung der (Auto)fluorophore die Emission depolarisiert wird durch die Anisotropie beschrieben. Änderungen der molekularen Umgebung haben einen Einfluss auf Emissionsspektren und Anisotropie. Somit können Messungen von Spektrum und Polarisation Aufschluss über die chemische Zusammensetzung und z.B. die Viskosität geben.

NLSM von Schimmelpilzen

In Kapitel 2 wird NLSM als Methode näher beschrieben. Dabei wird die Summe der Fluoreszenz(spektren) aller im Organismus angeregter autofluoreszenter Biomoleküle gemessen. Die NLSM basiert auf einem kommerziellen Multiphotonenmikroskop. Dadurch ist das System anwenderfreundlich, da es z.B. schnelles Navigieren zu den zu unter-

suchenden Regionen ermöglicht und Standardanwendungen wie Hellfeldmikroskopie verfügbar sind. Außerdem kann man auch Ein-Photonen-Fluoreszenz anregen. Darüberhinaus kann man mit dem selbstgebauten Detektor zeitgleich sowohl Fluoreszenzspektren, als auch Anisotropie messen. Der Detektionsbereich (440 - 620 nm) deckt fast den gesamten sichtbaren Wellenlängenbereich ab und ist so gewählt, dass der Emissionsbereich autofluoreszenter Moleküle in Schimmeln, komplett erfasst wird. In Kapitel 3 und 4 zeige ich, dass die Emission im blauen, grünen und roten Spektralbereich verwendet werden kann um die Frische von Champignons zu bestimmen. Für diese Zwecke ist das derzeitige Gerät jedoch sehr kostspielig. Daher sollte untersucht werden, ob die kostengünstigere Ein-Photonen-Anregung mit ähnlichen Resultaten einsetzt werden kann. In diesem Fall könnte eine Anordung von Diodenlasern oder LEDs in Kombination mit 2 oder 3 Detektrokanälen zum Einsatz kommen. Die Entwicklung von handlichen, tragbaren NLSM Systemen stellt eine andre Anwendung dar. Diese werden derzeit für die medizinische Diagnostik entwickelt.

Der Vorteil der Spektroskopie liegt darin, dass das gesamte gemessene Emissionssignal in die Teilsignale der jeweiligen Komponenten zerlegt werden kann. Für dieses sogenannte unmixing, habe ich die Phasor Analyse eingesetzt. Dieser Phasor Algorithmus beruht auf einer Fouriertransformation der Spektren, wobei jedes Spektrum als Punkt in einer Ebene dargestellt werden kann. Die Phasor Analyse ist eine visuelle Methode, die es ermöglicht die Teilsignale leicht aus den Abständen zwischen den reinen Komponente und der Mischung zu bestimmen.

Um nicht nur die Teilsignale der verschiedenen Komponenten zu erfassen, sondern auch ihre Interaktion mit der Umgebung zu messen, kann die bildgebende Spektroskopie (spectral imaging) mit der Anisotropie kombiniert werden. Diese misst die Beweglichkeit von Molekülen als Folge ihrer Wechselwirkung mit der Umgebung (Viskosität) oder der Bindung an andere Moleüle, wie z.B. Enzyme. Da die Emission autofluoreszenter Moleküle jedoch sehr schwach ist, ist es sehr schwer insbesondere bei den Anisotropiemessungen ein gutes Signal-Rausch-Verhältniss zu erzielen. Dies erschwert unter anderem auch

die kombinierte Analyse von Spektum und Anisotropie. Um das volle Potential auszuschöpfen, sollte die kombinierte Analyse von Spektum und Anisotropie weiter erforscht werden.

Überwachung des Stoffwechsels mit NLSM

Für die Optimierung von biotechnologischen Prozessen, wie auch für die kommerzielle Erzeugung von Speisepilzen, ist es von Vorteil, wenn man die Stoffwechselaktivität von Schimmelpilzen überwachen kann. Dafür gibt es verschiedene Methoden. Die meisten dieser Verfahren sind jedoch invasiv und benötigen daher Zellextrakte, Gewebeschnitte oder zellfremde Markermoleküle, die verstoffwechselt werden und dann z.B. abhänging von der Zellaktivität fluoreszieren. Hier schlagen wir NLSM als nichtinvasive Methode vor um Zell – und Gewebeaktivität von Schimmelpilzen zu bestimmen (Kapitel 2, 3 und 4). Dabei bedient man sich der Autofluoreszenz von FAD und NAD(P)H (Energieträger im Stoffwechse), wobei das Verhältnis dieser beiden Komponenten als Maß für die Aktivität genommen wird. Eine Abnahme des FAD / NAD(P)H Verhältnisses wird gleichgesetzt mit der Zunahme der Zellaktivität. Diese Erkenntnis kann beispielsweise für die Bestimmung des Frischegrades von Speisepilzen eingesetzt werden, denn derzeit gibt es kein Verfahren, welches die Messung von Frische und damit eine Aussage über die Haltbarkeit erlaubt. Kommerziell werden Pilze, in diesem Beispiel Champignons, auf nährstoffreichem Kompost gezüchtet. Einer Lage Deckerde über dem Kompost ist nötig um den Pilz, der eigentlich nur der Fruchtkörper des Schimmels ist, zu erhalten (Kapitel 1, Figur 2). Der Schimmel wächst unterirdisch in einem weit verzweigten fadenartigen Netzwerk, dem sogenannten Myzel. In dieser Arbeit wurde der Frischegrad von Champignons, die bis zu 17 Tage bei 4 °C gelagert wurden und im gesamten Zeitraum keine Farb- und Formveränderung aufwiesen, bestimmt. Im Vergleich zu frischen Champignons, ist das FAD / NAD(P)H Verhältnisses innerhalb von 17 Tagen um das zweifache angestiegen (Kapitel 3). Wurden die Pilze im Ganzen gepflückt, anstelle sie, wie üblich am Stiel abzuschneiden, war das Verhältnis von FAD / NAD(P)H ungefähr 1,3 Mal niedriger. Vermutlich trägt das beim Pflücken am Pilz verbleibende Myzel und die daran gebundene Deckerde dazu bei,

dass dieser noch mit Nährstoffen versorgt und besser vor Austrocknung geschützt wird (Kapitel 3).

Die Fluoreszenzintensität von FAD war im Myzel im Kompost und in der Deckerde 2,3 Mal höher, als in Pilzen (Hutdurchmesser 4 cm). Die Fluoreszenzintensität von NAD(P)H hingegen war unverändert (Kapitel 4). Dadurch war das FAD / NAD(P)H Verhältnis des Myzels, im Vergleich zu den Messungen im Pilz, höher. Das bedeutet, dass Fruchtkoerper aktiver sind als Myzel. Darüberhinaus haben Pilze mit einem Hutdurchmesser von 1 - 4 cm ein 1,6 Mal niedrigeres FAD / NAD(P)H Verhältnis verglichen mit Pilzen mit einem Hutdurchmesser von 8 cm. Wie erste Pilotmessungen bestätigten, ist dies auch ein Hinweis darauf, dass kleinere Pilze länger haltbar sind.

Auf dem Weg zum Fruchtkörper durchläuft der Champignon mehrere Entwicklungsstadien: Zuerst bilden sich undifferenzierte flauschige Zellfadenknoten (Hyphenknoten), die dann ab einer Größe von 1 - 2 mm Primordia genannt werden und aus denen sich im weiteren Verlauf Fruchtkörpern bilden. Allerdings entwickeln sich nur 5-10% der Primorda letzendlich Fruchtkörpern. Daher wäre es von Vorteil, wenn man mit NLSM vorhersagen könnte, welche Priomorida sich weiterentwickeln werden. Jedoch ist die Anzahl der vermessenen Primordia zu diesem Zeitpunkt noch zu gering um darüber eine abschließende Aussage treffen zu können.

Zusammenfassend lässt sich sagen, dass das FAD / NAD(P)H Verhältnis ein Maß für den Stoffwechselstatus von Schimmelzellen und –geweben ist. Es kann zur Qualitätskontrolle des Myzels und zur Messung des Frischegrades von Pilzen eingesetzt werden und ermöglicht somit die Haltbarkeit zu bestimmen. Somit könnten weitere NLSM-Untersuchungen zur Optimierung von Ernteprozessen um letztendlich länger haltbare Champignons zu erlangen. Darüberhinaus ist diese Methode vielversprechend für die Überwachung des Myzels in industriellen Fermentationsprozessen und die Grundlagenforschung an Schimmelpilzen. Ausserdem kann NLSM potentiell auch für die Qualitätskontrolle von anderen leicht verderblichen Produkten, wie Obst und Gemüse eingesetzt werden.

Screening von melanin(artigen) Pigmenten mittels Verstärkung der Fluoreszenzintensiät

Viele Schimmelpilze bilden Melanin. Dieses hochmolekulare heterogene Pigment ist an Infektionsprozessen und an der Abwehr von Krankheitserregern und freien Radikalen, die u.a. durch UV-Bestrahlung entstehen, beteiligt. Das sogenannte Eumelanin, welches u.a. in menschlichem Haar und im Tintenfisch vorkommt, reagiert außergewöhnlich stark auf hohe Dosen Licht im Nahinfrarotbereich: Statt zu bleichen, wird die normalerweise schwer zu detektierende Fluoreszenz des Pigments in hohem Maße verstärkt. Das gleiche Verhalten habe ich bei synthetischem Melanin und Melanin, welches aus *A. niger* Sporen isoliert wurde, beobachtet (Kapitel 5). Selbst wenn nur Sporen von *A. niger* und dem Champignon direkt gemessen wurden, konnte bereits erhöhte Fluoreszenzintensität in der Zellwand, wo sich das Melanin befindet, gemessen werden. Überraschenderweise wurde das Phänomen der verstärkten Fluoreszenzintensität auch in *A. niger*-Stämmen, die in einem der Schritte ihrer Melaninbiosynthese blockiert waren, festgestellt. Diese Sporen weisen aufgrund ihrer verschiedenen Pigmente alle eine andere Farbe auf. Erstaunlicherweise wiesen selbst die Sporen des weißen ΔpptA Stammes eine erhöhte Fluoreszenzintensität auf, obwohl man davon ausging dass dieser Stamm kein Melanin oder Pigmentvorstufen bilden kann. Es gibt verschiedene Arten von Melanin (Kapitel 5, Figur 1). Im Falle von *A. niger* wird davon ausgegangen, dass DHN Melanin gebilted wird. Allerdings weisen die Ergebnisse des ΔpptA Stammes darauf hin, dass *A. niger*, wie *Aspergillus fumigatus*, auch in der Lage sein könnte eine andere Art von Melanin, Pyomelanin, zu synthetisieren. Geringe Mengen würden zwar für das Auge unsichtbar sein, aber dennoch ausreichen um zu einer erhöhten Fluoreszenzintensität zu führen. Zusammenfassend lässt sich sagen, dass Melanin, unabhänging vom Biosyntheseweg, auf hohe Dosen Licht im Nahinfrarotbereich immer mit einer Erhöhung der Fluoreszenzintensität reagiert. Selbst Vorläufermoleküle oder daraus abgeleitete Pigmente verhalten sich so.

In den Champignons wird Melaninbildung durch Beschädigung des Pilzes oder durch Infektionen ausgelöst. Beides führt zu der Entstehung von braunen Flecken auf der Pilzoberfläche. Unsere Ergebnisse

zeigen, dass Melanin auch in weißen Pilzhüten vorhanden ist, jedoch in geringeren Mengen als in beschädigten oder infizierten Pilzen, da in diesen Fällen eine geringere Lichtdosis/Energiedosis ausreichend war um zu einer Erhöhung der Fluoreszenzintensität zu führen (Kapitel 5). Außerdem bestätigten spektroskopische Messungen, dass die Melaninmänge in weißen Pilzhüten während eines Lagerzeitraum von 17 Tagen bei 4 °C ansteigt (Kapitel 3). Daraus folgt auch, dass sowohl das Melanin / NAD(P)H, als auch FAD / NAD(P)H Verhältnis um Frische und Haltbarkeit von Pilzen zu beschreiben.

Dass das Melanin biologisch eine wichtige Rolle spielt, wird auch deutlich, da NLSM Messungen des Myzels, der Pilze oder der Primorda ergeben habe, dass der Anteil des Melanins an der Gesamtfluoreszenz bis zu 20% betragen kann und das trotz ihres weißen Erscheinungsbildes (Kapitel 4 und 5). Auch im weißen Myzel von *A. niger* ist Melanin gemessen worden. Diese Daten legen nahe, dass melaninartige Pigmente eine strukturelle Komponente der Pilzzellwand darstellen. Dabei scheint die Melaninmenge im Myzel jedoch höher zu sein als im Pilz. Daher ist Melanin wahrscheinlich für die Verteidigung des Myzels gegen andere Mikroben oder oxidierenden Verbindungen im Kompost wichtig. Wenn das der Fall ist, sollte die Versuche einen melaninfreien Champignons zu erzeugen nochmals kritisch hinterfragt werden. Möglicherweise wäre dieses Myzel so geschwächt, dass das Wachstum und Entwicklung beeinträchtigt wären.

CURRICULUM VITAE

Helene Knaus was born on January 31st, 1982 in Dshambul, Kazakhstan. She completed her secondary education in 2000 with a Gymnasium-level diploma at the Joseph Haydn Gymnasium in Dresden, Germany. In the same year she began her coursework in process engineering with focus on bioprocess engineering at Dresden University of Technology (TUD). As part of her studies she did an internship on biosensors at the Helmholtz Centre of Environmental Research under the supervision of Dr. B. Strehlitz (Leipzig, Germany), followed by a second internship on rapid detection of bacteria in consumables in the bioprocess engineering group of Prof. Dr. T. Bley at the TUD. In 2003 Helene obtained her engineering diploma (equivalent to MSc) with an internship on protein folding studies using atomic force microscopy (AFM) under supervision of Dr. H. Janovjak and Prof. Dr. D. J. Müller at the BIOTEC (Dresden, Germany). After working on an integrated high resolution- (AFM) and wide-field fluorescence system at the Goethe University Frankfurt am Main (Germany), she started her PhD in 2009 on nonlinear spectral imaging of fungi with the Molecular Microbiology group under the supervision of Prof. Dr. H.A.B. Wösten and the Molecular Biophysics group under the supervision of Prof. Dr. H.C. Gerritsen at Utrecht University.

PUBLICATIONS

Knaus H., Blab G.A., van Veluw G. J., Gerritsen H.C., Wösten H.A.B. Label-free fluorescence microscopy in fungi. Fungal Biology Reviews 2013 (invited)

Knaus H., Blab G.A., Agronskaia A.V., van den Heuvel D.J., Gerritsen H.C., Wösten H.A.B. Monitoring the metabolic state of fungal hyphae and the presence of melanin by nonlinear spectral imaging. Applied and Environmental Microbiology 2013.

Knaus H., Blab G.A., Agronskaia A.V., Vos A.M., Gerritsen H.C., Wösten H.A.B. Monitoring melanin and the metabolic state during development of *Agaricus bisporus* by nonlinear spectral microscopy. in preparation

Knaus H., Segers F.J.J., Agronskaia A.V., Teertstra W.R., Blab G.A., Dijksterhuis J., Gerritsen H.C., Wösten H.A.B. Fluorescence intensity enhancement of fungal melanin and its precursors. in preparation

ACKNOWLEDGEMENTS

When I came to Utrecht for the first time the weather was gorgeous and all the streets along the grachten were lively, filled with students and other normal people. I immediately felt at home. (This happened after I stepped out of the train at about 16:30 at Utrecht Centraal, tried not to get run over by the incoming stream of people and seeing Hoog Catharijne). This first impression was not deceiving and I was lucky to meet great and helpful people everywhere.

Surely without Mika Ruonala (Goethe University Frankfurt) and Hans Gerritsen I wouldn't be here: Hans, thanks for inviting me, kindly hosting me in your group and for all the helpful discussions during my PhD. I am also deeply indebted to my promoter, Han Wösten, for all the freedom and trust I had during my PhD. Thanks to your enthusiasm I learned a lot about fungal biology, writing, getting things done and I do appreciate your support and advice, which always came along at the right time. Gerhard Blab, my copromotor, thanks for the honest discussions, your reliability, the data analysis plugin and the nice time.

I would like to thank the Molecular Biophysics group, especially Dave van den Heuvel (go-to person in any situation), Farzad Fereidouni (good timing with the phasor analysis), Imaad Mohammed, Matthia Karreman, Arjen Bader, Johan van Voskuilen, Giju Thomas and Hoa Truong (useful discussions) and foremost I want to thank Alexandra Agronskaia from whom I learned a lot about optical microscopy, life and Russian literature. I am also grateful to Alessandro Esposito (Cambridge, UK) for helping me getting started with the spectrograph and Jonathan Palero for the quick introduction into nonlinear spectral imaging. It was really fun to meet all the new PhDs (Sajjad Mohammadian, Sergey Loginov, Jantina Fokkema). Jacopo Antonello thanks for being such a nice lab housemate. I definitely would also like to acknowledge the Soft Condensed Matter group, particularly Anke Kuijk, Thijs Besseling, Bart de Nijs, Judith Wijnhoven and Wessel Vlug (coffee chats), Teun Vissers, Anjan Gantapara and Frank Smallenburg (introducing me to climbing, chats, dinners), Laura Filion, Marlous Kamp Jissy Jose and Nina Elbers (dinners, sharing de-

licious Indian recipes, support, yoga). Of course I also would like to thank the people from the Condensed Matter and Interfaces group, in particular Rosa Martin Rodrigues and Francesca Pietra (chats, spectrometer measurements), as well as Zachar Krumer (weather forecast, chats). I am also very grateful to the University workshop, which helped me solving quite some problems especially at the beginning of my PhD.

Although some of the Microbiology (Fungal) group members thought that I just had returned from my vacation (Luis), whenever I showed up (only for work discussions and growing *A. bisporus*), I am very grateful that you always have welcomed me in your group. Special thanks to Mayken Wadman, Roeland Berendsen, and Stefanie Kalkhove (introducing me to *A. bisporus*), Luis Lugones, Wieke Teertstra, Aurin Vos and Jordi Pelkmans (many helpful discussions about *A. bisporus* and melanin), Jerre van Veluw, Robert-Jan Bleichrodt and Arman Vinck (interesting collaborations), Hans de Cock, Fengfeng Wang, Brand Recter, Pauline Krijgsheld, Elsa Berends, Natalia Escobar Salazar and Florian Putker (helpful work discussions and fun time). I would also like to thank the whole bacterial group and the plant-microbe interactions group, especially Peter Bakker and Roeland (introducing me to *Pseudomonas spp.*), as well as Christos Zamioudis (all kinds of bacteria and lab questions). Of course I would also like to thank all the people from the CBS Fungal Biodiversity Centre, in particular Jan Dijksterhuis and Frank Segers (helpful work discussions, suggestions, collaborations, chats), as well as the group of Ronald de Vries, particularly, Ad Wiebenga, Isabelle Benoit and Aleksandrina Patyshakuliyeva (chats, work discussions), Sylvia Klaubauf (sharing my passion for cakes), Alexandra Vivas Duarte and Evy Battaglia (discussions, support and fun time). Furthermore, I also would like to acknowledge all the people working in the kitchen of the Microbiology group.

I take the opportunity to also thank my STW-user-committee for all the stimulating discussions: Johan Baars, Elsa Berends, Ko Hooijmans, Caroline van der Horst, Mark den Ouden, Erik Polman, Geert Weijers, Anton Sonnenberg, Wim Arts and Jan Vink.

Special thanks to my paranimfen: Wiebke, danke für die gute Laune, das Zuhören und die Spielerunden. Lieve Birgit, dank je wel voor de gezellige tijd op Hogeweide en het delen van mijn avonturen hier in Nederland.

My dear friends thank you all for your support, nice chats and fun time in The Netherlands: Birgit, Evy, Nina and Stefanie (support, teaching me Dutch), Alexandra and Wiebke (cheerfulness), Gergana (great Bulgarian dinners), Anneta (amazing Greek mountain tea), Diego, Sara and Carlo (lovely Italian dinners), Natalia (discovery of Spain), Oleg & Yulia (car retreats), Tom & Aspa (climbing & excellent dinners), Joke & Jonas (Flemish & playing board games), Roald and Mirte (vegetarian food), Visa & Patama (discovery of the Finnish Christmas market), and Anna-Carolina & Ward (adventures).

Ganz besonders möchte ich mich für die Unterstützung bei meinen Freunden und meiner Familie bedanken, insbesondere bei meinen Eltern: Unser Wiedersehen und die vielen Gespräche haben mir immer wieder Energie und einen frischen Blick auf die Dinge gegeben. Ohne euch währe das alles gar nicht möglich. Lieve Tim, dank je wel voor het delen van de stress, de spinazie lasagne zonder spinazie, voor alle avonturen en vooral bedankt dat je me neemt zoals ik ben.

So, finally you have made it though the acknowledgements! If you for any reason could not find your name I would like to take the opportunity and thank you now.